Modification of the silica nanoparticle surface with organosilanes

Introducing hydrophobicity for neutral wetting behavior

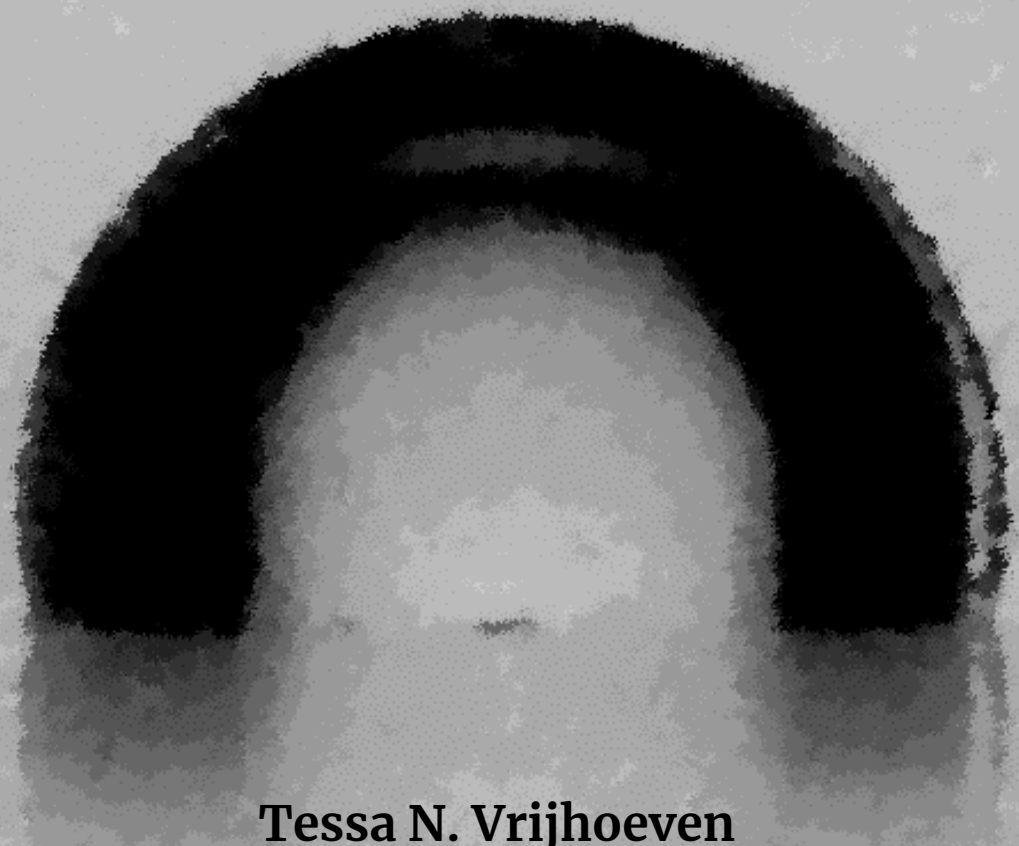

Tessa N. Vrijhoeven

Utrecht University

Master Thesis

Modification of the silica nanoparticle surface with organosilanes

Introducing hydrophobicity for neutral wetting behavior

Tessa N. Vrijhoeven

Supervisors:

Alessio J. Sprockel
dr. Katherine A. Macmillan
dr. Martin F. Haase

March 6, 2023

Van 't Hoff laboratory for Physical and Colloid Chemistry
Debye Institute for Nanomaterials Science
Utrecht University

Layman's abstract

The raincoat that keeps you dry when it is raining, a perfect example of a "water-disliking" surface. In chemistry the water-liking (hydrophilic) and water-disliking (hydrophobic) character of particles and liquids can be very important. If you for example add hydrophobic olive oil to a glass of hydrophilic water, the water and oil do not mix. The oil forms a layer on top of the water to avoid contact with the water molecules as much as possible. Why do we then use water to clean the rather oily dishes, you may wonder. Doing the dishes only works well if soap is added. Soap molecules are so-called surfactants. They consist of a hydrophobic and hydrophilic part. While doing the dishes the soap molecules attach to the oil-water interface, with the hydrophobic part into the oil phase and the hydrophilic part sticking out to the water phase. The outside of the oil droplet is now made hydrophilic by the soap molecules, allowing the oil droplet to be mixed with the water, and thereby make it possible to clean the dirty frying pan. Another way to mix water and oil is by adding an alcohol like ethanol. Removal of this alcohol will de-mix the water and oil again. Using specific amounts of water, oil and alcohol a so-called "spinodal" structure can be formed by the water and oil if the alcohol is removed as this induces a process called spinodal decomposition. In this spinodal structure the oil and water phase both form a continuous channel. The two channels are interwoven, resembling the coral structure depicted in Figure 1. This interwoven structure gives rise to a large interfacial area between the water and oil channel, making it interesting for numerous applications. However, water molecules still do not like to interact with the oil molecules, causing the interwoven structure to be instable and lost over time. Just as with the olive oil in a glass of water, the water and oil molecules will minimize contact with each other by forming a two-layer system. To maintain the interwoven structure stabilizing particles are required. These particles will, similarly to soap molecules, attach to the oil-water interface. Due to the presence of the particles at the interface the water and oil molecules do not have to interact, making the spinodal structure more stable. Such a particle-stabilized spinodal structure is called a "bijel", which stands for bicontinuous interfacially jammed emulsion gel. Often silica nanoparticles are used as stabilizing particles. However, silica is hydrophilic by nature because the surface contains a lot of negative charges that like to interact with water. To make the particles attach to the oil-water interface the particles must be made more hydrophobic such that they like to be in oil as much as they like to be in water. This is done by adding a positively charged surfactant. Due to the positive charge the surfactant will electrostatically adsorb onto the negatively charged silica surface, generating a more hydrophobic surface. However, using surfactants can be disadvantageous for applications of the bijel. In this work we researched if silica nanoparticles can be made more hydrophobic by covalently binding organosilanes, silicon-based compounds with an organic group that introduces hydrophobicity, and if this covalent modification can be used to eliminate the need for surfactants in the formation of bijels. Therefore, we have looked at three different silanes that differ in hydrophobicity and the number of bonds they can form with the silica surface.

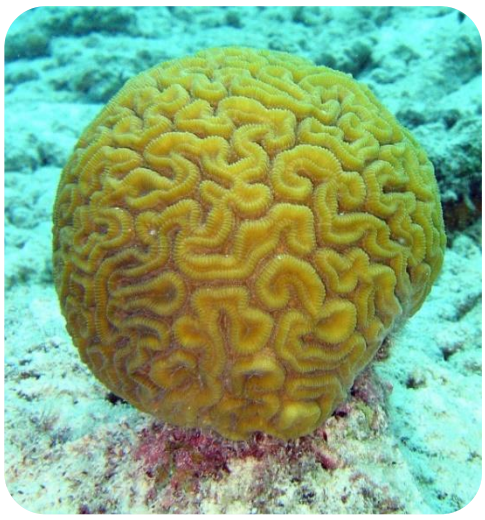

Figure 1 Picture of coral taken from https://en.wikipedia.org/wiki/Coral. The structure of coral can help the reader by visualizing the spinodal structure of bijels.

Abstract

The chemical industry utilizes enormous amounts of energy in their purification processes. A possible way to circumvent the need for energy costing processes like distillation is by applying bijels, bicontinuous interfacially jammed emulsion gels, as separative reaction media. Bijels have a bicontinuous structure consisting of two individual continuous channels, allowing for the combination of the reaction and separation process in one medium. Bijels can be continuously generated by the solvent transfer induced phase separation (StrIPS) method. In this method, the obtained structure is stabilized by CTA^+ (cetyltrimethylammonium) modified silica nanoparticles. The usage of surfactants like CTA^+ to hydrophobize the silica surface can be disadvantageous for possible applications. Therefore, it is desired to introduce surface hydrophobicity without using surfactants. A possible approach to achieve this is by functionalizing the particles with organosilanes. In this work, three organosilanes are studied, 3-(trimethoxysilyl)propyl methacrylate (TMSPM), n-dodecyltriethoxysilane (DTES), and hexamethyldisilazane (HMDS) to gain insight in their ability to create a hydrophobic Ludox TM-50 silica nanoparticles surface for potential application in bijels formed using a water/DEP/1-propanol system. The functionalization results were examined by FTIR, zeta potential, DLS, contact angle, and TGA measurements. We have successfully functionalized Ludox TM-50 particles with the three different silanes. Time-dependent studies showed that the functionalized particles could not be stored in water due to post-hydrolyzation. Additionally, the maximum silane coverage was found to be 40% for the Ludox TM-50 particles. Besides introducing hydrophobicity the trifunctional silanes, TMSPM and DTES, also introduced hydrophilicity. All three silanes did not introduce enough hydrophobicity to generate neutral wetting behavior with respect to water and diethyl phthalate (DEP), making these silanes unsuitable to stabilize bijels made using a precursor mixture consisting of water, DEP and 1-propanol. Additionally, testing the TMSPM functionalized particles in this precursor mixture revealed that there is a mismatch in the hydrophobicity required for stability in the precursor mixture and for bijel stabilization.

Keywords: silane functionalization, silica nanoparticles, contact angle, TMSPM, DTES, HMDS

Table of contents

Chapter 1

Introduction

Purification plays an important role in chemical industry. However, the processes involved in chemical separations are commonly very energy demanding as they require significant amounts of heat. In fact, 10 to 15% of the world's energy usage can be ascribed to chemical separation processes like distillation, as investigated by Sholl and Lively (1). In the United States these processes account for approximately half of the energy used in industry, see Figure 2. Replacing the energy demanding thermal separation processes could already save over 100 million tonnes of CO_2 emissions yearly in the US alone (1). As the emission of greenhouse gases like carbon dioxide is a major environmental problem it is of great importance to research alternative ways to separate chemicals.

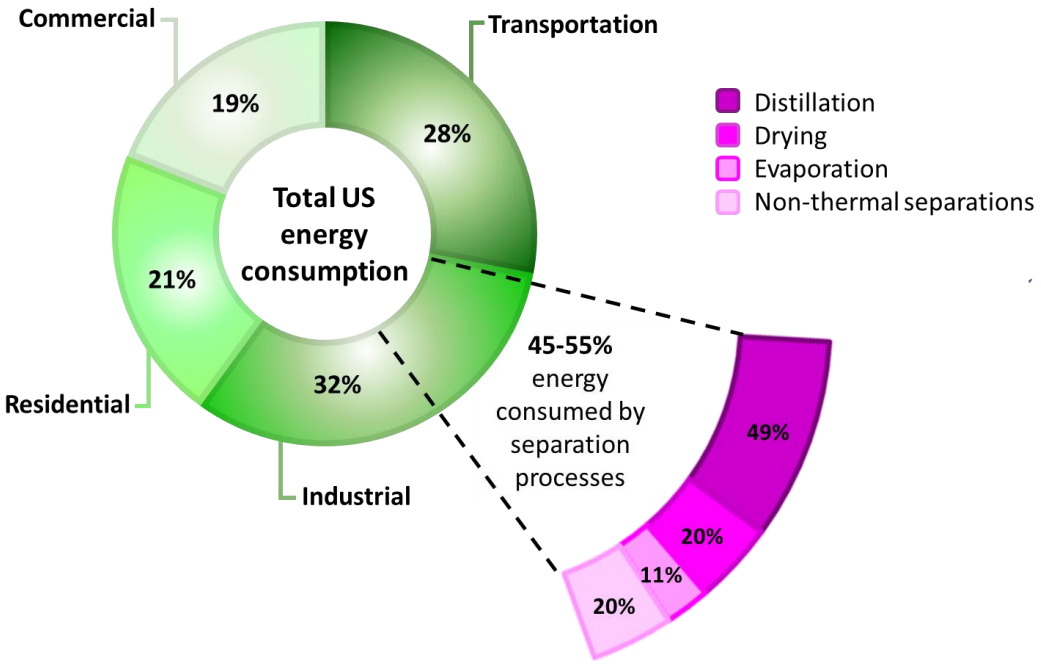

Figure 2 Overview of the energy consumption of the United States. Adapted from Sholl and Lively (1)*. Half of the energy used in industry in the US is consumed by separation processes.*

A potential alternative to distillation may be found in bicontinuous interfacially jammed emulsion gels, in short bijels. Bijels are a relatively new class of soft materials made from two immiscible fluids organized in a bicontinuous, channel-like structure with a fluid-fluid interface stabilized by interfacially jammed nanoparticles. The bicontinuous structure is formed by the phase separation of the two fluids via spinodal decomposition. As the phase separation proceeds, the interfacial tension between the two fluids increases. The high interfacial tension promotes the particles to position themselves at the liquid-liquid interface. In this way the unfavorable interfacial contact is minimized. Upon further coarsening of the fluid domains the interfacial area decreases, resulting in jamming of the particles on the interface, as depicted in Figure 3a. This happens because the nanoparticles cannot overlap, and the high interfacial tension makes it unfavorable for the particles to detach from the surface (2). The two particle-stabilized continuous channels give rise to a large interfacial area and allow for rapid mass transfer between the hydrophilic aqueous phase and the hydrophobic oil phase. These main characteristics makes bijels, amongst others, attractive to be applied as reaction media for continuous reactive separations. If stabilized by catalytically active particles, the reaction

can take place at the interface, and one phase can serve as supply channel while the other phase can be used to extract the product. Figure 3b shows a schematical graphic of a bijel operating as a reaction medium where the products are separated from the reactants in a continuous fashion. In this manner the reaction and separation process are combined in a single reaction medium, potentially eliminating the need for the energy demanding thermal separation processes like distillation.

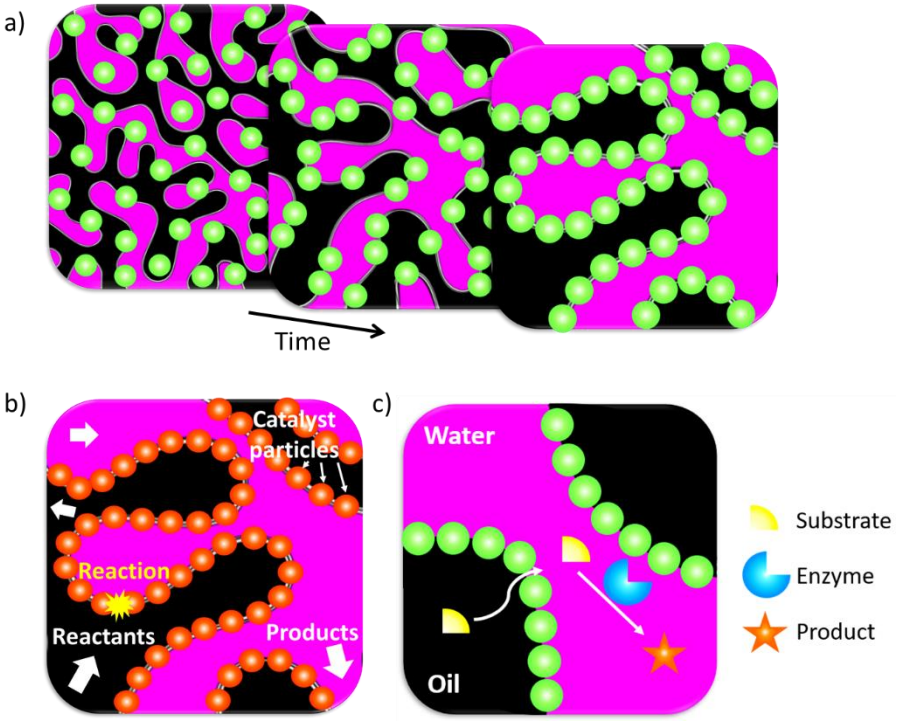

Figure 3 a) Illustration of particle jamming on the fluid-fluid interface over time. When time proceeds the interfacial area decreases resulting in jamming of the particles on the interface. b) Schematical illustration of a bijel as biphasic medium for continuous reactive separation. Reactants can be supplied to one channel while products can be subtracted from the other channel c) Schematical illustration of a bijel as reaction medium for the enzymatic conversion of hydrophobic substrates. The large interfacial area allows for transporting the hydrophobic substrate to the aqueous phase. Adapted from Cha et al. (3).

The first experimental method to fabricate bijels was reported by Herzig et al. (4). In this method the spinodal decomposition is induced by heating a close-to-critical mixture of two immiscible liquids and stabilizing particles through the critical solution temperature. For the spinodal structure to be trapped by the particles the three-phase contact angle must be close to 90°, also referred to as "neutral wetting behavior". Particles that are preferably wet by one of the fluid phases impose a preferred curvature on the fluid-fluid interface, resulting in stabilized emulsions droplets rather than spinodal structures. To achieve neutral wetting behavior Herzig et al. (4) tuned the drying procedure of the stabilizing silica colloids (4). In 2015 the so-called STrIPS, solvent transfer induced phase separation, method emerged to continuously generate bijels. In STrIPS the two immiscible liquids are mixed upon addition of a co-solvent rather than by decreasing the temperature. A precursor mixture is made from the two immiscible liquids and the co-solvent in a composition close to the critical point, stabilizing silica nanoparticles and cetyltrimethylammonium bromide (CTAB). Via CTAB the positively charged surfactant cetyltrimethylammonium (CTA^+) is introduced in the precursor mixture. This precursor mixture is then brought into a continuous phase where the solvent diffuses out of the mixture into the continuous phase, inducing phase separation. The added surfactant electrostatically adsorbs onto the nanoparticle surface, making the particles partly hydrophobic and thereby enable the particles to stabilize the bicontinuous structure (5). Recent research has shown that, when water and diethyl phthalate (DEP) are utilized as immiscible liquids and 1-propanol as solvent, STrIPS can produce so-called "small domain" bijels with domain sizes below 500 nm (6).

Besides the positive effects of changing the surface chemistry and wettability of the sililca nanoparticles, the usage of surfactants like CTA^+ has it drawbacks. Removal of the CTA^+ in a post-processing step is challenging, resulting in CTA^+ residues. This residual CTA^+ can be disadvantageous for potential applications (7). For example when bijels are applied as biphasic reaction medium for the enzyme-catalyzed conversion of hydrophobic substrates, see Figure 3c. Enzymes are generally soluble in water while some hydrophobic substrates are not. This reduces the enzyme-catalyzed conversion of a hydrophobic substrate significantly as there is little substrate present in the aqueous enzyme-rich phase. The large interfacial area of a bijel can already increase the conversion rate as it allows for rapid mass transfer between the aqueous and oil phase of the bijel, as shown by Cha et al. (3). However, the usage of surfactants in the bijel preparation might limit the conversion rates one can achieve due to enzyme activity being influenced by the surfactant. Binding of the surfactant to the enzyme can influence the enzyme structure and thereby influence whether the enzyme can still serve as catalyst or not (8). Thus, to make the utmost use of the potential of bijels, it is desired to have a surfactant-free synthesis route to continuously fabricate bijels. Recent research has already shown that short-term stable STrIPS bijels can be formed when acrylate-functionalized silica nanoparticles are used in the synthesis. Functionalization with 3-(trimethoxysilyl)propyl acrylate, an organosilane, renders the inherently hydrophilic nanoparticles partially hydrophobic and thereby facilitates the particles to be surface active and stabilize the bicontinuous structure. However, long-term stability could only be achieved by the addition of CTAB. The required amount of surfactant was significantly less compared to nonfunctionalized particles, illustrating the potential of silane functionalization (9). The research to date, however, has not been able to synthesize long-term stable bijels completely without the usage of surfactants.

1.1 Aim and outline

Therefore, this thesis sets out to find a method to fabricate surfactant-free bijels with the water/DEP/1-propanol system that exhibit long-term stability using the STrIPS method. Part of the aim of this thesis is to explore the ability of different silanes to hydrophobize the silica nanoparticle surface to enable neutral wetting behavior of the particles in the water/DEP system. Therefore, we studied three different organosilanes: 3-(trimethoxysilyl)propyl methacrylate (TMSPM), n-dodecyltriethoxysilane (DTES) and hexamethyldisilazane (HMDS). TMSPM and DTES are both trifunctional silanes but differ in the hydrophobicity of the functional chain. HMDS, on the other hand, is monofunctional allowing for a comparison between trifunctional and monofunctional silanes. Additionally, the implementation of the TMSPM functionalized particles in the bijel system is examined. Are the functionalized particles stable in the precursor mixture? Can covalent modification be used to generate neutrally wetting nanoparticles for bijel stabilization?

This thesis is composed of seven chapters. Chapter 2 aims to give the reader theoretical background knowledge that might be helpful in further reading and understanding this thesis. In the third chapter the TMSPM functionalization is discussed. Here, the techniques used to characterize the functionalized particles are treated in depth. Chapter 4 focuses on the functionalization with DTES, the more hydrophobic trifunctional silane. The fifth section analyses the HMDS functionalization. In chapter 6 the different silanes are compared. The final chapter summarizes the key findings and conclusions of this project and gives an outlook with ideas for further research.

Chapter 2

Theory

This chapter discusses the theory underlying the research that is done in this master thesis, which can help the reader by further reading this work.

2.1 From Pickering emulsion to bijels

It is well known that water and oil do not mix but rather form an emulsion upon vigorously shaking, see Figure 4. An emulsion is defined as a dispersion of two liquids that are non-miscible. One liquid forms the internal phase, the droplets that are dispersed. The other liquid forms the continuous phase, the liquid phase where the droplets are dispersed in. An example of a water-in-oil emulsion is given in the middle figure of Figure 4. Here, the continuous phase is formed by the oil, and the internal phase by the water. For an oil-in-water emulsion it is the other way around. For droplet sizes in the size range of 0.5-10 µm, the emulsion is referred to as macroemulsion. Macroemulsions are thermodynamically metastable or unstable. Over time the system will minimize its Gibbs free energy by droplet coalescence. When the droplets coalesce, the overall interfacial area, and thereby the Gibbs free energy, is decreased. The situation of two bulk phases has the smallest interfacial area and therefore the lowest Gibbs free energy. Hence, macroemulsions have a tendency to undergo demulsification where they split into the two bulk phases again, see Figure 4, as this is the energetically most stable configuration (10).

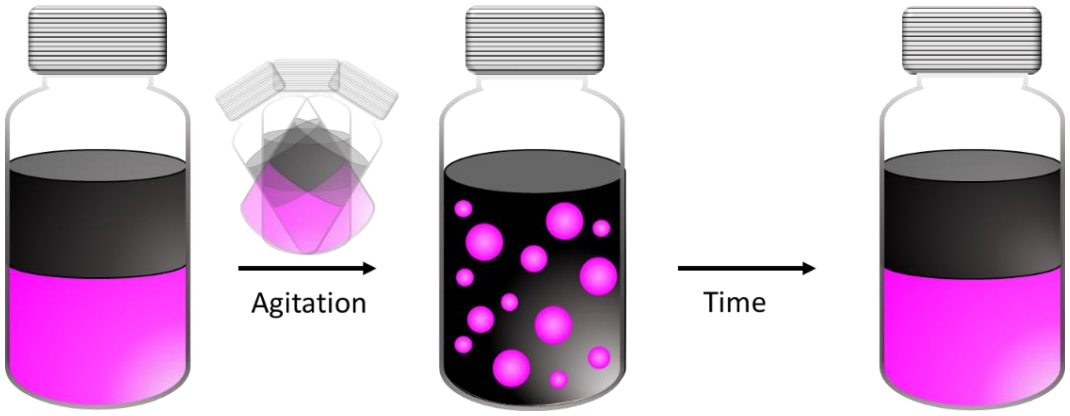

Figure 4 Emulsification and demulsification of a water-oil system. When oil (black) is added to water (magenta) a two-layer system is formed because water and oil do not mix. Upon agitation an emulsion is formed, in this case a water-in-oil emulsion. Over time the emulsion phase separates due to the minimization of the system's Gibbs free energy by minimizing the interfacial area.

2.1.1 Particle stabilized emulsions: Pickering emulsions

To avoid demulsification solid particles can be added to stabilize the emulsion. Such an emulsion stabilized by solely surface-active solid particles is called a "Pickering emulsion", after one of the pioneers in the field, Spencer Umfreville Pickering. In 1907 Pickering observed that oil-in-water emulsions could be protected from spontaneous demulsification by adding solid particles that were found to adsorb onto the oil surface (11). In 1903 Ramsden, the other pioneer in the field, already reported on the stabilization of emulsions by solid particles (12). The same phenomenon that causes the macroemulsion to phase separate over time, the energy-costing interface, drives the stabilization of Pickering emulsions. When a particle is positioned at the interface between the two non-miscible liquids, this simply reduces the unfavorable contact area between the two phases, causing the interface to become stabilized (13). These nanoparticle-stabilized emulsions can be made in a similar manner as the macroemulsions (14). The stronger the agitation, the smaller the droplet size. To

stabilize macroemulsions with droplet sizes of a few microns the stabilizing particles must be in the nanometer size range. The particle layer that is constructed by the adsorption of the particles at the interface sterically protects the emulsion droplets from coalescence, giving rise to long-term stability as shown in Figure 5 (14). Nonetheless, these particle-stabilized emulsions are still metastable.

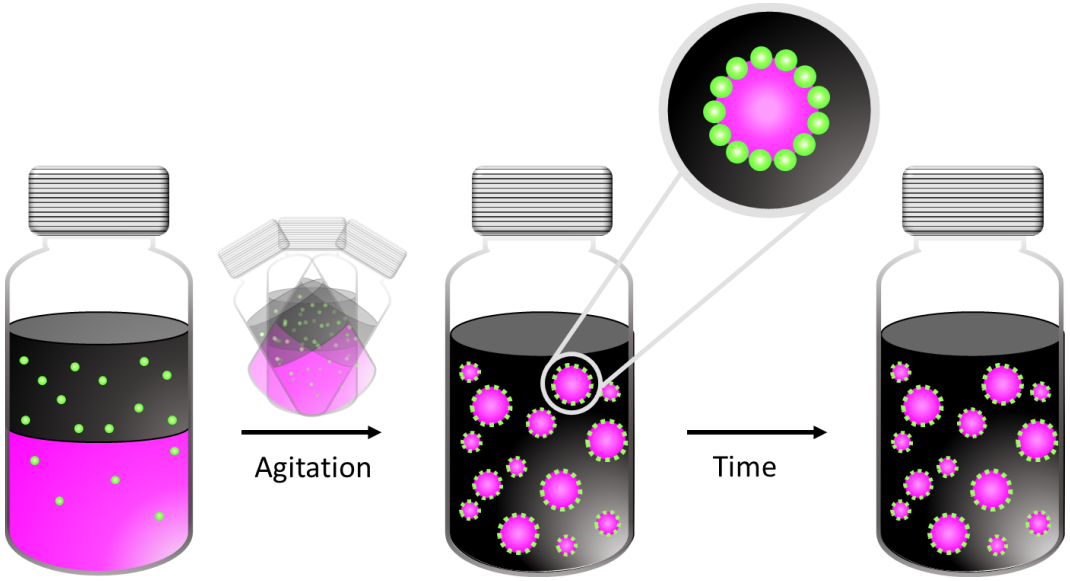

Figure 5 Formation of a water-in-oil Pickering emulsion. Upon agitation the water phase is broken into droplets. The solid particles adsorb on the interface that is generated by the agitation. Over time the emulsion remain stable as the particle layer protects the emulsion droplets from coalescence.

2.1.2 Bicontinuous Pickering emulsions: bicontinuous interfacially jammed emulsion gels (bijels)

In contrast to Pickering emulsions where the interfacial area is increased by agitation, quenching a fluid mixture into the spinodal regime is what gives rise to the large interfacial area of bijels. In the spinodal regime two continuous domains are formed rather than emulsion droplets in a continuous phase. Similarly to Pickering emulsions the liquid-liquid interface in bijels is stabilized by adsorbed solid particles, allowing for the solidification of the bicontinuous structure (15). Essentially, bijels are bicontinuous Pickering emulsions. Bijels were first computationally predicted by Stratford et al. (16) in 2005. Experimental realization followed in 2007 by Herzig et al. (4). Before diving into the details of the commonly used bijel fabrication method, it is of interest to understand the influence of the wettability of the stabilizing particles at fluid interfaces on the stabilization.

2.2 Contact angle, wettability and attachment energy

The three-phase contact angle θ is a fundamental aspect in both Pickering emulsions and bijels. More generally speaking, the three-phase contact angle is of great importance when considering solid particles located at liquid interfaces. Young's equation describes the dependence of the contact angle on the interfacial tensions of the interfaces present. For a particle at the oil-water interface the contact angle depends thus on the particle-oil (γ_{po}), the particle-water (γ_{pw}) and the oil-water interfacial tension (γ_{ow}). Young's equation is then given by (17),

$$\cos\theta = \frac{\gamma_{po} - \gamma_{pw}}{\gamma_{ow}} \qquad (1)$$

How this contact angle is created by a particle located at the oil-water interface is illustrated in Figure 6.

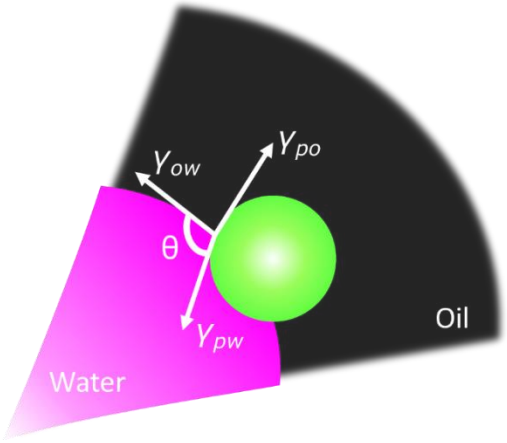

Figure 6 Particle located at the oil-water interface, showing the contact angle θ created by the particle at the interface. The contact angle depends on the interfacial tensions of the particle-oil, particle-water and oil-water interface, and is traditionally measured through the hydrophilic phase. Adapted from Björkegren et al. (18).

2.2.1 Contact angle & wettability

For particles that obey neutral wetting behavior the particle-oil and particle-water interfacial tensions are equal, indicating a three-phase contact angle of 90°. When a particle is hydrophilic it is preferably wet by water, and thus γ_{po} is larger than γ_{pw}. Hence, the contact angle of hydrophilic particles is 0° ≤ θ < 90°. Hydrophobic particles, on the other hand, are preferably wet by oil, with γ_{po} smaller than γ_{pw}. For hydrophobic particles the contact angle is thus 90° < θ ≤ 180° (17). The contact angle, whether the particles are hydrophilic or hydrophobic, greatly affects the shape of the interface. The Gaussian curvature K is the intrinsic curvature at a certain location on a surface. K is given by the product of k_1 and k_2, the principal curvatures. If K equals zero at least one of the principal curvatures is zero, meaning that the surface is uncurved in one or both of the directions. Examples of geometrical shapes with a zero gaussian curvature are a plane, where both k_1 and k_2 are zero, and a cylinder, where k_1 or k_2 equals zero. A positive Gaussian curvature gives rise to a spherical geometry as both k_1 and k_2 have the same sign, implying that the surface curves in a similar manner in both directions. The surface is a local minimum if k_1 and k_2 are both negative, and a maximum if k_1 and k_2 are both positive. If k_1 and k_2 have different signs the surface has a negative Gaussian curvature, and is bent differently in each direction. This is the case for saddle-like geometries (19). The three different types of curvatures are depicted in Figure 7.

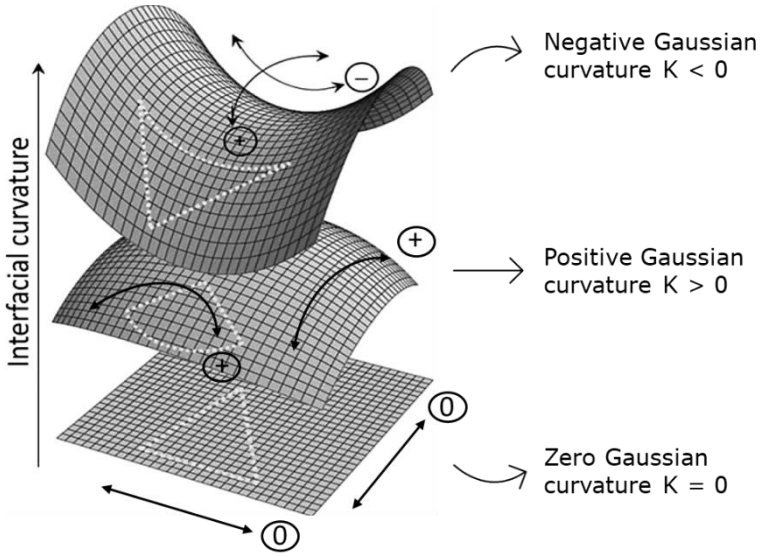

Figure 7 Schematic of the Gaussian curvature K. For K=0 the surface is uncurved in one or both directions. If K>0 the surface is bent similarly in both directions. For K<0 the surface bends differently in the two directions. Adapted from Gupta and Saxena (19).

For contact angles below and above 90° the particles position themselves at the interface in a manner that prefers a positive Gaussian curvature, forming emulsion droplets of one phase in the other. Particles with θ < 90° curve the interface such that an oil-in-water emulsion is stabilized. Particles with θ > 90° curve the interface in a manner that a water-in-oil emulsion is stabilized. Only particles with a contact angle close to 90° can curve equally to both the water and the oil phase. This enables the interface to have a negative Gaussian curvature, allowing for bicontinuous structures to be stabilized (13). McDevitt et al. (20) determined the Gaussian curvature of bijel-derived structures using micro-computed tomography, and showed that the Gaussian curvature of such spinodal structures is indeed predominantly negative (20). Figure 8 shows the different types of wettability, hydrophilic (θ < 90°), neutral (θ = 90°) and hydrophobic (θ > 90°) and the corresponding curvatures of the interface. If the particle surface is extremely hydrophilic it will be completely wetted by the water phase. The particle will stay dispersed in the water phase instead of adsorbing onto the interface. Likewise, an extremely hydrophobic particle will remain dispersed in the oil phase (14). These particles do not stabilize emulsions nor bijels.

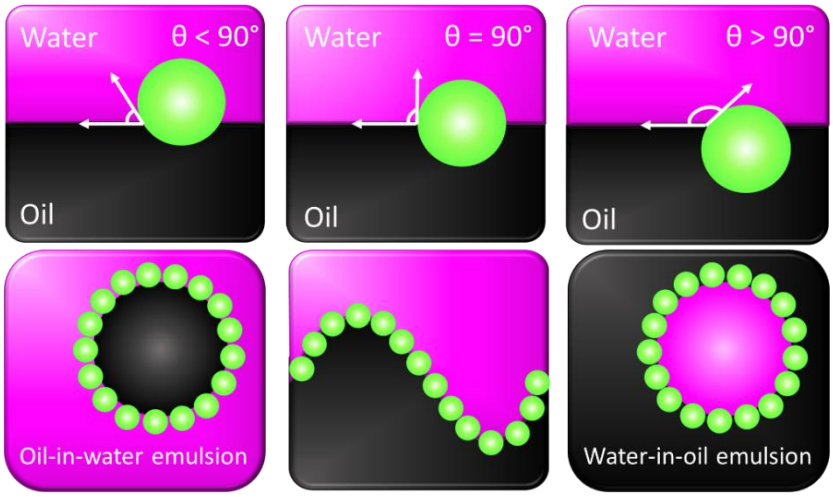

Figure 8 Particle imposed curvature of the interface. For θ < 90° the particle is preferentially wet by the water phase. For θ > 90° the particle is preferentially wet by the oil phase. In both situations the particles impose a positive Gaussian curvature on the interface, resulting in emulsions. For θ = 90° the particles are equally well wetted by both fluid phases, allowing for a negative Gaussian curvature. Adapted from Tran & Haase (13).

2.2.2 Contact angle & attachment energy

The wettability of the particles can not only influence the curvature of the oil-water interface but also influences the attachment energy of the particles to the fluid-fluid interface. When a particle attaches to the oil-water interface the area of the oil-water interface A_{ow} decreases and two new interfaces are generated, the particle-oil and the particle-water interface with area A_{po} and A_{pw}, and interfacial tensions γ_{po} and γ_{pw}, respectively. The attachment energy of a particle to the oil-water interface is given by (13,17);

$$\Delta G_{attach} = \gamma_{po}A_{po} + \gamma_{pw}A_{pw} + \gamma_{ow}A_{ow} = -\pi \cdot r^2 \cdot \gamma_{ow} \cdot (1 - |\cos\theta|)^2 \qquad (2)$$

Here, r represents the particle radius, γ_{ow} the interfacial tension of the oil-water interface and θ the three-phase contact angle determined via the water phase. This expression allows us to plot the relation between the attachment energy and the three-phase contact angle for a known particle size and γ_{ow}. The Ludox TM-50 particles used in this work have a particle size of around 30 nm according to transmission electron microscopy (TEM) as shown in Figure 9a (21), corresponding to a radius of 15 nm. The measured interfacial tension of a DEP droplet in water is 12.3 mN/m. Figure 9b shows the DEP droplet surrounded by water of which the interfacial tension was measured. Using the values for the DEP/Ludox TM-50/water system results in the attachment energy evolution depicted in Figure 9c. This plot clearly shows that the attachment energy is maximum at a contact angle of 90°. Here, the attachment energy is more than two thousand times k_bT. Due to this high attachment energy

the particles strongly attach to the oil-water interface. The higher the attachment energy, the less likely it is for the particles to detach from the interface.

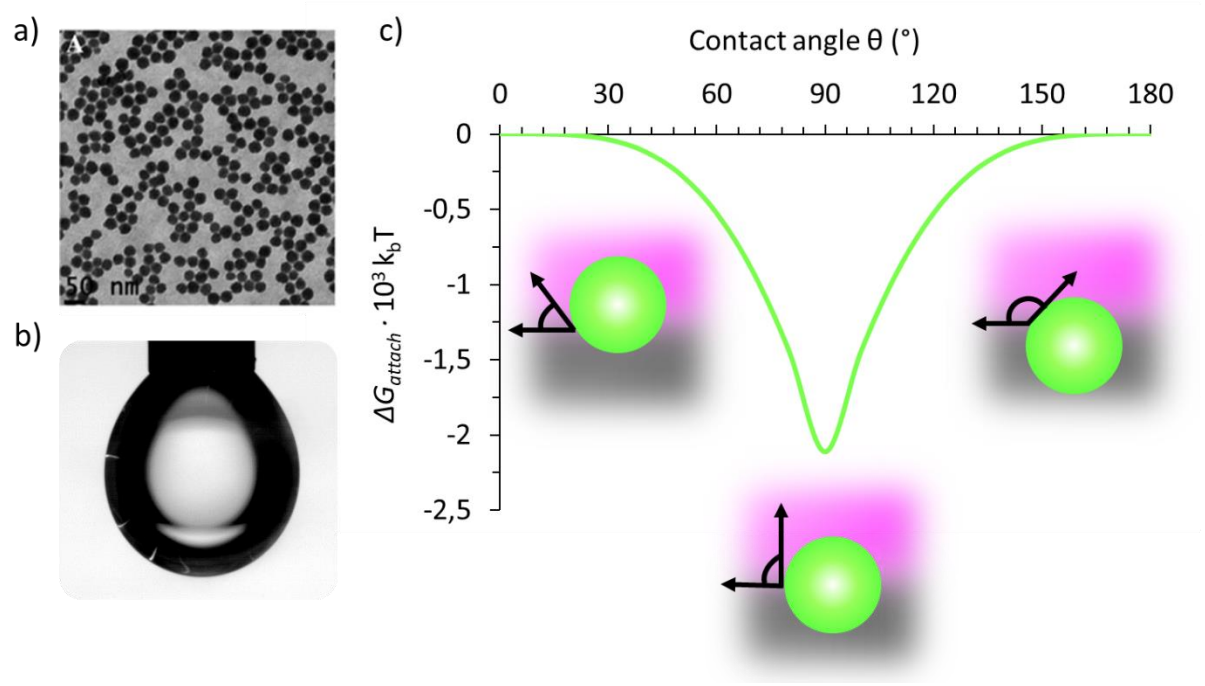

Figure 9 a) TEM image of Ludox TM-50 silica nanoparticles. Reprinted from Orts-Gil et al. (21)*. b) Interfacial tension measurement of a DEP droplet in water. The measured value was 12.3 mN/m. c) Evolution of the attachment energy in 10^3 k_bT with increasing contact angle from 0° to 180° using Equation 2. The particle radius and oil-water interfacial tension are 15 nm and 12.3 mN/m, respectively.*

2.3 Bijel synthesis: Solvent Transfer Induced Phase Separation (STrIPS)

As introduced in Chapter 1 bijels can be fabricated via a temperature-based method, often referred to as thermal quenching (4), and via the so-called STrIPS method that relies on the removal of the co-solvent (5). This is not the only fabrication method that is based upon removal of the solvent. In 2020 vaporization-induced phase separation (VIPS) was introduced by Wang et al. (22). In VIPS the co-solvent is removed by evaporation, enabling the formation of bijels under ambient conditions (22). One can also simply mix two immiscible liquids with a high viscosity, nanoparticles and surfactants to obtain a bicontinuous structure stabilized by particles (23).

2.3.1 The ternary phase diagram, the principle underlying STrIPS

In this work the STrIPS method introduced by Haase et al. (5) is applied. An important principle underlying the STrIPS method is the ternary phase diagram. In STrIPS the two immiscible liquids are mixed by adding a co-solvent. Hence, the ternary phase diagram can be used to understand the mixing behavior. The binodal line, the black curve in Figure 10a, splits the miscible region from the immiscible, biphasic region. A ternary mixture with a composition that lies in the immiscible region will divide along the tie-line into an oil-rich and a water-rich mixture. The colored lines in Figure 10a represent the tie-lines and the black point towards which the tie-lines converge is the critical point, also referred to as the plait point. For the water/DEP/1-propanol ternary diagram the tie-lines have a negative slope, indicating that the 1-propanol partitions mostly in the oil-rich phase (7). Besides the separation between the miscible and biphasic region by the binodal, the biphasic region itself can also be separated into an unstable part and a metastable part. A mixed phase in the metastable part does not become unstable when the local composition slightly changes. The boundary between the unstable and metastable region is called the spinodal line. At the critical point the binodal and spinodal line meet each other, as depicted in Figure 10b (24). When the liquid mixture is brought

from the miscible phase to the immiscible phase by only crossing the binodal line, phase separation occurs via nucleation and growth, resulting in metastable water-in-oil or oil-in-water emulsions. If the initial composition of the liquid mixture is close to the critical point, both the binodal and spinodal are crossed simultaneously, and the phase separation occurs via spinodal decomposition. In spinodal decomposition continuous water and oil channels are formed that are arranged in an intertwined fashion (6,24).

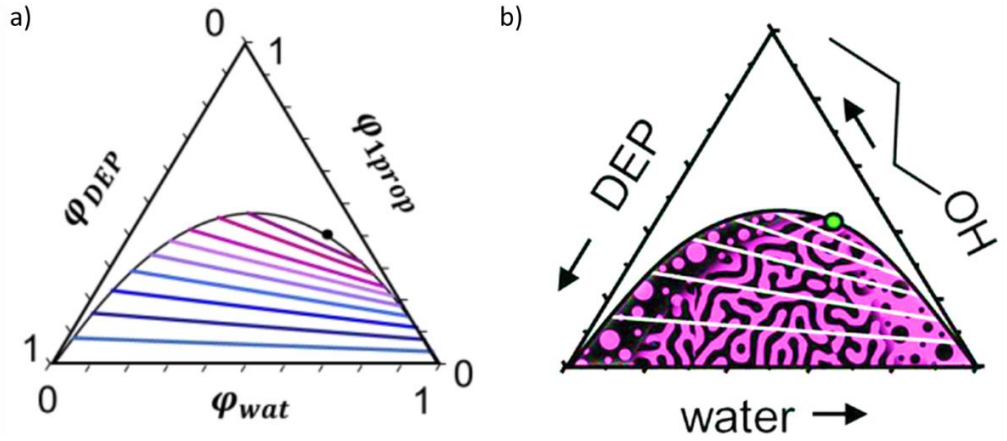

Figure 10 a) Ternary phase diagram of the water/DEP/1-propanol system. The colored lines are the different tie-lines. The negative slope of the tie-lines indicates that the 1-propanol partitions predominantly in the oil-rich phase. The critical point is indicated with the black point. Reprinted from Khan & Sprockel et al. (25)*. b) The water/DEP/1-propanol ternary diagram with the unstable spinodal region and the metastable region shown. Reprinted from Khan & Sprockel et al.* (6)*.*

2.3.2 Particle stabilization and the formation of bijels by STrIPS

Due to the high interfacial energy the lifetime of this bicontinuous, interwoven fluid structure is short. As time proceeds the interfacial area will be reduced until eventually a two-layer system is formed, see top figure in Figure 11a. This configuration has the smallest oil-water interfacial area and thereby the lowest interfacial energy (6). On its own the bicontinuous structure is thus not stable. That is why in STrIPS silica nanoparticles and the positively charged surfactant CTAB are added to the ternary mixture of the two immiscible liquids and the solvent. The mixture of the immiscible liquids and solvent at a composition close to the critical point together with the particles and the CTAB will from now on be referred to as precursor mixture. Besides aiding in the dispersibility of the silica nanoparticles in the precursor mixture, the CTAB allows the particles to attach to the interface. CTAB electrostatically adsorbs onto the silica surface, and thereby alters the hydrophobicity of the particles to make them neutrally wetting (5). Only if the particles are equally well wetted by the oil and the water phase, they are able to freeze the bicontinuous structure formed upon spinodal decomposition, see bottom figure in Figure 11a. Both the by the particles imposed curvature and the particle attachment energy show to be optimal for bijel stabilization at contact angles close to the neutrally wetting angle of 90°. As discussed in Section 2.2 there is no preferred curvature imposed on the interface and the attachment energy is high if the three-phase contact angle is 90°. Due to the absence of a curvature preference, there should be no formation of emulsion droplets. The high attachment energy of a few thousand k_bT makes that the particles almost irreversibly attach to the interface, allowing for jamming. Therefore, we aim in this work to functionalize particles to the extent where they have a three-phase contact angle close to this optimum of 90°.

In STrIPS the precursor mixture is rapidly injected into a continuous phase. The solvent used to enable the mixing of the two non-miscible liquids diffuses from the precursor mixture into the continuous phase, triggering the phase separation. The solvent diffusion changes the composition of the mixture such that it is shifted from the miscible region into the spinodal region in the ternary phase diagram. In other words, the solvent diffusion induces the spinodal decomposition. The resulting bicontinuous, channel-like structure coarsens further as more solvent diffuses out until the

spinodal structure is arrested, and thereby stabilized, by the silica nanoparticles. The particles with adsorbed CTAB molecules attach to the formed oil-water interface during the process of phase separation. Upon coarsening of the structure the number of attached nanoparticles increases, and the interfacial area decreases. The particles cannot overlap, and the attachment energy is too high for the particles to detach. Hence, the interface is jammed by the particles at a certain point in the phase separation, causing the spinodal structure to be arrested (5,7,13). Haase et al. (5) showed that using STrIPS it is possible to continuously fabricate bijels. This is achieved by flowing the precursor mixture through a cylindrical capillary that is positioned in the center of a second, slightly larger cylindrical capillary. Through the outer capillary the continuous phase is flown, allowing for the solvent diffusion (5). This experimental setup is depicted in Figure 11b.

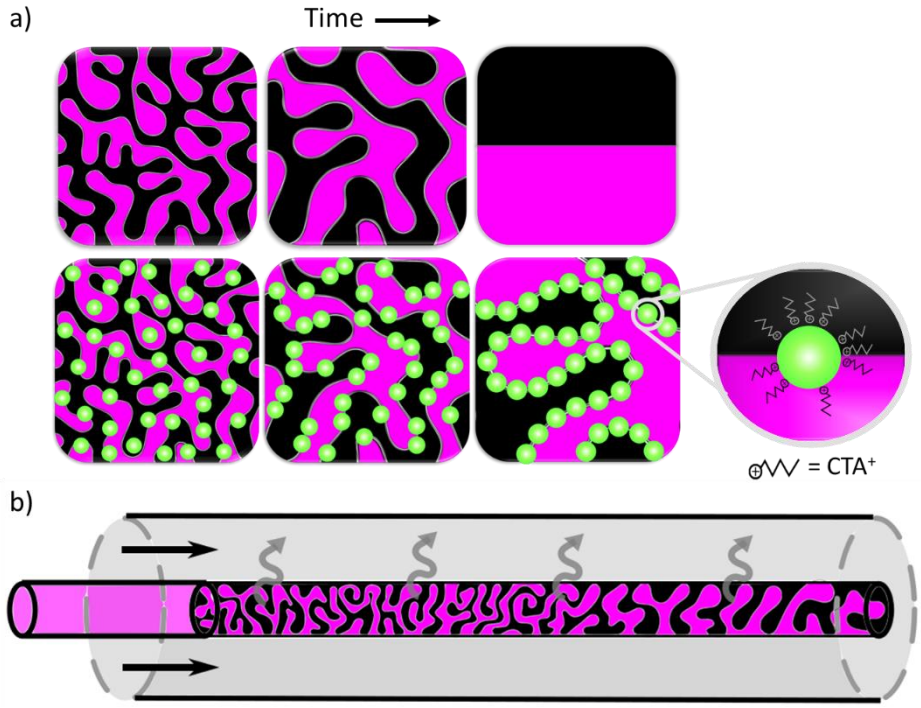

Figure 11 a) The top figure shows the coarsening of the spinodal structure if there are no particles present. Eventually two bulk phases are formed as this minimizes the unfavorable interfacial area. The bottom figure shows the coarsening and arresting of the spinodal structure by jammed nanoparticles. Due to the CTAB the particles attach to the interface. As phase separation proceeds more nanoparticles are attached to the oil-water interface, resulting in jamming of the particles at the interface. Adapted from Khan & Sprockel et al. (6). *b) Experimental setup for performing STrIPS. The precursor mixture is flown through the inner capillary while the continuous phase is flown through the outer capillary. As the solvent diffuses out of the precursor mixture into the continuous phase spinodal decomposition is induced. The more solvent diffuses out, the further the structure coarsens until the structure is arrested by the jammed particles. Adapted from Haase et al.* (5).

2.4 Reaction of the silane with the silica surface: hydrolyzation and condensation

In literature numerous examples can be found where silica is functionalized with silanes to alter the hydrophobicity of the silica. Björkegren et al. (18), for example, used silane functionalization to obtain long-term stable Pickering emulsions. By combining both hydrophilic and hydrophobic silanes the surface chemistry of the silica nanoparticles is adjusted such that the emulsification performance of these particles was significantly enhanced (18). In addition, Wang et al. (26) showed that flame-made silica nanoparticles could be hydrophobized with relatively high grafting content by introducing 3-methacryloxpropyltrimethoxyl silane in the flame spray pyrolysis process (26).

2.4.1 Silica-trialkoxysilane reaction

Modification of the silica surface is commonly done with organosilanes containing one organic group (R') and three hydrolyzable alkoxy groups (OR). Before a trialkoxysilane can react with the silica surface the alkoxy groups must undergo hydrolysis to generate silanol groups. According to Arkles (27,28) the silane-silica reaction consists of four steps. As mentioned above the first step is the hydrolysis of the OR-substituents. This step requires the presence of water. However, one does not necessarily have to add water. It can also originate from the atmosphere or just be present on the surface of the substrate. The three subsequent steps, condensation, hydrogen bonding and bond formation, can take place simultaneously. After the hydrolysis the silanes can be subjected to a condensation reaction, resulting in oligomers. These oligomers can then form hydrogen bonds with the surface silanol groups of the silica nanoparticle, which leads to bond formation over time. Usually, the silane molecule only forms one bond with the silica surface (28). The hydrolyzed silanes can also directly form hydrogen bonds with the silanol groups of the silica surface, instead of first undergoing the condensation reaction, followed by bond formation. The remaining silanol groups of the silane can either remain in their free form or undergo condensation reaction with the adjacent silanol groups of the neighboring silane molecule. Figure 12 shows the different steps of the silica-silane reaction. Another possibility, not shown in Figure 12, is that all three hydrolyzed alkoxy groups form hydrogen bonds with three neighboring silanol groups on the silica surface. Subsequent bond formation leads to three O-Si-O bonds.

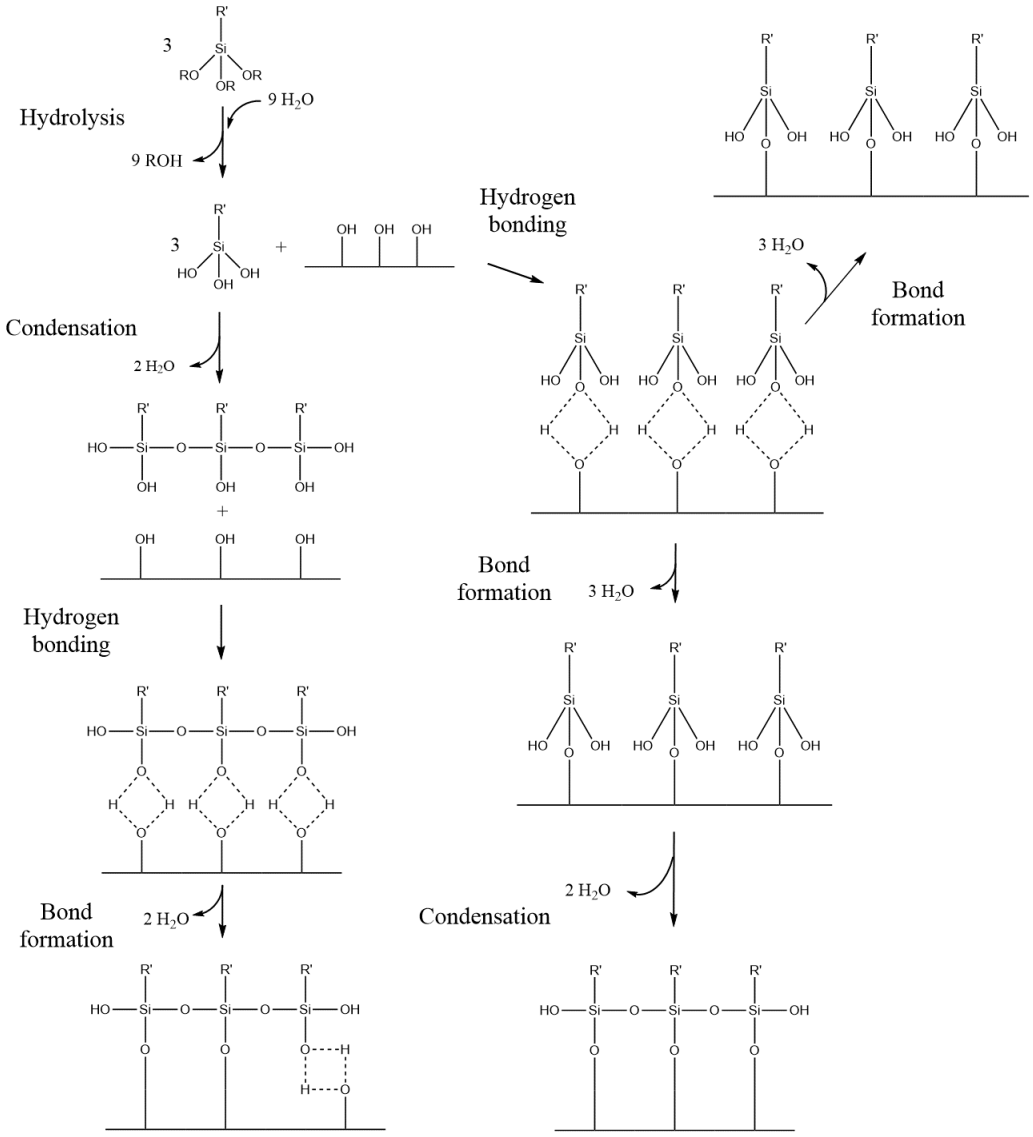

Figure 12 The possible reaction pathways for the reaction between trialkoxysilanes and the silica surface. Adapted from Arkles (27).

2.4.2 Silica-HMDS reaction

The overall reaction between the silica surface and HMDS, a monofunctional silane, is given in Figure 13. This reaction can follow two reaction schemes. It can be an one-step, concerted reaction where the surface silanol groups react in pairs. The silanol groups must be in sufficiently close vicinity to react according to this one-step reaction. The other reaction scheme is a two-step reaction. In the first reaction the HMDS reacts with a surface hydroxyl group to form an intermediate, which is assumed to be adsorbed on the hydroxyl group. Subsequently, this intermediate reacts with another surface OH group to form the end products. The rate-determining step is likely to be the second reaction where the adsorbed intermediate reacts with the OH group (29).

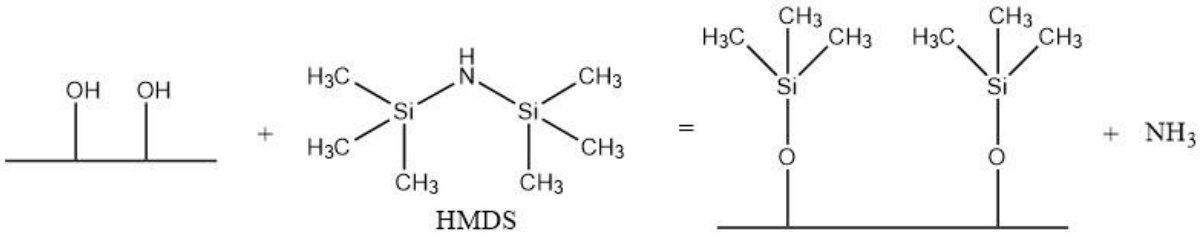

Figure 13 The overall reaction between HMDS and the surface silanol groups of the silica surface. Adapted from Hertl & Hair (29).

According to Gun'ko et al. (30) the probability of the one step, concerted mechanism is small. They reasoned that because the HMDS molecule contains only one nitrogen atom with one lone pair, at most one strong hydrogen bond can be formed between HMDS and the surface silanol group. In addition, the neighboring silanol groups must be at a distance similar to the Si-Si distance in HMDS to generate the transition state, which can only be possible if the two OH-groups are bound to the same silicon atom, i.e. geminal silanols. Theoretical investigations by Gun'ko et al. (30) indeed suggested that the HMDS-silica reaction is a two-step reaction, see Figure 14. In the first step the HMDS reacts with one surface silanol group, forming a trimethylsilyl surface group and trimethylaminosilane. This trimethylaminosilane reacts with another silanol group forming another trimethylsilyl surface group in the second step of the reaction. In this step ammonia is released as byproduct (30).

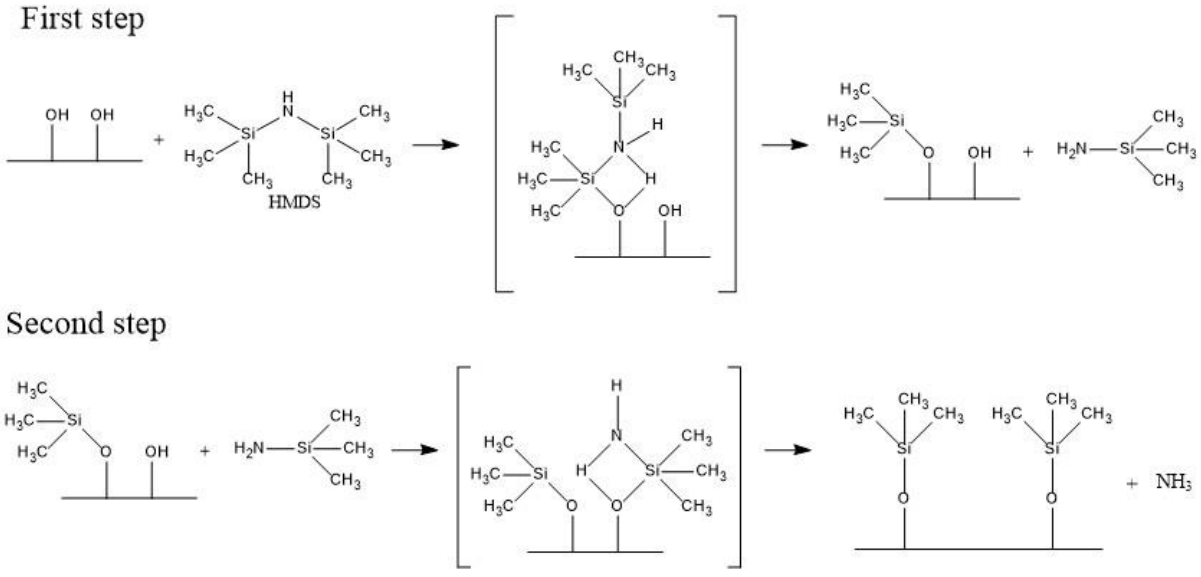

Figure 14 The two-step reaction mechanism for the reaction between HMDS and the silanol groups of the silica surface. In the first step a trimethylsilyl surface group and trimethylaminosilane are formed. The trimethylaminosilane reacts with the silica surface in the second step to create another trimethylsilyl surface group and ammonia. Adapted from Park et al. (31).

In the above described reaction HMDS reacts with the silica surface in the absence of water. However, just like the trialkoxysilanes described in Section 2.4.1, HMDS is prone to hydrolyzation if water is present. This gives rise to a second possible way for HMDS to react with the silica surface (32). Figure 15 displays the reaction of HMDS with the silica surface in the presence of water.

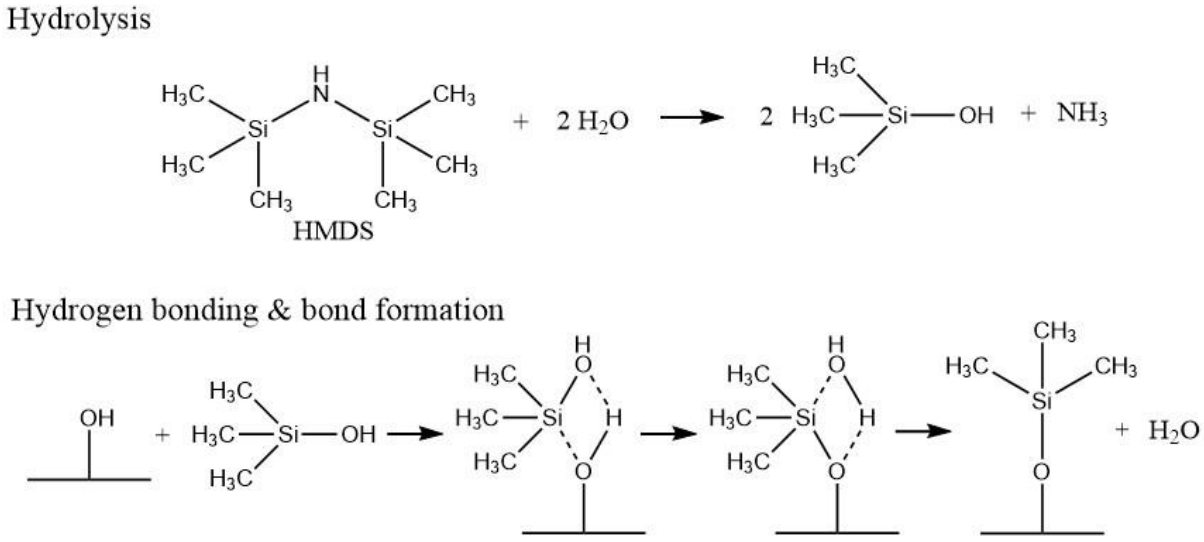

Figure 15 Reaction of HMDS with the silica surface in the presence of water. HMDS first hydrolyses before it binds to the silica surface. Adapted from Jones (32).

2.4.3 Factors influencing the ability of organosilanes to create hydrophobic surfaces

According to Arkles (28) there are four factors that contribute to the surface hydrophobicity of silane-functionalized surfaces:

1. The organic group R'
2. The degree of surface coverage
3. Unreacted groups from both the silica surface and the organosilane,
4. The silane distribution on the silica surface.

Obviously, the organic group R' must be a hydrophobic, non-polar entity to allow the silane to hydrophobize the surface. Distinctions between hydrophobic substituents can be made based upon their structure. The more sterically closed the structure of the substituent is, the more the van der Waals contact is minimized, the more hydrophobic the substituent. A methyl-substituted alkylsilane will thus succeed better in generating a hydrophobic surface than a linear alkylsilane. The other three factors are interrelated. The silica surface is a polar surface with hydroxyl groups distributed over the surface. These hydroxyl groups serve as hydrogen bonding sites. If both hydrogen bonding and the interaction between the polar, hydrophilic surface and water are hindered, the hydrophobic coating is considered to be successful. Hindrance of the surface-water interaction can be achieved by generating a non-polar interface that shields the hydrophilic surface. The lower the degree of surface coverage, the more hydroxyl groups are present, increasing the number of hydrogen bonding sites and thereby the hydrophilicity. The same holds true for unreacted hydroxyl groups, both from the silica surface and the hydrolyzed silane alkoxy groups. These groups allow for hydrogen bonding and thereby increase the hydrophilicity of the surface. Additionally, a higher degree of surface coverage results in the presence of more organic groups. A larger area of the surface is then shielded by the organic groups. The silane distribution also affects the shielding. Different types of silica have different number of surface silanol groups per squared nm. If fewer surface silanol groups are present, the surface has fewer binding opportunities. The reacted silanes will now be distributed over the surface in a way that leaves a significant amount of the surface area accessible for water molecules. Hence, the surface will remain rather hydrophilic (28). Figure 16 schematically depicts the influence of residual hydroxyl groups and shows the effect of fewer binding opportunities.

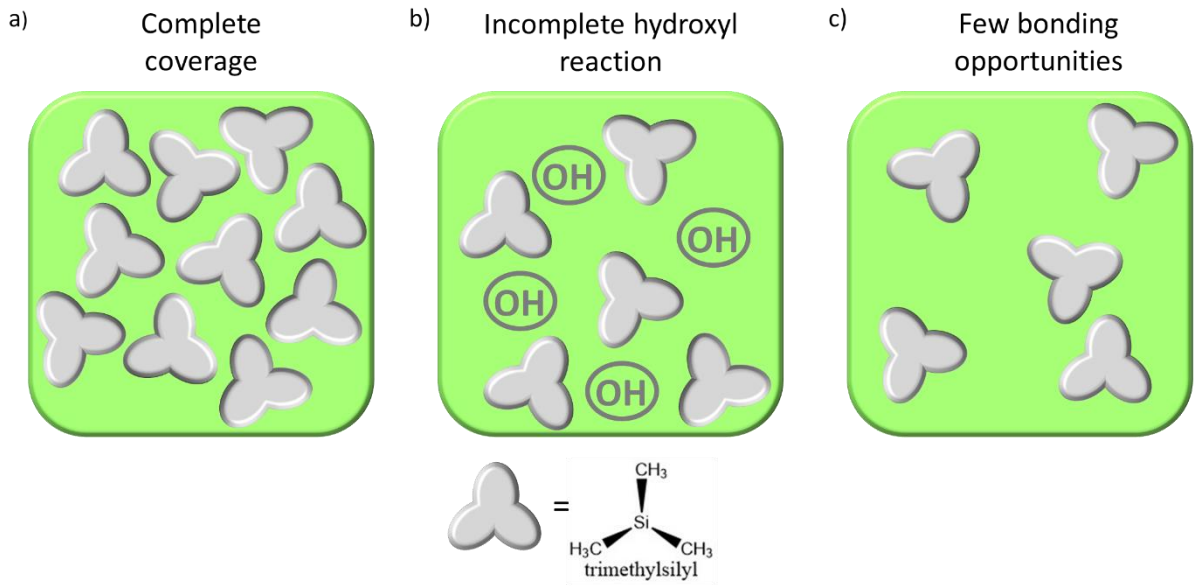

Figure 16 Schematic illustration of a silica surface covered with trimethylsilyl groups. a) If the surface coverage is complete all the silanol groups are substituted by the functional trimethylsilyl group. There are no hydrogen bonding site present and the surface is sufficiently shielded. b) When not all hydroxyl groups on the surface have reacted with the silane the surface coverage is incomplete. Hydroxyl groups remain present, allowing for hydrogen bonding, and the surface is not completely shielded. c) For silica types with relatively few hydroxyl groups at the surface, complete coverage is unachievable. Adapted from Arkles (28).

2.4.4 Calculation of the silane surface coverage

As mentioned above the wettability of the silica nanoparticles can be changed by functionalizing the silica nanoparticle surface with silanes. The degree of the functionalization, i.e. how much of the surface is covered with functional silanes, will influence the hydrophobicity of the surface and thereby its wettability. The amount of silane that is required to cover a certain percentage of the silica nanoparticle surface can be calculated by assuming that the silica nanoparticle surface contains four silanol groups per nm^2, see Figure 17a, and by making an assumption on the surface area of the used silica nanoparticles, as shown by Boakye-Ansah et al. (33). In this research Ludox TM-50 silica nanoparticles are used. These Ludox TM-50 particles have a particle size of around 30 nm (21) and the surface area is reported to be 140 m^2 per gram (34). Using this surface area, the total number of silanol groups per gram of silica nanoparticle can be calculated as

$$n_{SiOH} = \frac{N_{SiOH}}{N_{av}} = \frac{4\ SiOH\ molecules\ nm^{-2} * 140\ m^2 g^{-1}}{6.0223 * 10^{23}\ molecules\ mol^{-1}} = 9.3 * 10^{-4}\ mol g^{-1} \qquad (3)$$

with N_{SiOH} the total number of silanol groups on the Ludox TM-50 particles and N_{av} Avogadro's number. The amount of silane that one has to add to the system for a specific surface coverage depends on the added mass of silica nanoparticles, as this dictates the total amount of silanol groups in the system, and the desired fraction of functional silane on the nanoparticle surface. The number of moles of silane to be added, n_{silane}, can thus be calculated as follows,

$$n_{silane} = n_{SiOH} * \Delta m_{snp} * S \qquad (4)$$

where Δm_{snp} is the mass of silica nanoparticles that is added to the system and S the desired fraction of silane on the nanoparticle surface. The added volume of Ludox TM-50, ΔV_{snp}, is known and can be used to calculate the added nanoparticle mass using Equation 5,

$$\Delta m_{snp} = \Delta V_{snp} * \rho_{snp} * w_{snp} \qquad (5)$$

Here, ρ_{snp} is the silica nanoparticle density and w_{snp} the weight fraction of the silica nanoparticles (33). Both are given by the suppliers and are therefore known. According to the suppliers the used dispersion of Ludox TM-50 particles has a density of 1.4 g/mL and a weight fraction of 50 w% (34). The calculated required amount of moles of silane can then easily be converted into the volume of silane one has to add by multiplying it with the silane molar mass, M_{silane}, and subsequently divide it by the silane density, ρ_{silane} (33). It is important to note that this calculation assumes mono-grafting mode, meaning that each silane molecule only binds to one silanol group as depicted in Figure 17b.

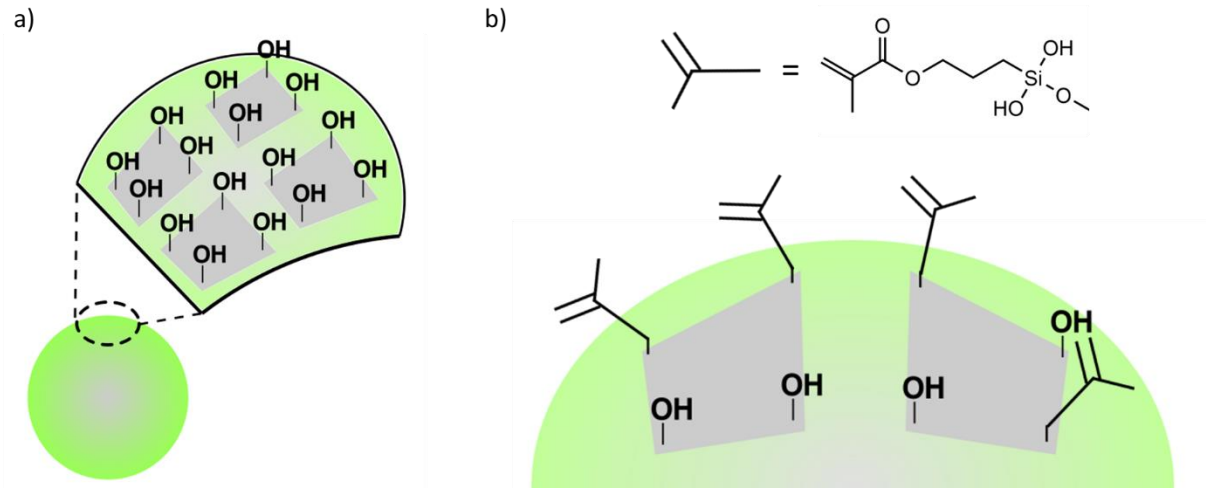

Figure 17 a) Illustration of the silica surface containing 4 silanol groups per nm^2. The grey planes represents a squared nm. b) Depiction of the silica surface after functionalization with 3-(trimethoxysilyl)propyl methacrylate assuming only mono-grafting of the silane molecules. Adapted from Boakye-Ansah et al. (33).

For trifunctional silanes that contain three silanol groups after hydrolysis, like trimethoxy silanes and trichloro silanes, di-, tri- and ladderlike-grafting modes may also be possible. Wu et al. (35) studied these four grafting modes for a 3-mercaptopropyl trimethoxy silane (MPTMS) modified silica surface using Density Functional Theory (DFT). They concluded that the mono-grafting mode is the most stable, followed by the ladderlike-grafting mode. The tri-grafting mode is the least stable grafting mode. The di-grafting mode stability is in between the ladderlike-grafting mode stability and the tri-grafting mode stability. The mono-, di- and ladder-like grafting mode are depicted in Figure 18. Wu et al. (35) found that the favorable grafting mode depends on the MPTMS concentration. For low concentrations the mono-grafting mode is favored whereas for high concentrations the ladderlike-grafting mode is more likely. This ladderlike-grafting mode is formed upon self-condensation of two silane molecules. Once bound to the silica surface these by self-condensation attached silane molecules can cause some silanol groups to be inaccessible for other silane molecules due to steric hindrance (35). Hence, this ladderlike structure may cause the surface coverage to be lower than calculated. The calculation described above serves thus only as an indication of the surface coverage.

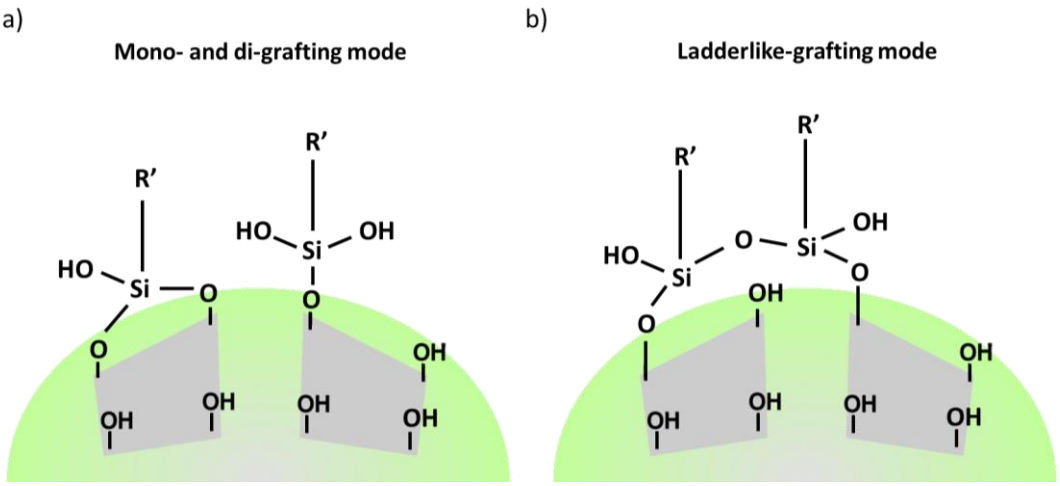

Figure 18 Most likely grafting modes of trifunctional silanes on the silica surface. a) At low silane concentration the mono-grafting mode is most likely followed by the di-grafting mode. b) At high silane concentration the ladderlike-grafting mode is favorable. Adapted from (35).

2.5 Silanol groups and zeta potential

The zeta potential, ζ, relates electrophoretic mobility of colloidal particles to their charge. Essentially, the zeta potential is the electric potential at the so-called plane of shear. When a colloidal particle migrates through a liquid, it takes a thin layer of surrounding liquid with it that moves with the same velocity as the particle. This layer ends at the point where the shear forces are large enough to move the liquid with respect to the particle surface. The electrophoretic mobility μ of the object is dependent on the surface potential of the moving object. In this case the moving object is the colloidal particle plus the thin layer of surrounding liquid that moves along, and thus the electrophoretic mobility is dependent on the potential of the shear plane, the zeta potential. For small particles, a few nm in size, at "low" ionic strength the electrophoretic mobility μ is related to the zeta potential as follows (36);

$$\mu = \frac{2}{3}\frac{\varepsilon_0 \varepsilon_r}{\eta}\zeta \qquad (6)$$

Here, η represents the viscosity, ε_0 the permittivity of vacuum and ε_r the dielectric constant of the medium. For the Ludox TM-50 nanoparticles, 15 nm in radius, this formula holds for NaOH concentrations up to 4.2 μM. If the salt concentration is higher, up to 4.2 M, the electrophoretic mobility relates to the zeta potential as (36)

$$\mu = f(\kappa a)\frac{2}{3}\frac{\varepsilon_0 \varepsilon_r}{\eta}\zeta \qquad (7)$$

where *f(κa)* is Henry's function which changes from 1 to 3/2. The zeta potential gives insight in the charge of colloidal particles. Besides informing on whether or not the dispersed particles are charged, it also gives information on the sign of the charge, i.e. if the particles are predominantly negatively of positively charged (36). The larger the absolute value of the zeta potential, the more charged the particles. Applied to the system of interest, the zeta potential can inform on the relative silane density on the silica surface.

The neutral surface silanol groups, Si-OH, can protonate or dissociate depending on the acidity of the environment, according to the equilibrium reactions described below (37);

$$Si - OH + H_3O^+ \leftrightarrow Si - OH_2{}^+ + H_2O \qquad (8)$$

$$Si - OH + H_2O \leftrightarrow Si - O^- + H_3O^+ \qquad (9)$$

$$Si - OH + OH^- \leftrightarrow Si - O^- + H_2O \qquad (10)$$

Duval et al. (38) showed the presence of Si-OH, Si-OH_2^+ and Si-O^-, the three surface species, and determined the surface density of the species for the quartz-water interface using X-ray photoelectron spectroscopy (XPS). Quartz has its isoelectric point (IEP), solution pH where the zeta-potential is equal to zero, between 0.5 and 3.5. The XPS results showed that the density of the positively charged species is highest at a pH of 0 and rapidly decreases with increasing pH. The density of the negatively charged species gradually increases with increasing pH. At pH 2 the amount of Si-OH_2^+ and Si-O^- determined by Duval et al. (38) were almost equal. Silanol groups can thus be charged depending on the pH. At a pH below the isoelectric point the surface silanol groups are predominantly positively charged, in the form of Si-OH_2^+. At a pH above the isoelectric point the surface silanol groups are predominantly negatively charged, in the form of Si-O^-.

During the functionalization the silanol groups on the silica surface undergo a condensation reaction with the silanol groups of the silane resulting in a covalent bond between the silane and the silica surface. If the condensation reaction is successful, the silica surfaces "loses" a silanol group. By substituting a silanol group with a silane molecule, a potentially chargeable surface group is replaced by a non-chargeable group, assuming that the silane does not contain chargeable groups. This allows for examination of the successfulness and the tunability of the silane-silica reaction by zeta potential measurements at a pH where the silanol groups are significantly charged. The more surface silanol groups are substituted for silane molecules, the less silanol groups are present that can be charged upon protonation or dissociation, and thus the lower the absolute value of the zeta potential.

When the zeta potential is measured at a pH far above the isoelectric point the remaining silanol groups are negatively charged. The more silane has reacted with the silica surface, the more silanol groups are lost, and the less negative the zeta potential will be. However, this does not have to hold for trifunctional silanes. In theory all the three silanol groups formed upon hydrolyzation of the alkoxy groups can condensate with the silica surface. This enables three types of binding, provided that the silane reacts with the silica surface. In case there is no condensation reaction between the silane silanol groups and the silanol group present on the silica surface the number of chargeable silanol groups on the surface does not change, see Figure 19a. The surface charge and thereby the zeta potential will not change if no reaction took place. If all the three silanol groups react with the silica surface the number of chargeable silanol groups is significantly reduced, resulting in a small absolute value of the zeta potential as depicted in Figure 19b. When two of the three hydrolyzed alkoxy groups condensate with the silica surface, see Figure 19c, this also reduces the number of silanol group. However, this reduction is less compared to the situation where all three hydrolyzed groups react with the surface, giving rise to an intermediate absolute value of the zeta potential. The last proposed situation is that of one hydrolyzed alkoxy group bound to the silica surface as shown in Figure 19d. On the same footing, the absolute value of the zeta potential will now increase as there are more chargeable silanol groups. Hence, both an increase and decrease can indicate that the surface reaction was successful.

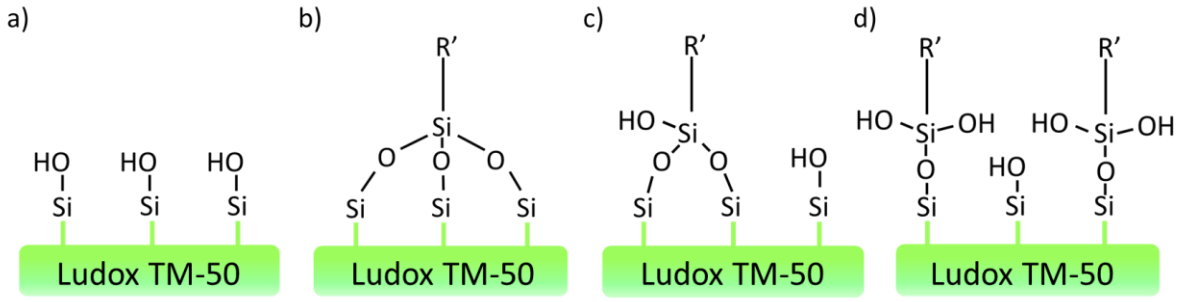

Figure 19 Different possible types of binding between a trifunctional silane and the silica surface. a) Silica surface without silane functionalization. b) Situation where all hydrolyzed alkoxy groups have condensed with the silica surface. c) Silica surface with a trifunctional silane of which two silane silanol groups have reacted with the surface. d) Trifunctional silane that has formed one bond with the silica surface.

Chapter 3

3-(Trimethoxysilyl)propyl methacrylate

The first silane that we investigated in this work is 3-(trimethoxysilyl)propyl methacrylate. As mentioned in the introduction, previous research by Boakye Ansah et al. (9) has shown that temporally stable bijels could be formed using silica nanoparticles functionalized with 3-(trimethoxysilyl)propyl acrylate as the stabilizing nanoparticles. They produced bijels with a relatively large pore size, around 10 µm, using a ternary comprising ethanol, BDA and water (9). When using CTAB to modify the silica nanoparticle wettability and a ternary mixture consisting of 1-propanol, DEP and water bijels can be synthesized with pore sizes below 500 nm as shown by Khan & Sprockel et al. (6). As a starting point for possibly synthesizing such "small domain" bijels without the usage of surfactants we researched the ability of 3-trimethoxy propyl methacrylate as functional group to adjust the silica nanoparticle wettability. 3-(Trimethoxysilyl)propyl methacrylate is chemically comparable to 3-(trimethoxysilyl)propyl acrylate as they only differ one methyl group, see Figure 20. Previous research has shown that the acrylate-functionalization can offer the right wettability properties for the formation of bijels with domain sizes of a couple of µm using a BDA/water/1-propanol system. Possibly, this might also be the case for the bijels with sub-micrometer sized domains that are formed using the water/DEP/1-propanol system. In this chapter the experimental approach for the surface modification with 3-(trimethoxysilyl)propyl methacrylate (TMSPM) will be discussed. The bond formation between the TMSPM functional group and the silica surface is examined with transmission Fourier Transform Infrared spectroscopy (FTIR) and zeta potential measurements. The effect on the surface hydrophobicity is explored by measuring the three-phase contact angle. The results of these studies will be discussed in Section 3.2. Additionally, the ability of the particles to disperse in a water/DEP/1-propanol precursor mixture and the outcoming structures will be discussed in Section 3.3.

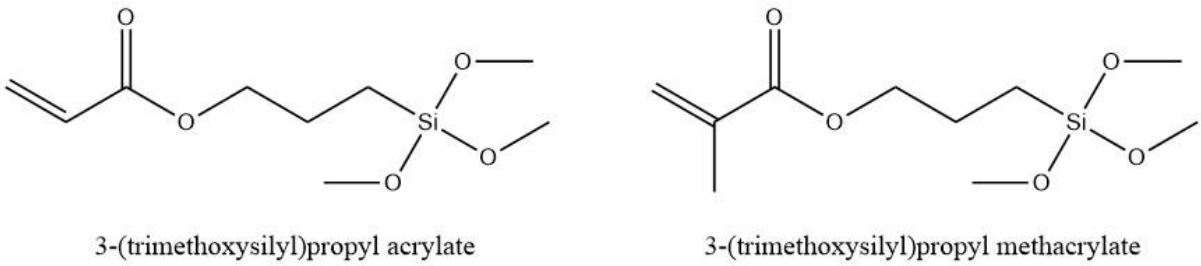

Figure 20 The chemical structures of 3-(trimethoxysilyl)propyl acrylate and 3-(trimethoxysilyl)propyl methacrylate.

3.1 Functionalization of SiO_2 nanoparticles with 3-(trimethoxysilyl)propyl methacrylate

The experimental approach used for the functionalization is based on the method reported by Boakye-Ansah et al. (9). In this method a silica dispersion is made from 33.3 v/v deionized water, 33.3 v/v acetic acid, 38.1 v/v ethanol and 9.5 v/v Ludox TMA silica nanoparticles. Subsequently, the dispersion is heated to 70 degrees Celsius, nitrogen is bubbled through, and 3-(trimethoxysilyl)-propyl acrylate is added. The functionalized particles were washed three times with deionized (DI) water and subsequently redispersed in ethanol. To completely remove the residual water dialysis was performed in ethanol (9). As we aim to implement the functionalized particles in the water/DEP/1-propanol precursor mixture, slight adjustments were made to the method described above. Instead of ethanol the particles were redispersed in 1-propanol. Additionally, a washing step with 1-propanol was added. The detailed description of the performed functionalization method is given in Section 3.1.2, and a schematical overview is given in Figure 21.

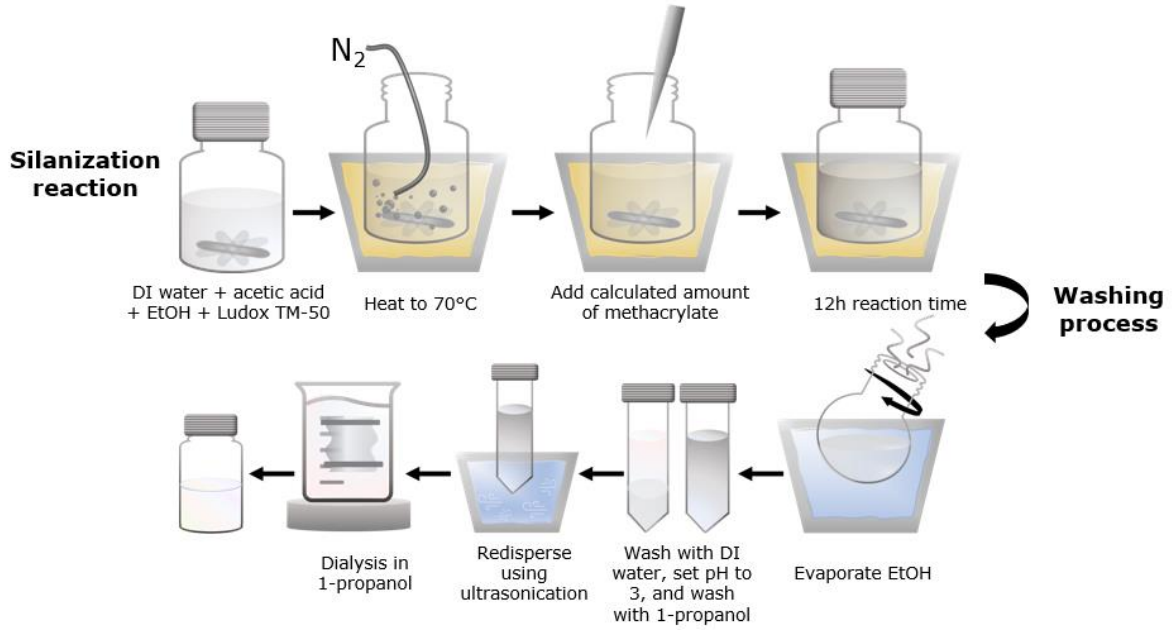

Figure 21

Figure 21 Schematical overview of the experimental method for the functionalization of Ludox TM-50 with 3-(trimethoxysilyl)propyl methacrylate. The silica dispersion consisting of deionized water, ethanol, acetic acid and Ludox TM-50 is heated to 70°C. To prevent polymerization of the methacrylate N_2 is bubbled through before adding the methacrylate. After 12 hours of reaction time the ethanol is removed, the particles are washed and the pH is set. Lastly, the particles are redispersed in 1-propanol and a dialysis is carried out.

3.1.1 Chemicals

All chemicals used in this part of the work is tabled in Table 1. The water used in this work is purified before use by the Millipore Synergy purification system and has a resistivity of 18.2 MΩcm at 25°C. From now on, the purified water will be referred to as MilliQ water.

Table 1 Used chemicals with their purity, application and supplier.

Name	Purity	Application	Supplier
Ethanol, EtOH	Absolute for analysis, 100%	Solvent	Merck
Acetic acid (glacial)	Anhydrous for analysis, 100%	Acid	Merck
Ludox® TM-50	50 wt.% in H_2O	Silica nanoparticles	Sigma Aldrich
3-(Trimethoxysilyl)propyl methacrylate, TMSPM	98%	Silane	Sigma Aldrich
Sodium hydroxide, NaOH	99%	Base	Merck
1-Propanol	99.5%	Solvent	Sigma Aldrich
Diethyl phthalate, DEP	99%	Oil	ThermoFischer
Glycerol	>99%	Optical transparency	Thermo Scientific
Toluene	>99%	Continuous phase	Thermo Sienctific
n-Hexane	HPLC grade	Optical imaging	Biosolve
Nile red	Microscopy grade	Fluorescent dye	Sigma Aldrich
Potassium bromide, KBr	IR grade, >99%	IR pellets	Acros Organics

3.1.2 Experimental method functionalization

A silica nanoparticle dispersion was made by mixing 160 mL MilliQ water, 80 mL acetic acid, 160 mL ethanol and 20 mL Ludox TM-50. The dispersion was placed in a preheated oil bath of 70 degrees Celsius under continuous stirring and nitrogen was bubbled through for approximately 10 minutes to remove the oxygen from the dispersion. The calculated amount of TMSPM for the desired degree of functionalization was added to the dispersion which was left overnight to react. For a methacrylate density of 60%, 80% and 100% the corresponding amounts of TMSPM are given in Table 2. After 16 hours the dispersion was removed from the oil bath and the ethanol was evaporated using a Hei-VAP core rotary evaporator by Heidolph® at a bath temperature of 60 degrees Celsius, rotation of 250 rpm and a setpoint pressure of 250 mbar. After 50 minutes most of the ethanol was removed, resulting in an opaque dispersion which might indicate that the silica nanoparticles became relatively hydrophobic by the functionalization as the particles show not to be stable in water. The nanoparticles were washed two consecutive times. Each washing step consist of adding approximately 200 mL of MilliQ water, centrifugation using a Beckman Coulter Allegra® X-12R centrifuge at 3750 rpm until a clear supernatant was obtained and subsequent redispersion of the white sediment by vortex mixing (Scientific Industries Vortex-Genie 2) and ultrasonication (Branson 1800). Next the pH of the silica nanoparticles is conditioned by adding 1M NaOH until a pH of 3 is reached. Subsequently the dispersion is washed once more, and the supernatant is decanted. To the white sediment 1-propanol is added. Vortex mixing and ultrasonication is used to redisperse the particles. Upon redispersing the dispersion becomes less opaque. Once completely redispersed a dialysis was performed in 1-propanol overnight to remove residual water from the dispersion using the Spectra/Por® 4 dialysis membrane. For the 80% and 100% TMSPM covered particles an extra washing step with 1-propanol was performed prior to completely redispersing the particles and the dialysis. To the 60% covered particles 1-propanol was added and the particles were redispersed using ultrasonication and vortex mixing after the dialysis. To remove any aggregates in the dispersions, all three the dispersions were subjected to 10 minutes of centrifugation at 3750 rpm.

Table 2 Amounts of TMSPM added during the functionalization to obtain 60%, 80%, and 100% TMSPM covered particles together with the particle weight fraction of the obtained dispersions.

Degree of functionalization (%)	Amount of added TMSPM (mL)	Particle weight fraction (w%)
60	1.86	33
80	2.48	34
100	3.10	32

As we want to have an indication on how many particles are added to a ternary system it is important to know the amount of particles in the obtained dispersion. For the determination of the weight fraction of the obtained dispersion the mass of 200 uL of dispersion was determined. Subsequently the solvent was evaporated, and the mass of the dry nanoparticles was determined.

3.1.3 Sample preparation DLS and zeta potential measurements

For the dynamic light scattering (DLS) and zeta potential measurements the samples were prepared by adding two drops of particle dispersion to about 10 mL of MilliQ water at pH 9. The pH of the diluted particle dispersion in water was brought up to 10 by adding 1M NaOH. Overnight equilibration caused the pH to shift to values close to 9. Before the measurement the pH was brought up to 10 again using a 0.1M NaOH solution. Any formed aggregates were removed by centrifugation for 4 min at 14500 rpm before the measurement. Each sample was measured using a folded capillary (DTS1070). Both the zeta potential measurement and the DLS measurement were repeated thrice for each sample.

3.1.4 Sample preparation transmission FTIR using KBr pellets

To measure the transmission infrared spectra of the functionalized particles the dispersions were first dried overnight at 60°C. For each sample 250 mg of potassium bromide (KBr) was measured on a scale. To this 1-2.5 mg of dried particles was added per sample. The mixture of KBr and particles

was left overnight to dry at 60°C. After drying the mixture was pressed into a transparent pellet using a hydraulic press. For each sample three transmission FTIR spectra were collected with the KBr pellet FT-IR spectrometer (PerkinElmer). The wavelength range for each spectrum was set to 4000 cm^{-1} to 400 cm^{-1} with a resolution of 4 cm^{-1}. For each sample the three collected spectra were averaged by taking the average value of the transmission at each wavelength. The average spectra were integrated, and the transmission values were divided by the integration area to plot the spectra in one figure.

3.1.5 Spin coating procedure for contact angle measurements

To be able to measure the contact angle of the functionalized particles, a uniform layer of particles is needed. Therefore, we developed an experimental setup that allows us to spin-coat microscope slides with a thin film of particle dispersion. A microscope slide holder was designed in Autodesk Inventor Professional 2023. The design was inspired by so-called spin coater "chucks" (39). These chucks are commercially available for vacuum-free spin coaters. Generally, spin coaters secure the substrate by using vacuum, which can negatively influence the uniformity of the film. To circumvent this, Ossila® invented a top unit that can be placed on top of a vacuum-based spin coater, keeping the substrate mechanically in position. In this way, no vacuum is required for the spin coating procedure (40). We reproduced such a vacuum-free spin coating setup by attaching a 3D-printed microscope slide holder to a motor, see Figure 22. The slits allow for removal of the excess particle dispersion and the dimensions were chosen such that the microscope slide fits tightly in the holder, keeping it in place while spinning. The spin coating procedure was inspired by the procedures used by Zhou & He (41) and Brassard et al. (42). We used 5 w% dilutions of the particle dispersions. Before spin coating the diluted dispersion onto the microscope slide, the dispersion was subjected to centrifugation for 2 minutes at 14500 rpm to remove aggregates. The presence of aggregates in the sample might induce extra surface roughness. This can result in misinterpretation of the hydrophobicity of the film. On each glass slide 100 uL of 5 w% dispersion was added while the slide was spun at 1000 rpm, as depicted in Figure 22a. The spinning was kept at 1000 rpm for approximately 40 seconds. After 40 seconds the motor was turned off and the speed decreased rapidly to zero. By eye one could see a glossy, transparent layer on top of the microscope slide. To completely dry the film the slide was placed in the oven for at least 1 hour at 60 degrees Celsius. To be able to measure the three-phase contact angle between particles, water and DEP, mimicking the bijel system, a glass container is used such that water can be applied as ambient phase, see Figure 22b. For the coated glass slide to fit in the container the edges of the slide must be broken off. To neatly break the glass slide a diamond scribing pen was used. By breaking off the edges of the slide the best part of the coating was preserved.

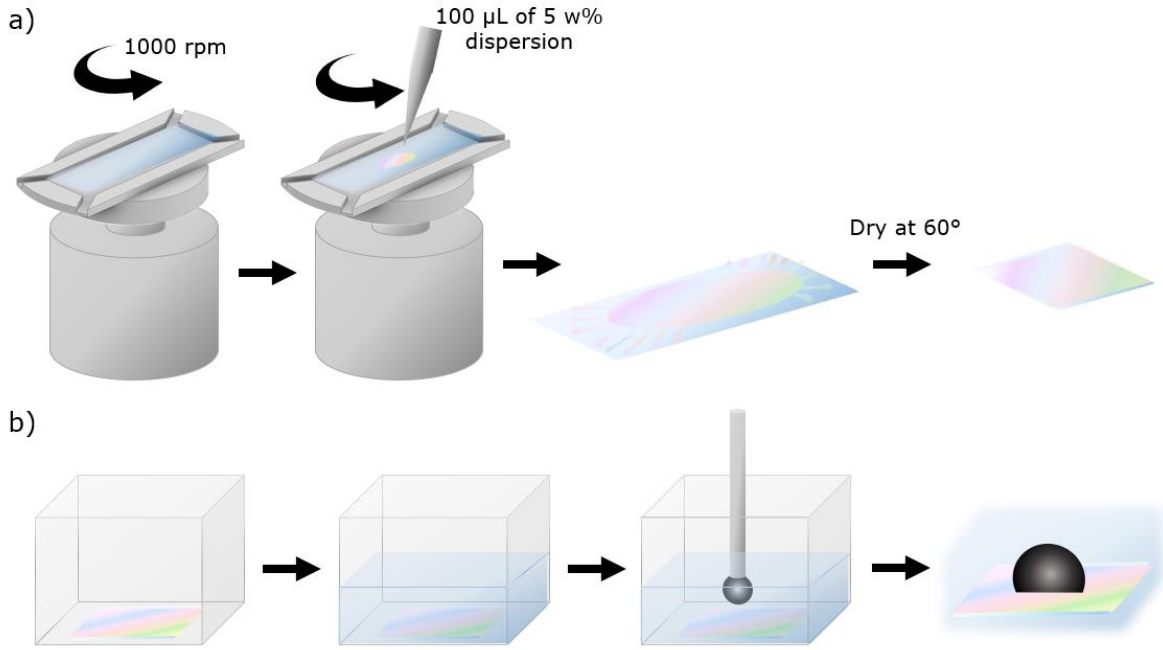

Figure 22 a) The spin coating procedure. A microscope slide is placed in the 3D-printed holder and spun at 1000 rpm. 100 uL of 5 w% dispersion is rapidly added in the middle of the spinning slide, and left to spin at 1000 rpm for approximately 40 seconds. The coating is then dried at 60°C. To ensure that the slide fits in the sample container the edges of the slide, where the coating is incomplete, are broken off. b) Sample container used in three-phase contact angle measurements. After the slide is placed in the container it is filled with deionized water. Via a needle a drop of DEP is dispensed on the coated slide.

3.2 Results and discussion

The particles with a methacrylate surface coverage of 60% appeared to be dried out after the dialysis. Presumably the sediment contained a significant amount of water. The dialysis membranes are permeable for water but 1-propanol cannot migrate into the dispersion via the membrane. Therefore, if there is a significant amount of water present in the dispersion this can cause all the water to migrate into the dialysis bath resulting in dry particles. To avoid this the particles can be washed with 1-propanol prior to completely redispersing them and performing the dialysis. To obtain the weight fraction the mass of the dried nanoparticles is divided by the mass of the dispersion. Ideally, the dispersion should have a nanoparticle weight fraction around 30-35%. The calculated weight fractions for the different methacrylate densities are given in Table 2. Before implementing the functionalized particles in a water/DEP/1-propanol precursor mixture for the formation of bijels, it is insightful to verify whether the reaction was successful. In this thesis three main particle characteristics are examined to gain insight in the successfulness of the functionalization reaction: their FTIR-spectra, zeta potential, and three-phase contact angle with water and DEP.

3.2.1 Determining the presence of TMSPM functional groups using FTIR

By functionalizing the silica nanoparticles with organosilanes like 3-(trimethoxysilyl)propyl methacrylate, amongst others, hydrocarbon groups are introduced in the chemical composition of the particles. The presence of hydrocarbons and other functional groups introduce peaks at absorption values different from the absorption values of characteristic peaks of silica. The FTIR-spectrum of pure silica has six distinct typical vibrations which are tabled in Table 3. The appearance of peaks at 2950 cm^{-1}, 1400-1300 cm^{-1} and 780 cm^{-1} indicate the presence of CH_2 and CH_3 groups as these peaks correspond to the different stretching modes (symmetric, asymmetric and scissor-like) of the hydrocarbon groups (43). Besides the hydrocarbon groups, there is also a carbonyl group introduced when the silica surface has reacted with TMSPM. The carbonyl species axial deformation gives rise to a band at 1716 cm^{-1} (43). For TMSPM-functionalized silica nanoparticles it is thus

expected to observe peaks at 2950 cm^{-1}, 1400-1300 cm^{-1}. 780 cm^{-1} and 1716 cm^{-1}. The presence of these peaks can confirm that part of the surface -OH groups are replaced by 3-trimethoxy propyl methacrylate groups whereas absence of these peaks indicate that the reaction was not successful.

Table 3 The six characteristic FTIR peaks for pure silica.

Wavenumber (cm^{-1})	Species
3390	Si-OH (44)
1630	Si-OH (45)
1130-1000	Si-O-Si (44)
950-810	Si-OH (44)
800	Si-O-Si (45)
460	Si-O-Si (45)

The FTIR spectra of the TMSPM functionalized particles are plotted with an offset in Figure 23. The spectrum of the Ludox TM-50 serves as reference spectra. Here, the Si-O-Si bands and two of the three Si-OH bands are clearly visible. The band at 950-810 cm^{-1}, expected for the Ludox TM-50 silica nanoparticles, could not be detected in the obtained spectra. This band likely overlaps with the Si-O-Si band at 1113 cm^{-1}. The peaks present in the FTIR spectra of the DTES functionalized particles are tabled in Table 4. Compared to the spectrum of Ludox TM-50, the spectra of the TMSPM-functionalized silica have a peak around 1710 cm^{-1}. As discussed above, this peak can be attributed to the presence of the C=O group (43). Wang et al. (26) also observed that when silica nanoparticles are functionalized with 3-methacryloxypropyltrimethoxyl silane, another name for TMSPM, a peak arises around 1717 cm^{-1}, and ascribed this to the carbonyl stretching mode (26). The presence of this band in the FTIR spectra indicates that there is TMSPM bound to the silica surface.

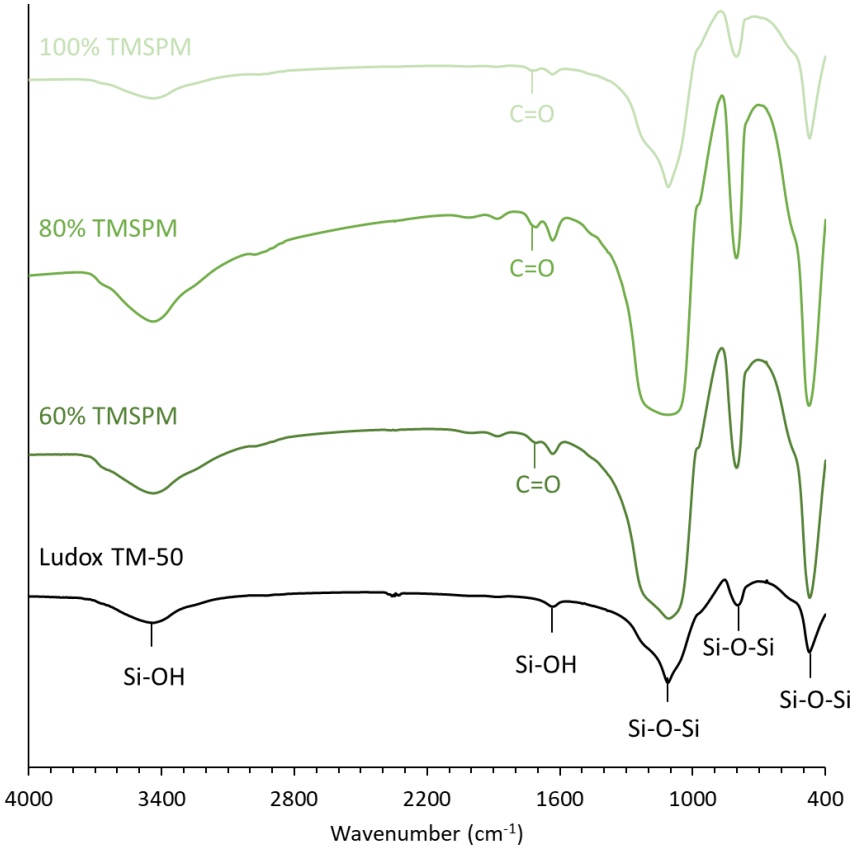

Figure 23 The average FTIR spectra of Ludox TM-50 and the TMSPM-functionalized Ludox TM-50. The spectra are plotted with an offset. The presence of the peak around 1710 cm^{-1} indicates the presence of a carbonyl group, and thus the presence of TMSPM at the silica surface.

Table 4 Overview of FTIR bands observable in spectra of TMSPM functionalized particles.

Wavenumber (cm^{-1})	Species	Appearance
3437	Si-OH	Broad
1720-1707	C=O	Weak
1632	Si-OH	Weak
1113	Si-O-Si	Strong
797	Si-O-Si	Medium
473	Si-O-Si	Strong

Whether or not there is TMSPM present at the surface is not the only information that can be deduced from the FTIR spectra. Upon binding of the TMSPM functional group to the silica surface a surface silanol group is replaced by the functional group. When more TMSPM has reacted with the surface, this should result in less remaining silanol groups. An indication of the relative change in the amount of silanol groups present can be obtained by looking at the Si-OH/Si-O-Si peak ratio. A back of the envelope calculation of the ratio of total surface silanol groups versus the Si-O-Si groups present at the interior of a silica nanoparticle gives a value of 0.048. This value indicates that the number of Si-O-Si groups is more than 20 times as large as the total number of silanol groups at the surface. When part of the surface silanol groups are replaced by a functional group, this will have little effect on the number of Si-O-Si group present. Hence, the Si-O-Si band can be used as internal standard. According to Kulkarni et al. (46) the characteristic, low frequency Si-O bands indeed do not vary with silanization of the surface. Both Kulkarni et al. (46) and Wagh et al. (45) observed a decrease in the intensity of the OH band at 3400 cm^{-1} as a result of trifunctional silane surface modification. The Si-OH/Si-O-Si ratio is determined by dividing the area of the Si-OH band at 3437 cm^{-1} by the area of the Si-O-Si band at 473 cm^{-1}. The areas are determined by standard PerkinElmer software. For the Si-OH band the area between 3780 cm^{-1} and 3100 cm^{-1} is taken in each original spectrum. For the Si-O-Si band the area is defined between 525 cm^{-1} and 400 cm^{-1} in the initial spectrum. For each individual spectrum the peak ratio is calculated. The average ratio for each degree of functionalization is calculated form the peak ratios of the three corresponding spectra, and are shown in Figure 24.

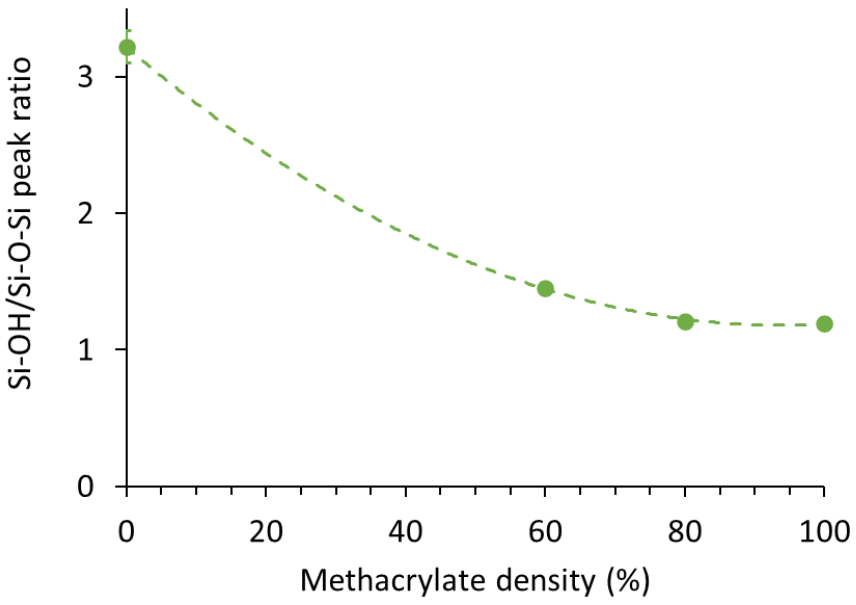

Figure 24 The average ratio between the area of the Si-OH band and the Si-O-Si band for the different degrees of functionalization. The error bars indicate the standard deviation in the data. For the TMSPM functionalized particles the standard deviation is too small to be observable in the graph. A second order polynomial trendline was added which has a R^2 value of 0.9999.

Figure 24 shows that for the TMSPM functionalized particles the Si-OH/Si-O-Si ratio is lower compared to the non-functionalized Ludox TM-50. This indicates that silanol groups are lost after the reaction with TMSPM, reinforcing the idea that the functionalization reaction took place and that the TMSPM has condensed with the silica surface. The peak ratio seems to decrease with increasing TMSPM surface coverage, but the differences are rather small. Moreover, we have only looked at three different degrees of functionalization. Therefore, one cannot deduce a clear trend. To further examine the successfulness of the reaction the zeta potential was measured.

3.2.2 Change in surface charge examined by zeta potential measurements

In this work the Malvern Zetasizer Ultra is used to measure the zeta potential via electrophoretic light scattering (ELS). In ELS light scattering and electrophoresis are combined in order to evaluate the electrophoretic mobility μ of dispersed particles which is subsequently used to determine the zeta potential. This measurement is carried out in a sample cell that contains two electrodes. Upon applying an electrical field the present charged particles will move towards the electrode with opposite charge. The velocity of the migration depends on the charge of the particle and determines the electrophoretic mobility that is measured (47). For the determination of the electrophoretic mobility a laser beam is split in two. One beam serves as reference beam and the other beam irradiates the sample. The particles present in the dispersion scatter the light of the laser beam that passes through the sample. This scattered light is detected under a low angle. Before detection the two beams are combined. As a consequence of the electrophoretic movement of the particles the frequency of the scattered light beam is changed. Hence, combining the two beams results in optical beat interference, which allows for calculating electrophoretic velocity and mobility (36).

In this thesis we work with Ludox TM-50 silica nanoparticles. As beforementioned in Section 2.5 the isoelectric point is of importance when considering the charge of silanol groups. Therefore, the zeta potential was measured as a function of the pH using the titrator unit of the Malvern zetasizer. The measurement was performed by Alessio Sprockel. In the measurement the zeta potential is measured at different pH values, starting at pH 9.9 going to pH 1.1. The resulting zeta potential curve is given in Figure 25. Here, it can be observed that the zeta potential is negative for pH values between 1.6 and 9.9. The values obtained for pH close to 1 vary significantly, indicating that the particles are no longer stable. Whether the zeta potential crosses the 0 mV at pH 1.1 cannot be said. Presumably, the isoelectric point of the Ludox TM-50 particles is close to pH 1. The zeta potential decreases from -4.5 mV at pH 1.6 to -42 mV at pH 8. For pH values above 8 the zeta potential remains rather constant, indicating there is no change in the charge of the silanol groups. When measuring the zeta potential at pH 10 it can thus be assumed that all the silanol groups are charged.

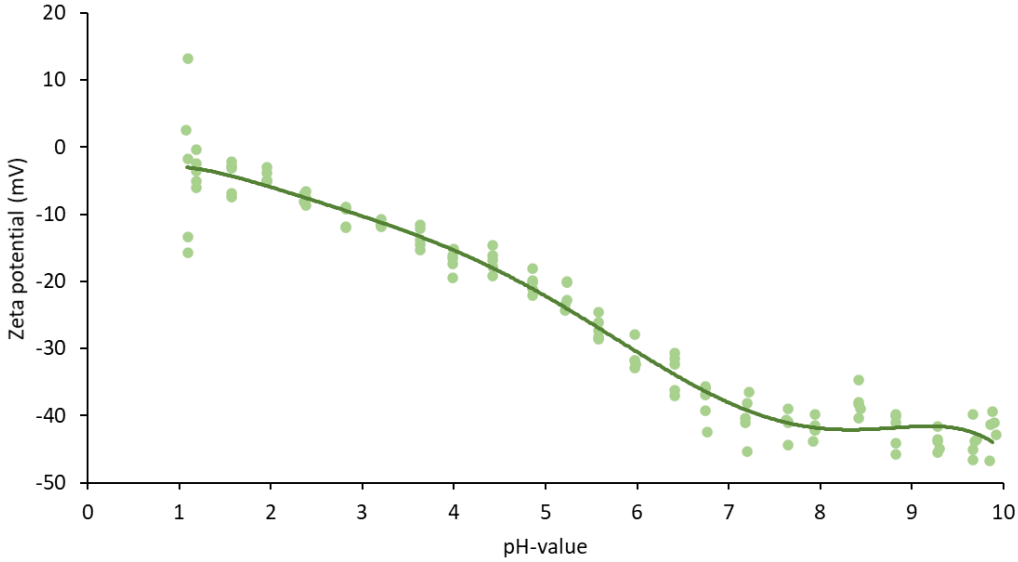

Figure 25 The zeta potential of Ludox TM-50 particles as a function of the pH. Over the complete pH range, going from 1.1. to 9.9 the zeta potential is negative. The isoelectric point of the Ludox TM-50 particles is thus below pH 1.1

The average of the three zeta potential measurements is given in Figure 26. Figure 26a shows the distribution of the zeta potential for Ludox TM-50 and the TMSPM functionalized particles. The distributions of Ludox TM-50, 60% TMSPM and 80% TMSPM are rather broad and overlap significantly. The broadness suggests that there are particles with different surface charges present in the sample. The charge of the particles is thus not uniform across the sample. The zeta potential distribution of the 100% TMSPM is notably sharper and shifted to smaller absolute values. The 100% TMSPM particles are thus more uniformly charged and this charge is smaller compared to the other particles. Figure 26b shows the average value of the zeta potential together with the standard deviation in the measurements. The zeta potentials of 60% and 80%TMSPM functionalized particles show no significant increase nor a significant decrease as can be observed in Figure 26b. The zeta potentials remained close to -39.6 mV, the value measured for pure Ludox TM-50 particles in water at pH 10, for both functionalization densities. The absolute zeta potential does decrease for the 100% TMSPM particles. The absence of a significant change in zeta potential for the 60% and 80% surface coverages can indicate that the surface silanol groups of Ludox TM-50 were not replaced by the functional silane in the reaction, suggesting that the reaction was not successful for these methacrylate densities. Perhaps the concentrations used for these functionalizations are too low because the 100% TMSPM does show an altered zeta potential. However, it is crucial to first look at the size distribution.

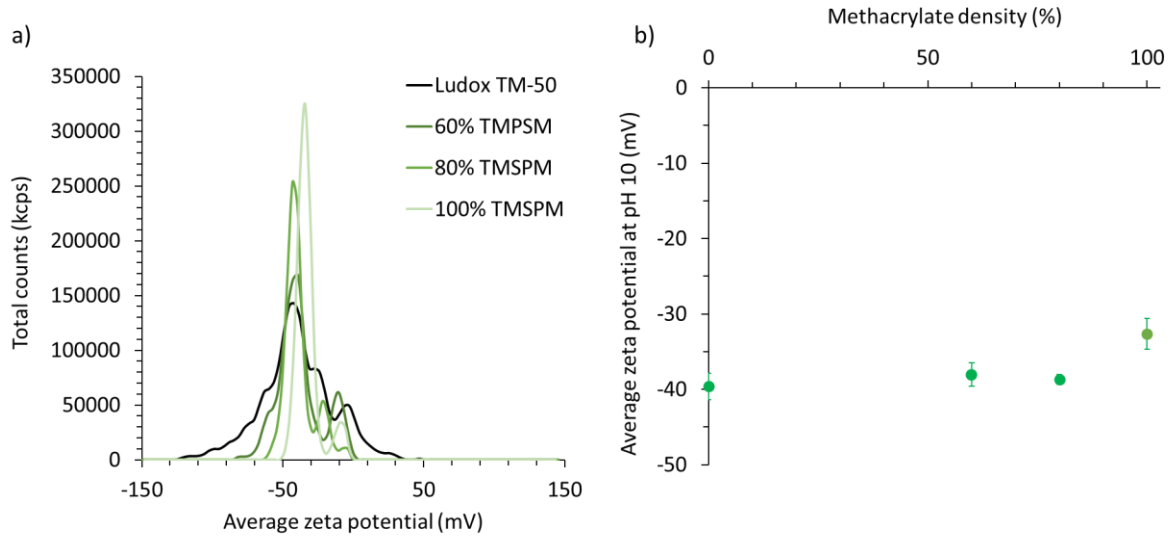

Figure 26 Zeta potential results. a) Average zeta potential distribution. b) Average zeta potential for the different degrees of functionalization. The error bars represent the standard deviation in the data.

Subsequently to the zeta potential measurements the size was measured using the DLS option of the Malvern Ultra Zetasizer. In DLS the particle size is measured by irradiating a sample with a laser beam. The particles present in the sample exhibit Brownian motion and scatter the incident light. The Brownian motion causes the local particle density to fluctuate and thereby gives rise to fluctuations in the intensity of the scattered laser light. Analyzation of the intensity fluctuations yields the diffusion constant. From the diffusion constant the hydrodynamic radius R_h can be deduced making use of the Einstein-Stoke relation (48),

$$R_h = \frac{k_b T}{6\pi\eta D} \qquad (11)$$

Here, D is the translational diffusion coefficient in m^2s^{-1}, η is the viscosity in Pa·s, and k_bT the thermal energy in J.

It is important to know whether the particles are significantly aggregated. If so, the obtained value for the zeta potential might not be representative for the individual particles. Besides that, the

aggregation behavior can give insight into the particle stability. The more prone to aggregation, the less stable the particles are in dispersion. Figure 27a shows the volume-weighted average size distribution. What stands out is that the higher the surface coverage, the broader the size distribution becomes. Especially for the 80% and 100% methacrylate density. Here, multiple size populations are present, indicating that the particles have aggregated. Figure 27b gives the average size for the different surface coverages. The average size clearly increases with increasing surface coverage. For the 100% TMSPM the size has increased by a factor of four. The zeta potential measured for this functionalization might thus not represent the zeta potential for the individual particles. Based on the zeta potential and DLS measurements it is difficult to conclude whether the surface reaction was successful. The aggregation behavior of the particles has changed, which can be a result of the surface modification. However, the Ludox TM-50 particles also tend to aggregate without modification of the surface. Thus, aggregation does not necessarily indicate that the surface is modified. The change in zeta potential for the 100% TMSPM can also be due to the particles being present in the aggregated form, and thus also not have to indicate a successful surface modification.

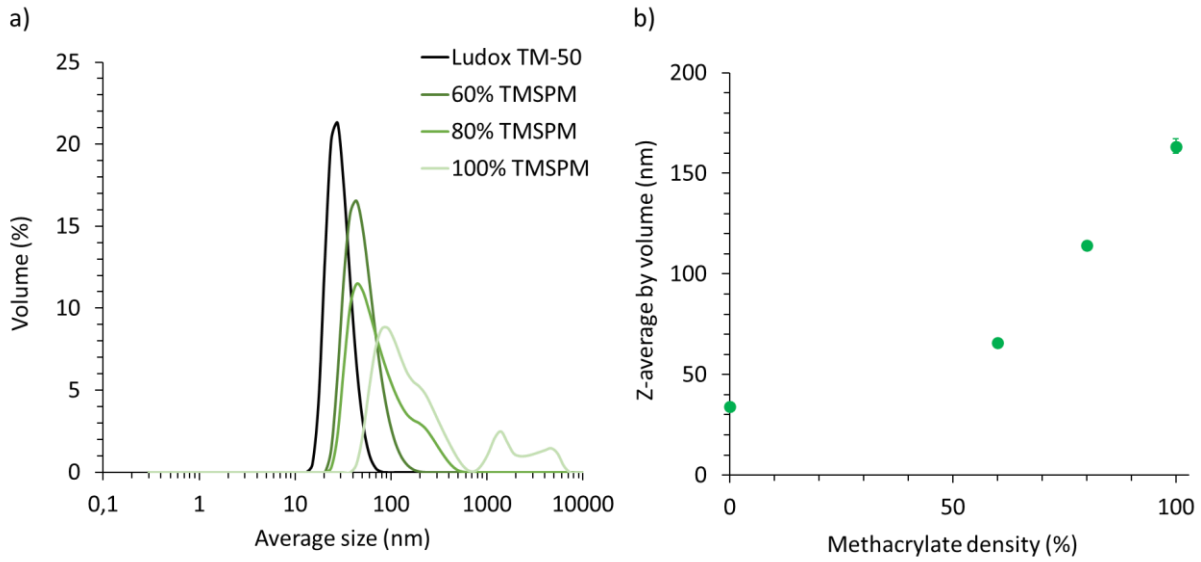

Figure 27 DLS results. a) Average size distribution by volume. b) Average size for the different degrees of functionalization. The error bars indicate the standard deviation in the data.

3.2.3 Influence on the wettability studied by the three-phase contact angle

When the particles are sufficiently functionalized this should alter the surface hydrophobicity. Hence, measuring the contact angle can give insight into the extent of the functionalization reaction. First, a study was done to verify whether the spin coating method is sufficient to coat a glass slide with a uniform layer of nanoparticles. Only if the layer is uniform the three-phase contact angle between two liquids and the functionalized particles can be measured. To verify the uniformity of the coating, two different type of glass slides were used, the more hydrophilic microscope slides and the more hydrophobic cover slips. Figure 28 depicts the differences in the hydrophobicity when a droplet of water is added on the two different glass slides.

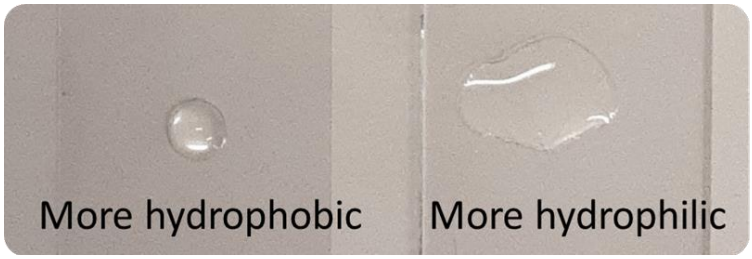

Figure 28 The more hydrophobic cover slip and more hydrophilic microscope slide. The water droplet on the more hydrophobic cover slip remains in a droplet shape and does not wet the surface very well. On the other hand, the water droplet on the more hydrophilic microscope slide wets the surface well.

For both type of slides the three-phase contact angle that it forms with DEP and water was measured by adding a droplet of DEP on the slides while they are submerged in water, as depicted in Figure 22b. Per slide four droplets of DEP were deposited and measured unless specified otherwise. For each droplet measured in this work 100 contact angle measurement runs are done using the Optical Contact Angle (OCA) meter with SCA20 software. This software measures the contact angle via the droplet phase, in this case the DEP. Convention in the field of contact angles is to measure the contact angle via the water phase. Assuming a straight baseline the values given by the SCA20 software can be translated to contact angles measured through the water phase via

$$180° - \theta measured\ through\ oil\ phase\ =\ \theta measured\ through\ water\ phase \qquad (12)$$

A schematical overview of the situation is given in Figure 29. Experiments performed by Dominique Thies-Weesie indeed suggest that contact angles measured with water as the drop phase and DEP as the ambient phase give similar results as the ones obtained by translating the contact angle measured via the oil phase to contact angles measured through the water phase for DEP as the drop phase and water as the ambient phase. Even if the values differ slightly, this should not influence the trend that is obtained. In addition, the conclusions on the hydrophobicity or hydrophilicity of the particles is not affected by translating the contact angels according to Equation 12. If the contact angle measured through the oil phase is >90° the surface is hydrophilic. The translated contact angle through the water phase will be <90° and thus also indicates that the surface is hydrophilic.

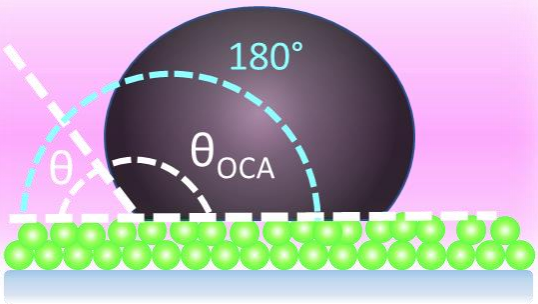

Figure 29 Schematical overview of a contact angle measurement. θ_{OCA} is the contact angle measured by the SCA20 software if DEP is used as the drop phase. Convention is to measure the contact angle through the water phase. Assuming the baseline is straight, the θ_{OCA} can be translated to θ through the water phase via Equation 12.

Equation 12 is used to translate all the contact angle values measured by the SCA20 software. The average contact angle and standard deviation is calculated using Excel. The resulting average values for the contact angle are 35°±5° and 58°±1° for the more hydrophilic slide and the more hydrophobic slide, respectively. The obtained droplet shapes are shown in the top figure of Figure 30. When both slides are now covered with a diluted particle dispersion, the contact angle measured for both slides should be determined by the hydrophobicity of the particles and thus be similar. To

verify this, a microscope slide and cover slip were spin coated with 5w% of 80% TMSPM covered Ludox TM-50 particles. For each slide three droplets were measured. The obtained droplet shapes are depicted in the bottom figure in Figure 30. The average contact angle of the more hydrophilic microscope slide spin coated with 80% TMSPM covered silica nanoparticles was 43°±0.5°. For the more hydrophobic cover slip the corresponding contact angle was 49°±3°. These obtained values are similar, suggesting that the particles indeed dictate the measured contact angle.

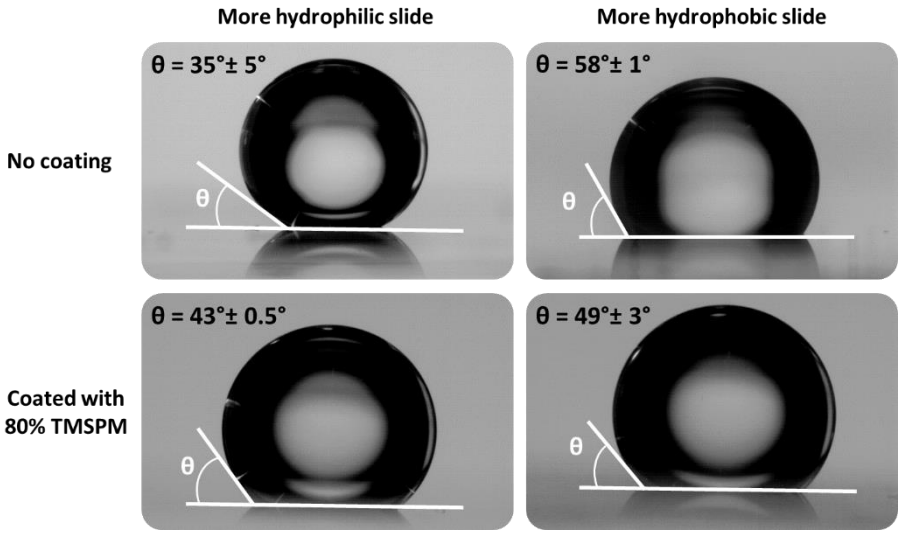

Figure 30 Contact angle measurements using more hydrophilic and more hydrophobic slides. The top figures give the droplet shapes obtained for the uncoated slides. The bottom figures give the droplet shapes obtained for the 80% TMSPM silica nanoparticle coating. The value in the top left of each figure is the average value of the contact angle with the standard deviation.

Complementary to this study Scanning Electron Microscopy (SEM) was used to visualize the coating formed upon spin coating. For this a microscope slide was broken into small pieces before spin coating it with 80% TMSPM covered silica nanoparticles. In this way a small piece of coated microscope slide could be obtained without having to perform pressure onto the coating after it has been spin coated. This piece was placed on a SEM specimen stub. Subsequently, the surface was sputter coated with 8 nm of platinum using the Cressington® Sputter Coater 208 HR. The SEM images were collected using the Zeiss EVO high resolution SEM operated by Dominique Thies-Weesie. Figure 31 shows SEM images of the coating. The coating appears to be rather uniform. The larger irregularities that can be observed are likely dust particles. The inset shows a magnification of the area marked by the grey rectangle. Here, small cracks are visible in the coating. These cracks appear not to completely penetrate through the depth of the coating, indicating that there are particles present along the entire surface of the coating. Besides the cracks, the inset also shows how uniform the remainder of the coating is. Together with the similarity in the contact angle for more hydrophilic and more hydrophobic slides the SEM images led to the conclusion that the coating is uniform and allows for measuring the three-phase contact angle with the functionalized particles.

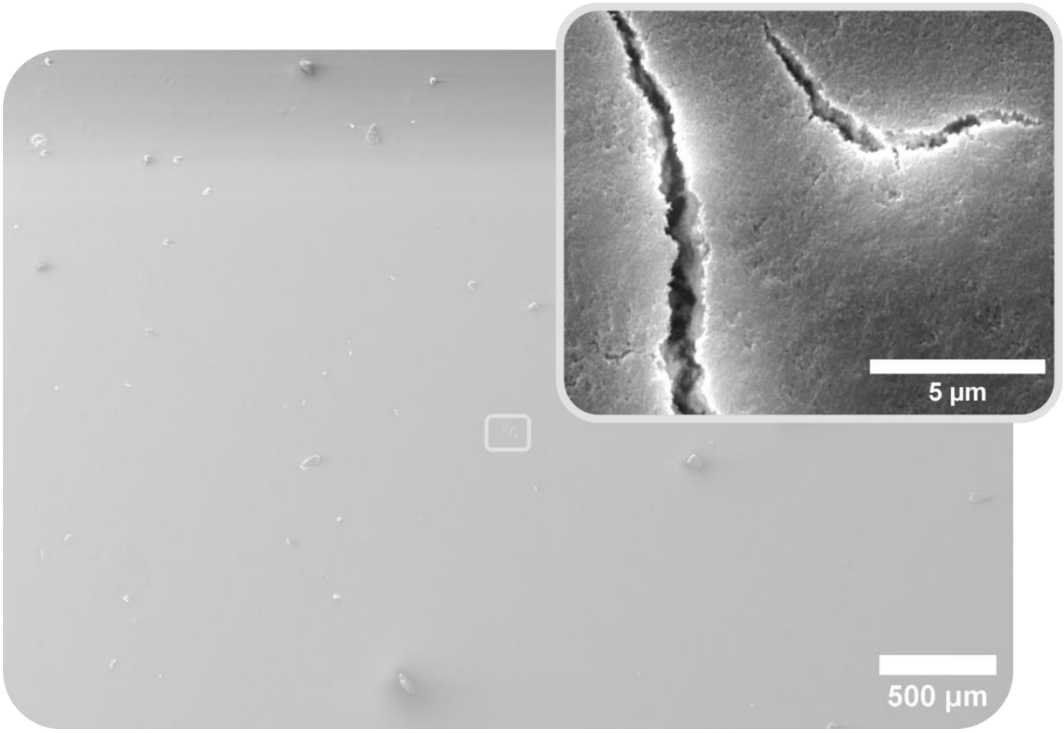

Figure 31 SEM images of a glass slide coated with the 80% TMSPM covered Ludox TM-50 particles. The coating appears to be rather uniform. The inset shows a magnification of a defect. The cracks are only present at the surface, meaning that over the total width of the coating particles are present.

Now we have verified the spin coating method it can be used to investigate the influence of the silane-coating on the three-phase contact angle. The contact angle results of the 60% TMSPM, 80% TMSPM, and 100% TMSPM coverage are shown in Figure 32. The average contact angles in Figure 32 are again based on three droplets for each sample. To get insight into the reproducibility of the measurement, each sample is measured twice. Between the first and second measurement was a period of six weeks. The measurements were reproducible as the average contact angle values differed 15° at most. Concerning contact angles, this is a small deviation. Noticeable, the contact angles of the second measurement are consistently 13° to 15° lower compared to the first measurement. Whether this is only due to the error in the contact angle measurement or also partly due to a slight decrease in hydrophobicity, by for example hydrolyzation of the attached TMSPM molecules, is difficult to say based on three measurements. Despite the presence of TMSPM, as shown by the FTIR results, the obtained contact angles are close to 50° for all the three functionalizations. These contact angles indicate that the particle surface is still hydrophilic. When comparing the different degrees of functionalization, there is no significant difference in the contact angle. The more functionalized particles do not give rise to a less hydrophilic contact angle. This might suggest that there is a maximum silane coverage that can be achieved, and that this maximum is already reached for 60% silane coverage. Based on the contact angle measurement it can be concluded that the surface modification with TMSPM as described in Section 3.1.2 is not successful in generating a hydrophobic nanoparticle surface. It is good to keep in mind that in these experiments the macroscopic contact angle is measured. This contact angle can differ significantly from the microscopic contact angle that is formed by the nanoparticle at the liquid-liquid interface due to the line tension that influences the nanoscale force balance as discussed by Winkler et al. (49). These microscopic contact angles are very difficult to determine experimentally, whereas the macroscopic contact angle can relatively easily be determined by these sessile drop experiments. The contact angle results presented in these thesis thus serve as an indication of the hydrophobicity but not necessarily give the contact angle that is formed by the nanoparticles at the DEP-water interface.

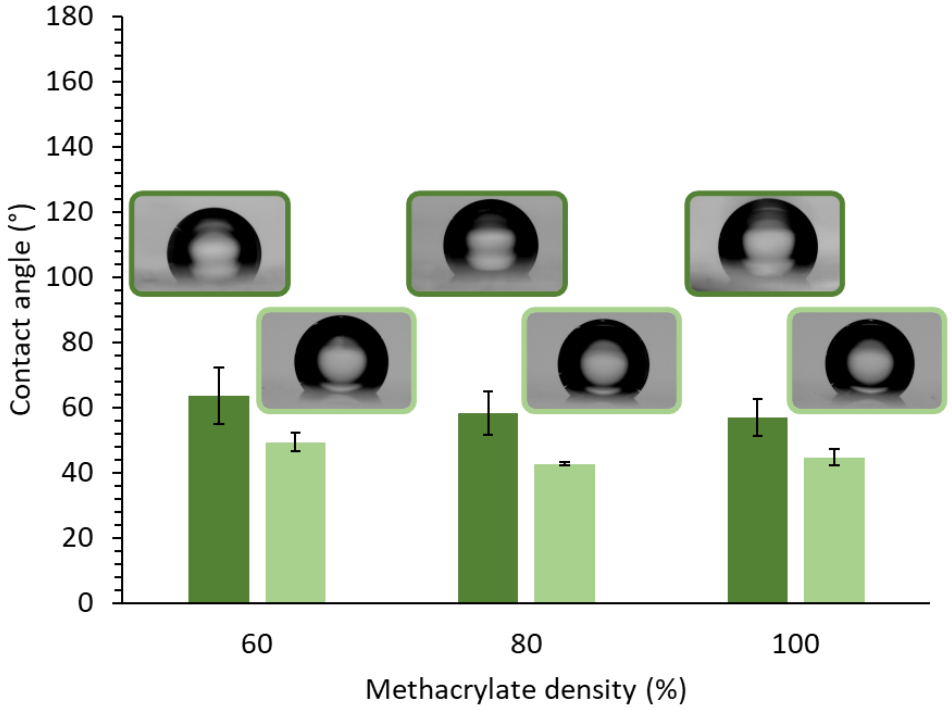

Figure 32 Contact angle measurements of the TMSPM functionalized particles. The figure shows the average contact angle versus methacrylate density of the two measurements. The error bars represent the standard deviation in the data. The insets show the corresponding DEP droplet shapes.

3.3 Precursor mixture preparation using 3-(trimethoxysilyl)propyl methacrylate functionalized SiO_2 nanoparticles and outcoming structures

In order to research the dispersibility of TMSPM functionalized nanoparticles precursor mixtures were prepared with the TMSPM covered particles as stabilizing particles. For functionalized particles to be able to stabilize any structure formed by immiscible liquids, they first need to be dispersible in the precursor mixture. The ternary composition for bijel fabrication using the water/DEP/1-propanol system, derived from Khan & Sprockel et al. (25), is 46 v% water, 9 v% DEP and 45 v% 1-propanol. This is a rather hydrophilic mixture of liquids due to the large contribution of water compared to DEP. Potentially, the hydrophobicity of functionalized particles can hamper the dispersibility of the particles in a precursor mixture.

3.3.1 Precursor mixture preparation

Precursor mixtures were prepared with the TMSPM functionalized particles. Prior to mixing the three liquids and the particles a 50 w.% glycerol stock was made. To 18.7 mL of MilliQ water at pH 3 with 50 mM NaCl 15 mL of glycerol was added. Glycerol is added to the precursor mixture to improve the optical transparency when the obtained structures are examined with optical microscopy. After combining all the components as listed below in Table 5 the precursor mixtures were subjected to vortex mixing.

Table 5 The used amounts in µL of the components of the precursor mixture.

	60% TMSPM	80% TMSPM	100% TMSPM
DEP	70	70	70
MilliQ water (50 w.% glycerol)	211	211	211
MilliQ water (pH 3, 50 mM NaCl)	289	289	289
Particle dispersion in 1-propanol	394	373	406
1-Propanol	93	115	84

Using the amounts tabled in Table 5 the precursor mixture made with 80% TMSPM covered particles showed phase separation. To enhance the miscibility 50 µL of 1-propanol was added to this precursor mixture. When subjected to centrifugation at 14500 rpm for two minutes the particles formed a relatively large sediment, indicating that the particles are not stable in the precursor mixture. To increase the particle stability 100 µL of 1-propanol was added to each precursor mixture. The obtained precursor mixtures are shown in Figure 33a. Obviously, these precursor mixtures are opaque, suggesting that the particles aggregated. When again subjected to centrifugation (14500 rpm, two minutes), the amount of sediment had decreased significantly. The supernatant still contained particles as can be seen by the scattering that is visible in Figure 33b. These particles can be considered to be colloidally stable as they do not sediment upon centrifugation. This supernatant is used as precursor mixture in the STrIPS process.

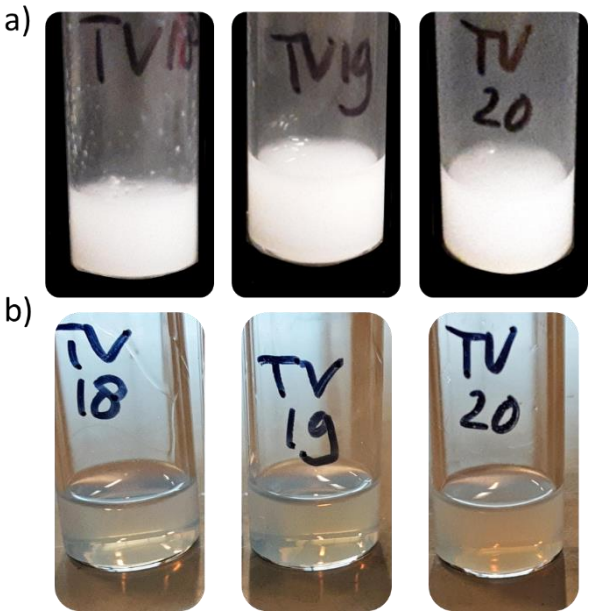

Figure 33 Precursor mixtures prepared using the TMSPM functionalized particles, a) before centrifugation and b) after centrifugation. The scattering visible in b) indicates that there are colloidally stable particles present.

Before testing the precursor mixtures it is insightful to combine the findings on the hydrophobicity of the TMSPM functionalized particles with the findings on their dispersibility in the precursor mixture. The three-phase contact angles showed that the particles remained hydrophilic after the TMSPM functionalization as $\theta \approx 50^{\circ}$. However, Figure 33a clearly shows that the particles are already too hydrophobic to be dispersible in the rather hydrophilic precursor mixture. This reveals one of the main difficulties of pre-modification of the particles for bijel formation using the water/DEP/1-propanol system. The used precursor mixture consist of mainly water, and does not allow for dispersing particles that are hydrophobic enough to ensure a three-phase contact angle of 90°, which is required for stabilization of the bijel structure. In other words, there is a mismatch in the particle hydrophobicity required for stability in the precursor mixture and bijel stabilization.

3.3.2 Quick fiber and outcoming structures

To test the precursor mixture the so-called "quick-fiber" method was used. A fiber extrusion device was assembled by gluing a 50 µm round glass capillary in a 200 µL pipette tip with Norland 89 UV-glue. To harden the glue the pipette tip was placed under UV-light for 10 minutes. To collect the sample and be able to examine the sample with confocal microscopy a container was built from 20 mL glass vial. The bottom of the vial was removed with a band saw. Using epoxy glue the vial was attached to a cover slip. The sample container was filled with water saturated toluene and the quick fiber tip was filled with 200 µL of precursor mixture prior to connecting the tip to the pipette. The tip of the 50 µm round glass capillary was positioned in the toluene bath and pressure was exerted

onto the pipette to flow the precursor mixture into the toluene continuous phase. Unfortunately, the tested precursor mixtures did not form fibers but round shaped blobs. The blobs were washed with n-hexane. First, the toluene was removed. n-Hexane was added and subsequently taken off to remove the residual toluene. Lastly, a mixture of n-hexane with Nile red was added. Nile red is an oil-soluble, fluorescent dye that exhibits solvatochromism, meaning that the fluorescent changes if the polarity of the environment is varied. A non-polar local environment will cause a blue-shift of the fluorescence whereas polar local environments cause the fluorescence to shift towards the red (50). Therefore, the oil phase and the particle phase can be distinguished using confocal microscopy.

The resulting confocal micrographs are given in Figure 34. Here, the phases are false colored after collecting the images. Magenta represents the water phase, the particles are colored green, and the oil is presented in black. Within the blobs there is almost no oil signal, meaning that the resulting structures are not bicontinuous. However, for the particles to be fluorescent it must have been in contact with the surrounding n-hexane with Nile red as Nile red causes the fluorescence. Within the blob some particle structure can be observed, suggesting that the n-hexane with Nile red has migrated into the structure to some extent. The structures formed by the particles are presumably caused by gelation of the particles. It can be observed that the particles are mostly present in the water phase, which is in accordance with the contact angle measurement results. The particles are too hydrophilic and preferably wet by the water phase. Besides the non-neutral wettability, the resulting structures might also be attributable to a too low particle weight fraction. During the centrifugation of the precursor mixture a significant amount of particles are lost. If there are too few particles present the formed structure cannot be stabilized. It is thus important to first achieve stable particle dispersion of which the particles also show to be stable in the precursor mixture.

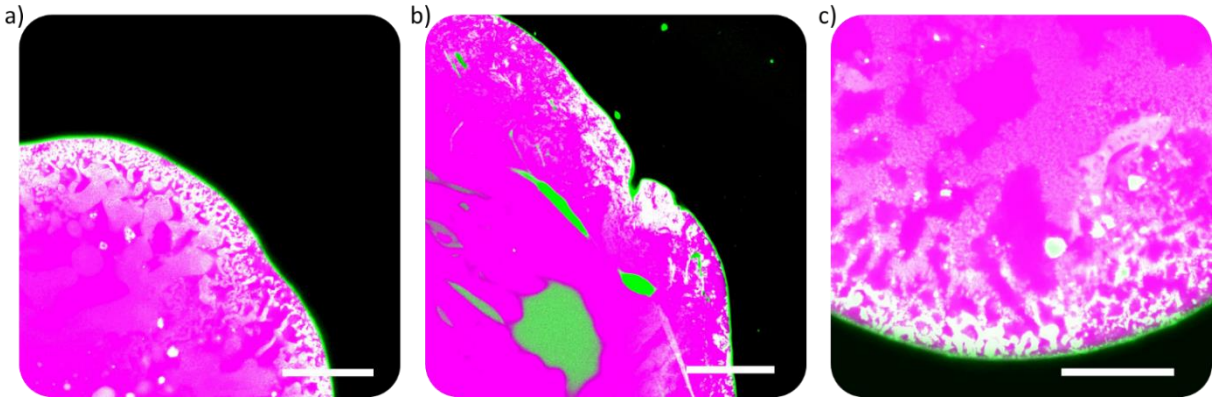

Figure 34 Confocal micrographs of the structures formed by the precursor mixtures made with TMSPM functionalized particles. a) Structure formed by precursor mixture containing 60% TMSPM covered Ludox TM-50. b) Structure formed by precursor mixture containing 80% TMSPM covered Ludox TM-50. c) Structure formed by the precursor mixture containing 100% TMSPM covered Ludox TM-50. The phases are false colored. The water phase is presented in magenta, the oil in black and the particles in green. Scale bars are 50 µm.

Chapter 4

Dodecyltriethoxysilane

Our previous attempt to hydrophobize the silica surface with TMSPM revealed that for the water/DEP/1-propanol bijel system this silane is not hydrophobic and/or not reactive enough to render the Ludox TM-50 particles neutrally wetting. When fabricating bijels, either with VIPS (22) or STrIPS (5,6), cetyltrimethylammonium cations (CTA^+) are commonly applied as the hydrophobizing agents. CTA^+ consists of a 16-carbon long alkyl chain with a positively charged quaternary ammonium head group. This charged head group electrostatically adorbs onto the negatively charged silica surface silanol group, providing a partially hydrophobic silica surface. To mimic this system of a silica nanoparticle surface covered with long alkyl chains, we researched the ability of dodecyltriethoxysilane to render the silica nanoparticle sufficiently hydrophobic. Dodecyltriethoxysilane is a trialkoxysilane with a 12-carbon long alkyl chain as the organic group, see Figure 35, resembling the structure of the CTA^+ surfactant. Roe et al. (51) showed the potential of alkylsilanes as "silane hydrophobes" for the hydrophobic treatment of cotton material. Alkylsilane-functionalized silica nanoparticles were applied to enhance the amount of hydrophobic silane that attaches during the treatment to the cotton surface. Comparison of alkylsilanes with different chain lengths, varying from 1 to 18 carbon atoms in the chain, showed that increasing the chain length further than 8 carbon atoms only slightly increased the value measured for the contact angle of the cotton fabric (51). This suggests that the difference in hydrophobicity of the dodecyl chains and hexadecyl chains is minimal. Pyo and Chang (52) utilized alkylsilanes to modify the surface of mesoporous silica particles. Again, the alkyl chain length was varied to enlarge the hydrophobicity using propyl-, octyl-, dodecyl- and octadecyltriethoxysilane, corresponding to a C_3, C_8, C_{12} and C_{18} chain. When the modification is conducted in hydrochloric acid, the changes in contact angle are most pronounced going from unmodified mesoporous silica particles to C_8-modified mesoporous silica particles. Increasing the chain length further to 18 carbon atoms increased the contact angle from 97.6° for C_8-modified particles to 102.1° for C_{18}-modified particles (52). Based on this previous research, it is thought that dodecyltriethoxysilane should be hydrophobic enough to alter the silica nanoparticle surface to an extent similar to CTA^+. In this chapter the dodecyltriethoxysilane functionalization is discussed. The experimental method will be treated together with the obtained results.

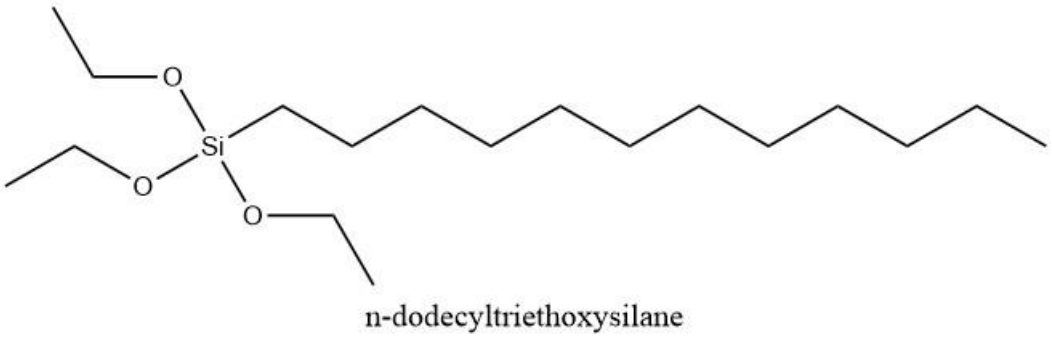

Figure 35 The chemical structure of n-dodecyltriethoxysilane.

4.1 Functionalization of SiO_2 nanoparticles with dodecyltriethoxysilane – dispersion in water

When implementing dodecyltriethoxysilane (DTES) in the functionalization method, the experimental method can be slightly altered. Unlike TMSPM, DTES cannot polymerize. Hence, it is not necessary to remove the present oxygen by flowing nitrogen through the reaction mixture. The work done on

the TMSPM revealed the importance of the dispersibility of the particles in the precursor mixture, predominantly consisting of water. Therefore, it is desired to have the particles dispersed in water. To achieve a stable dispersion the pH of the particles was increased to 11. At high pH values deprotonation of the surface silanol groups leads to a negatively charged silica surface, as discussed in Section 2.5. This negative surface charge can enhance the stability of the particles in water as the negatively charged particles will repel each other. A schematical overview of the experimental method for the DTES functionalization is given in Figure 36.

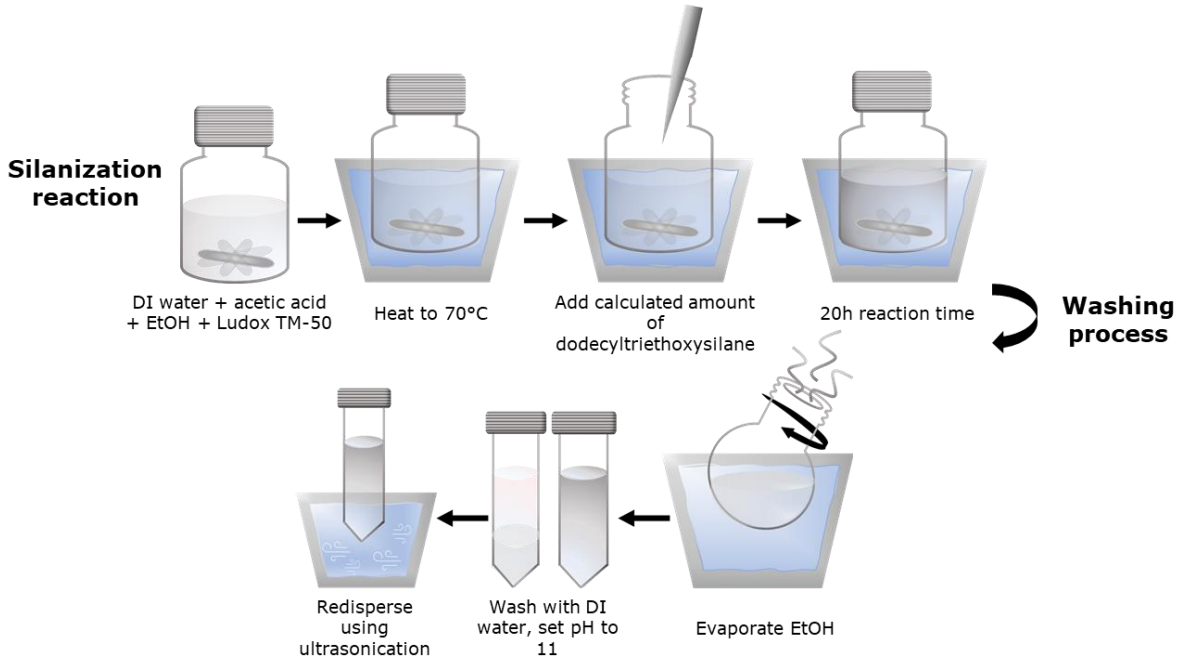

Figure 36 schematical overview of the experimental method for the DTES functionalization of Ludox TM-50. The reaction mixture consisting of DI water, acetic acid, ethanol, Ludox TM-50, and DTES is kept at 70°C for 20 hours. Subsequently, the ethanol is evaporated, the particles are washed, and the pH is set to 11. Lastly, the particles are redispersed in water using ultrasonication.

4.1.1 Chemicals

The n-dodecyltriethoxysilane used in this part of the work is purchased from Fisher Scientific and has a purity of 95%.

4.1.2 Experimental method functionalization

For each degree of functionalization 20 mL acetic acid, 40 mL MilliQ water, 40 mL ethanol and 5 mL were combined in a 100 mL bottle. Prior to combining the components of the reaction mixture a water bath was heated to 70°C under constant stirring. The bottles were placed in the water bath. Once the temperature had risen to 70°C, the calculated amounts of DTES were added. The exact amounts for the different degrees of functionalization are tabled in Table 6. The reaction mixture was left to react under constant stirring. After 20 hours of reaction time, the reaction mixture was removed from the water bath. The ethanol was evaporated using a Hei-VAP core rotary evaporator by Heidolph® at a bath temperature of 60 degrees Celsius and rotation of 250 rpm. The setpoint pressure was slowly decreased to 115 mbar. After 20 minutes the reaction volume was decreased from 110 mL to about 60 mL. Subsequently, the particles were washed. The washing procedure consisted of three consecutive washing steps of centrifugation using the Beckman Coulter Allegra® X-12R centrifuge followed by redispersion using the Scientific Industries Vortex-Genie 2 vortex mixer. In the first step 30 mL MilliQ water was added, in the second and third step 60 mL and 20 mL MilliQ water was added, respectively. During the first two steps centrifugation of 10 minutes at 3750 rpm was sufficient to obtain a clear supernatant for 40%, 60% and 80% surface coverage. For the 20% and 100% surface coverage 20 minutes of centrifugation were required, presumably these dispersions contained slightly more ethanol. For 40%, 60%, 80% and 100% DTES surface coverage

35 mL of MilliQ water was added in the third step. The dispersions of the 40%, 60% and 80% functionalized particles were then centrifuged for 30 min at 3750 rpm. The dispersion of the 100% functionalized particles was subjected to centrifugation for 1 hour. To the 20% covered particles a total of 140 mL MilliQ water was added in the third washing step. After 1 hour of centrifugation the supernatant remained slightly opaque, but it was possible to distinguish the sediment from the supernatant. To the sediment NaOH solution was added until the sediment formed a liquid-like dispersion upon vortex mixing and ultrasonication (Branson 1800). Once liquified the pH of the dispersions was measured using the Mettler Toledo FiveEasy pH meter. For all the degrees of functionalization the pH was between 11.13 and 11.20.

The particle weight fractions were determined by drying 100 µL of particle dispersion. Prior to drying the mass of the dispersion was weighted. After evaporating the water the mass of the particles is determined. Dividing the dried particle mass by the mass of the dispersion gives then the particle weight fraction.

Table 6 Amounts of DTES used in the functionalization method to obtain different degrees of functionalization together with the particle weight fraction of the obtained dispersions.

Degree of functionalization (%)	Amount of added DTES (mL)	Particle weight fraction (w%)
20	0.248	11
40	0.496	21
60	0.744	22
80	0.992	24
100	1.240	28

4.1.3 Sample preparation for DLS, zeta potential, FTIR, TGA, and contact angle measurements

The sample preparations were performed as described in Sections 3.1.4 and 3.1.5. The DLS and zeta potential measurement sample preparation was different as the particles are now conditioned at pH 11. To obtain the diluted dispersion with a pH of 10 required for the zeta potential measurements three drops were added to MilliQ water. The diluted dispersion was left overnight to equilibrate. Before measuring the zeta potential the pH was measured using a Mettler Toledo FiveEasy pH meter. Overnight the pH values had shifted towards pH 10.2. To further bring down the pH 0.1M HCl was added until a pH of 10 was reached. For the TGA samples the functionalized particles were immediately dried after the reaction. These dried particles were also utilized for the FTIR measurements.

4.2 Results and discussion

During the washing procedure a white layer could be observed on top of the clear supernatant for degrees of functionalization of 40% and higher, which is thought to be self-condensated DTES. This could indicate that not all DTES molecules react with the silica surface. The obtained values of the weight fractions are tabled in Table 6. Performing the functionalization as described in Section 4.1.2 generally yields a weight fraction of 20 w%. In addition to the FTIR, zeta potential, DLS and contact angle measurements and thermogravimetric analysis, in short TGA, was performed to research the functionalization.

4.2.1 Determining the presence of DTES functional groups using FTIR

As described in Section 3.2.1 there are six characteristic peaks in the spectra of pure Ludox TM-50, the Si-O-Si peaks and the Si-OH peaks. In addition to these peaks, only CH_2 and CH_3 stretches are expected for the dodecyltriethoxy functional group. The average spectra are given in Figure 37. An overview of the present peaks and the chemical species they have been ascribed to is given in Table 7. In addition to the characteristic peaks, there are two peaks arising around 2900 cm^{-1}. These peaks can be ascribed to the CH_2 and CH_3 stretches. Due to the presence of these peaks, it can be

concluded that there are dodecyltriethoxy groups bound to the silica surface for all degrees of functionalization.

Table 7 Overview of the peaks observable in the FTIR spectra of the DTES functionalized particles.

Wavenumber (cm^{-1})	Species	Appearance
3437	Si-OH	Broad
2926-2923	CH_2, CH_3	Sharp
2855-2852	CH_2, CH_3	Sharp
1632	Si-OH	Weak
1113	Si-O-Si	Strong
797	Si-O-Si	Medium
473	Si-O-Si	Strong

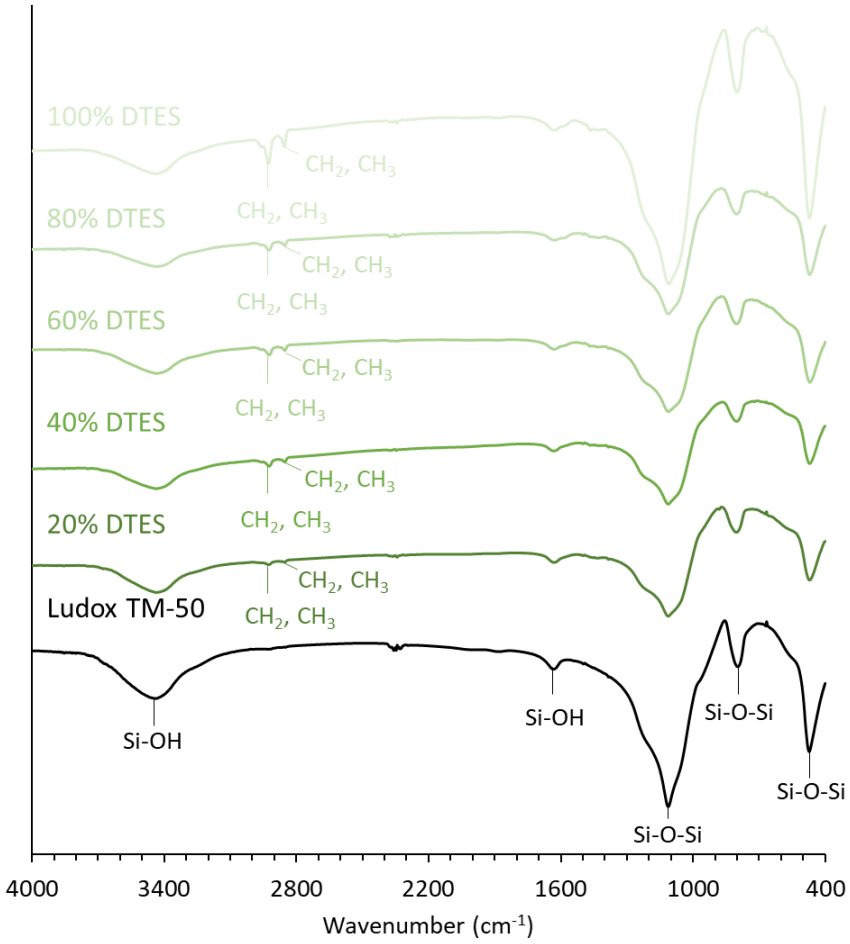

Figure 37 Average FTIR spectra of Ludox TM-50 and DTES functionalized Ludox TM-50 particles. The surface modification with DTES gave rise to CH_2 and CH_3 stretches located around 2900 cm^{-1}.

Figure 38 shows the average Si-OH/Si-O-Si peak ratio for the different amount of DTES. Similar to the TMSPM functionalization the Si-OH band decreases with respect to the Si-O-Si band upon increasing the DTES density. Assuming that a surface silanol group is substituted by a dodecyltriethoxy functional group in the surface modification, a decreasing Si-OH/Si-O-Si peak ratio suggest that the surface coverage can be tuned by adjusting the added amount of DTES during the reaction.

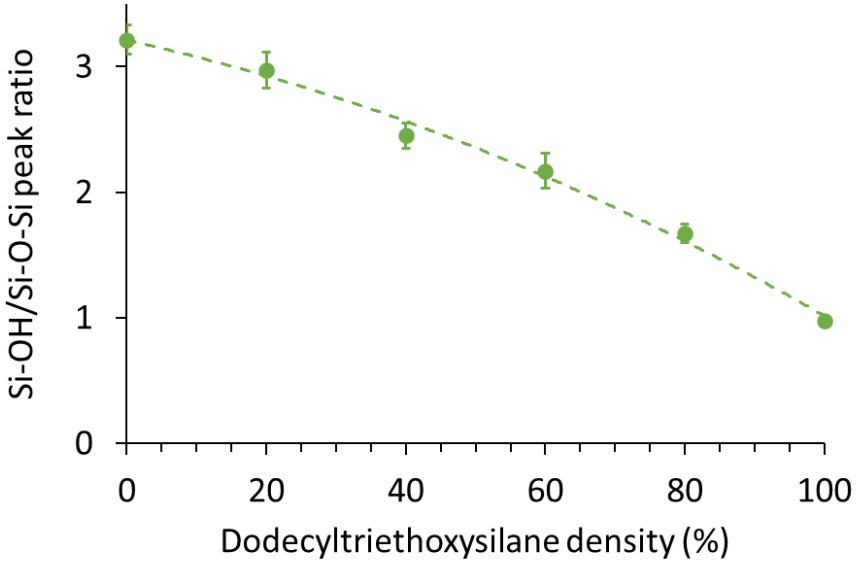

Figure 38 The average ratio between the area of the Si-OH band and the Si-O-Si band for the different degrees of functionalization. The error bars indicate the standard deviation in the data. A second order polynomial trendline was added corresponding to a R^2 value of 0.9936.

4.2.2 Change in surface charge examined by zeta potential measurements

Figure 39a gives the average zeta potential distributions for the DTES functionalized Ludox TM-50 particles. For all different degrees of functionalization the distribution consists of one peak, indicating that the particles present in the sample all have similar surface charges. For the 20%, 40% and 60% DTES the position of the peak shifts to more negative zeta potentials for higher degrees of functionalization. The peaks corresponding to 80% and 100% DTES are positioned at zeta potential values similar to that of the 60% DTES covered particles. When plotting the average value of the zeta potential versus the theoretical DTES density, see Figure 39b, indeed an increase in the absolute zeta potential can be observed upon increasing the surface coverage from 0% to 60%. Further increasement of the surface coverage did not influence the zeta potential significantly. As beforementioned in Section 2.5 the absolute value of the zeta increases if only one hydrolyzed alkoxy group condensates with the surface due to the increase in chargeable silanol groups. The increase in the absolute value of the zeta potential could thus be explained by the way how the DTES binds to the surface. For 0% to 60% surface coverage the impression is that dodecyltriethoxysilane predominantly forms only one siloxane bond during the reaction with the surface, resulting in additional chargeable silanol groups. For 80% and 100% surface coverage either the type of binding changes or 60% surface coverage is the maximum coverage that can be achieved. However, FTIR does not support the idea of an increasement in Si-OH groups for increasing degree of functionalization. It is good to keep in mind that the zeta potential measurements are conducted in water. Perhaps the presence of water can induce hydrolyzation of otherwise bound siloxane groups, resulting in chargeable silanol groups. The degree of functionalization might influence to what extent this hydrolyzation can take place.

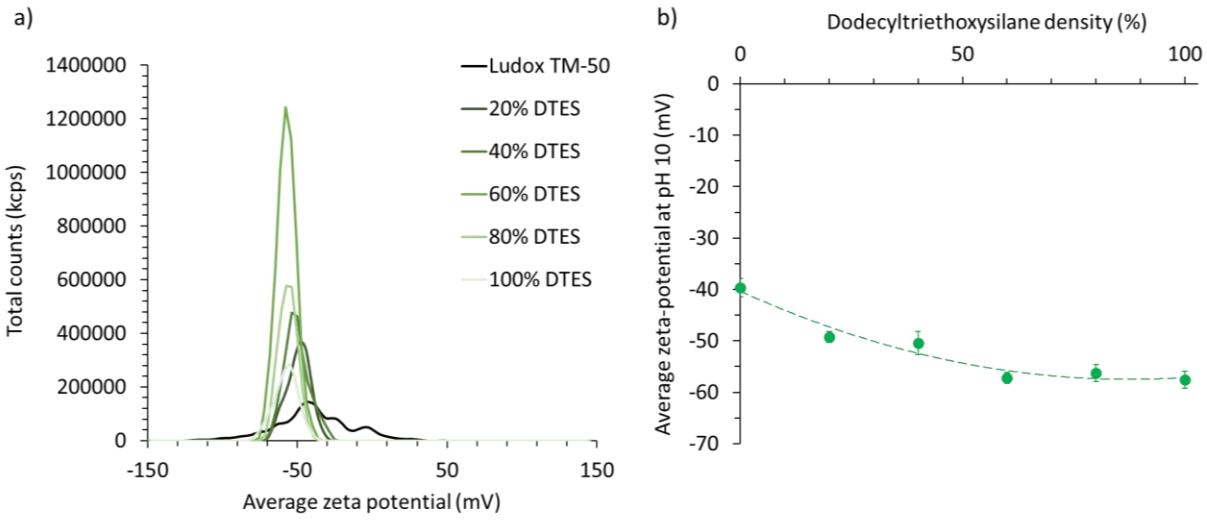

Figure 39 Results of zeta potential measurements. a) Average zeta potential distribution for different (theoretical) DTES densities b) Average zeta potential for different degrees of functionalization. A second order polynomial trend line was fitted to the average values of the zeta potential. R^2 of the trendline was 0.95.

The corresponding DLS results are given in Figure 40. The volume-weighted average size distribution in Figure 40a shows that for each DTES density there is only one size population as there is only one peak visible. The distributions significantly overlap, suggesting that the size remained rather constant for the different surface coverages. The plot of the volume-weighted average size in Figure 40b indeed shows that the size of the functionalized particles is between the 30 nm and 70 nm for all DTES densities. The absence of significant aggregation makes the zeta potential data more reliable.

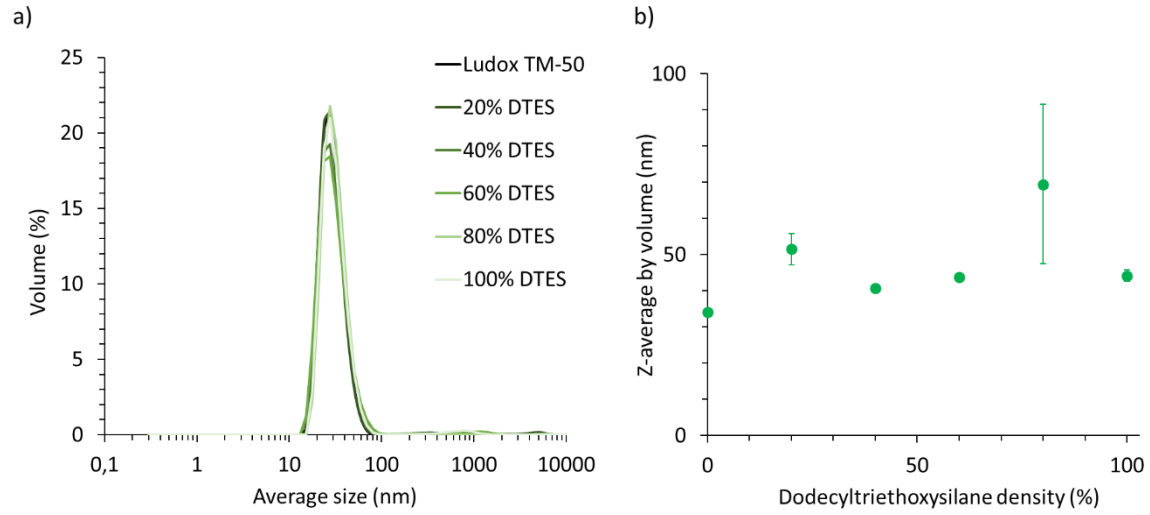

Figure 40 DLS results. a) Average size distribution by volume. b) Average volume-weighted size for the different DTES densities, with error bars indicating the standard deviation in the data.

4.2.3 Quantifying the DTES density using TGA

The beforementioned DTES densities are the theoretical surface coverages calculated as described in Section 2.4.4. However, reactions almost never have an efficiency of 100%. Hence, it is very unlikely that the 100% DTES density corresponds to a 100% surface coverage. To gain qualitative information on the amount of silane bound to the silica particles, TGA experiments were performed. The TGA experiments were conducted by Dennie Wezendonk from the Materials Chemistry and

Catalysis research group. In TGA the sample's weight is measured while the temperature is changed using a controllable temperature program (53). Applied to the silane functionalized silica nanoparticles, the silane consists of hydrocarbons that will decompose at temperatures in the 200°C-600°C temperature range (46,54). Silica, on the other hand, is thermally stable in this range. The resulting TGA curves are presented in Figure 41. Here, the temperature was increased from 30°C to 650°C with a heating rate of 10°C/min. Two weight loss steps can be deduced from the TGA curves. In the first step, 30°C to 100°C, both the Ludox TM-50 and the DTES functionalized exhibit a weight loss. This weight loss could be attributed to water that was physisorbed onto the particle surface. In the second step, 200°C to 600°C, the DTES functionalized particles show a significant weight loss while there is no weight loss observable for the Ludox TM-50 particles. This weight loss could be ascribed to the loss of silane molecules. A clear difference can be seen between the 20% DTES and the 60% and 100% DTES. The 20% DTES covered particles have a weight loss of 5.0% with respect to the unmodified Ludox TM-50. The weight losses for 60% DTES and 100% DTES were 11.3% and 10.7% with respect to Ludox TM-50, respectively. These percentages show that the 60% and 100% DTES covered particles have a surprisingly similar silane content, whereas the 20% DTES covered particles have a significantly lower silane content, as to be expected. The similarity of the 60% DTES and 100% DTES TGA curves reinforces the explanation of the zeta potential data. The 60% and 100% DTES indeed have similar silane content and thus it is likely that there is a maximum DTES coverage that can be achieved. Presumably, this maximum is around 60%.

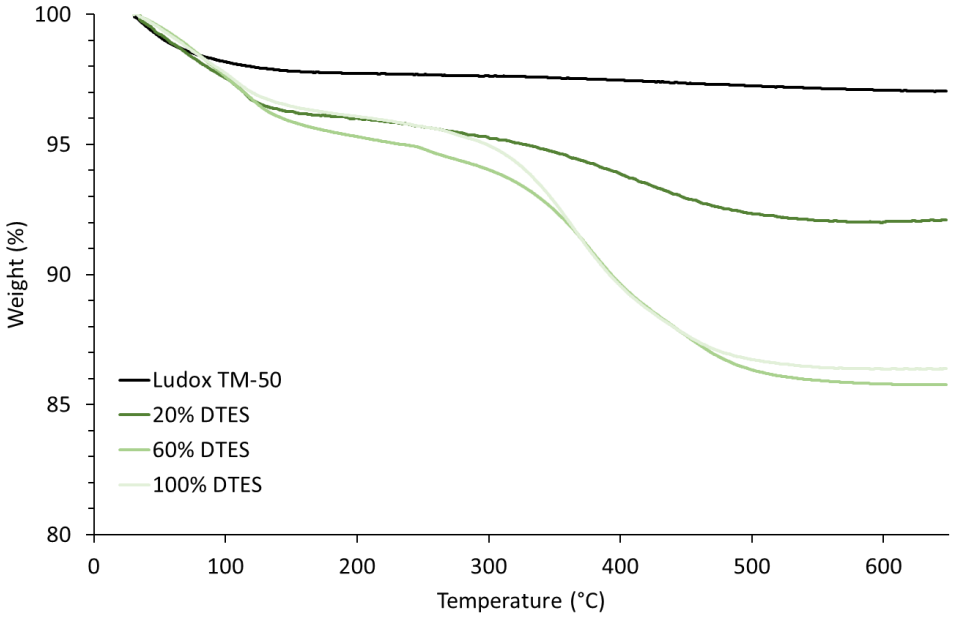

Figure 41 TGA curves for Ludox TM-50 and DTES functionalized particles. For non-functionalized Ludox TM-50 particles weight loss can only be observed up to 100°C. For the DTES functionalized particles an additional weight loss can be observed between 200°C and 600°C.

The TGA experiments were combined with mass spectrometry (MS). By burning off the organic silanes combustion products like CO and CO_2 will be released. Using mass spectrometry these products can be detected. In this way the weight loss at specific times can be coupled to a released compound. Therefore, the MS results can be used to verify whether the weight losses in the 30°C-100°C region and 200°C-600°C region are indeed due to water and the organic silanes, respectively. The mass spectrometer measures the ion current, which is a measure for the ion intensity for specific *m/z* values (55). The TGA results combined with the mass spectrometry results are depicted in Figure 42. The *m/z* value of 28, 18, and 48 correspond to CO, H_2O, and CO_2, respectively. The ion currents at *m/z*=18 confirm that the weight loss in the temperature range 30°C-100°C is due to the loss of water. At 100° there is also CO_2 formation, explaining why the TGA curve of the DTES functionalized particles start to differ from the reference Ludox TM-50 curve. Between 200°C and

600°C the ion current corresponding to CO_2 is increased. Most of the carbon containing silanes are thus combusted between 200°C and 600°.

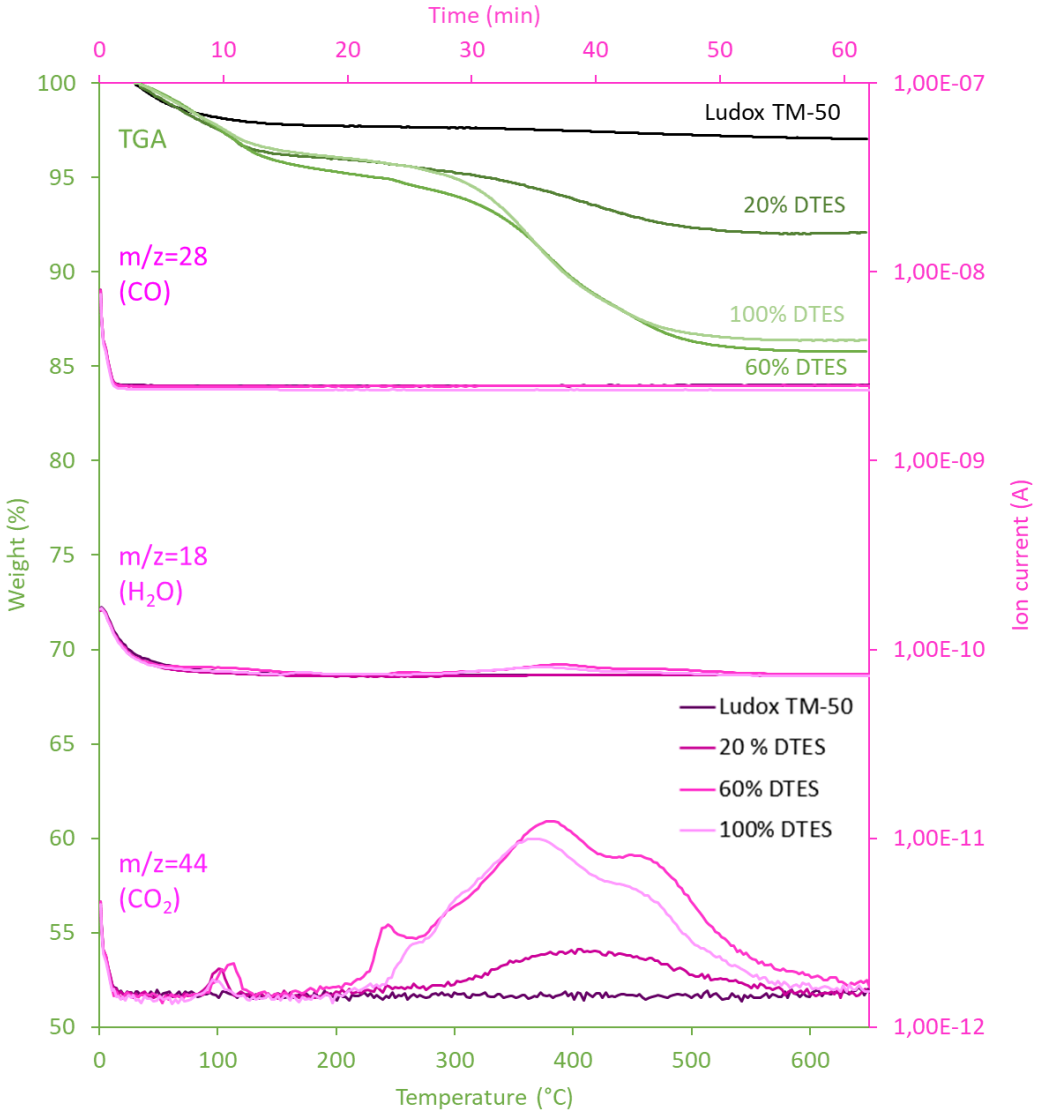

Figure 42 TGA results combined with the mass spectrometry results. The m/z values indicate the MS components. The m/z values of 28, 18, and 44 correspond to CO, H_2O, and CO_2, respectively.

For the pure Ludox TM-50 there is no peak observable in the ion current measured for *m/z*=44. Hence, the weight loss with respect to pure Ludox TM-50 can be completely ascribed to the DTES molecules and allows for calculating the mol fraction of DTES with respect to the Ludox TM-50 silica. For 20% DTES coverage the weight loss is 5.0%. Taking into account the DTES molecular weight of 332.6 g/mol this results in

$$\frac{(5.0\% * 1\ g)}{332.6\ g/mol} = 0.15\ mmol\ of\ DTES\ per\ gram\ of\ sample$$

For 60% and 100% DTES coverage there is 0.34 mmol and 0.32 mmol of DTES per gram of sample, respectively. The remainder of the mass at a temperature of 650°C are the silica nanoparticles. Using the weight loss at 650°C the amount of silica per gram of sample can be determined. Considering that $n_{SiOH} = 9.3 * 10^{-4}\ molg^{-1}$, see Section 2.4.4, the number of silanol groups present per gram of sample can be calculated. Both the amount of silica and the number of silanol groups per gram of sample are given in Table 8. Dividing the determined number of moles of DTES by the number of silanol groups present the actual degree of functionalization can be calculated. Here, it is assumed that each DTES molecule only binds to one surface silanol group. The actual degrees of

functionalization are also given in Table 8. For the lower degree of functionalization the theoretical value calculated as described in Section 2.4.4 is close to the degree of functionalization deduced from the TGA results. For the higher degrees of functionalization, on the other hand, the calculated values differ significantly. As expected, the 60% and 100% have a similar actual degree of functionalization, both are close to 40%. The actual maximum silane coverage that can be achieved is thus 40%.

Table 8 Amount of silica and number of silanol groups per gram of sample derived from the TGA results. Using these values the actual degree of functionalization could be calculated.

Degree of functionalization (%)	Amount of silica per gram of sample (g)	Number of silanol groups per gram of sample (mol)	Number of DTES molecules per g sample (mol)	Actual degree of functionalization (%)
20	0.921	$8.56*10^{-4}$	$0.15*10^{-3}$	17.5
60	0.858	$7.98*10^{-4}$	$0.34*10^{-3}$	42.6
100	0.864	$8.03*10^{-4}$	$0.32*10^{-3}$	39.8

4.2.4 Three-phase contact angles for functionalized particles stored in water – a time dependent study

The particles are now dispersed in water. By eye the coating looked different from the coatings obtained with the TMSPM particles dispersed in 1-propanol. To ensure that the film formed during spin coating sufficiently covers the glass slide the coating was examined with SEM. The obtained SEM images are shown in Figure 43. The overall coating appears to be smooth with particles present over the entire sample. Contrary to the SEM images of the coating of TMSPM functionalized particles, darker regions can be observed in the SEM images of the coating made from DTES functionalized particles. The inset in Figure 43 shows a magnification of such a darker region. Here, it can be seen that these regions also contain particles. Hence, it can be assumed that the coating is comparatively homogeneous, and that the contact angle measured on top of this coating is representable for the contact angle formed by the DTES functionalized particles.

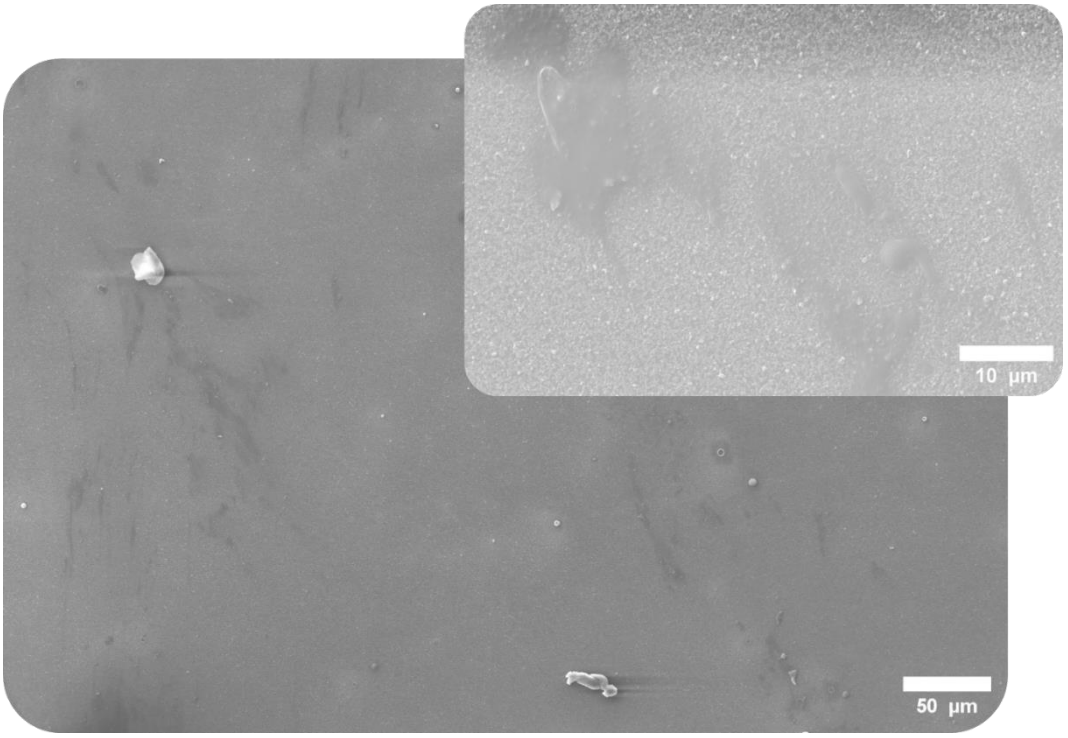

Figure 43 SEM images of the coating formed by the 100% DTES covered particle dispersion in water. The inset shows a magnification of the darker regions visible in the overview image.

Immediately after the functionalization the three-phase contact angles were measured using the OCA. Figure 44 shows the obtained values for the contact angle measured via the water phase. For reference the three-phase contact angle made by water, DEP, and a layer of dried Ludox TM-50 dispersion in water at pH 11.1 was measured. The overall trend that can be deduced from the contact angles is an increase in contact angle with increasing DTES density. The contact angle increases from 25° for unfunctionalized silica nanoparticles to 150° for 100% DTES functionalized silica.

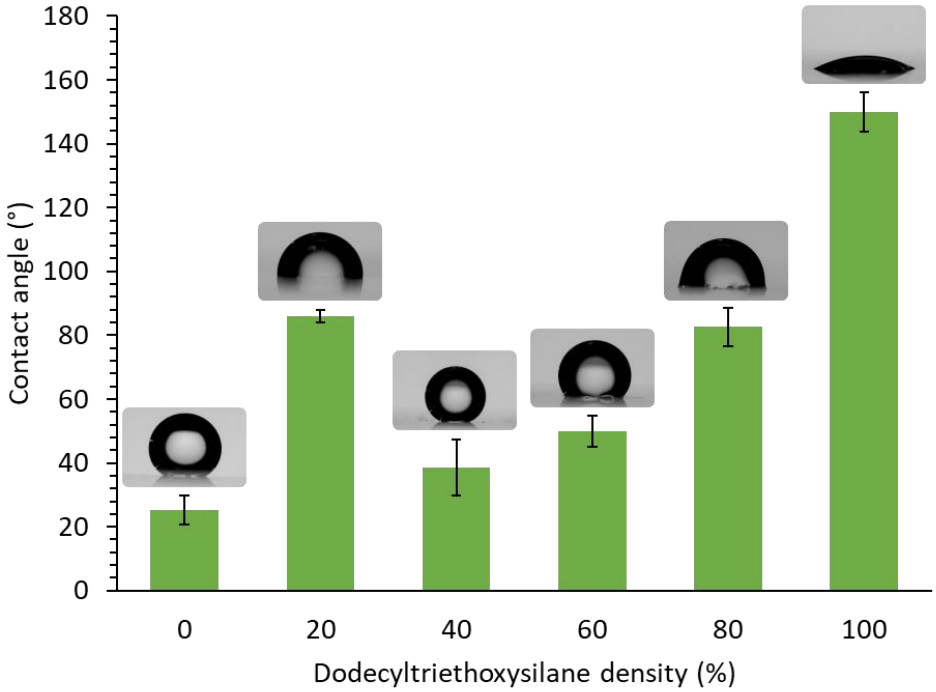

Figure 44 Three-phase contact angles measured directly after functionalization of the particles with DTES. The insets show the DEP droplets formed on top of the coated slides.

Noteworthy, the 20% DTES density particles gave rise to a relatively large contact angle. According to Li et al. (56) post-functionalization leads generally to inhomogeneous coverage. It could be possible that the inhomogeneity of the silanes on the particle surface causes the particles to assemble on the microscope slide in a certain manner, influencing the measured contact angle. This could explain the unexpectedly large contact angle for 20% DTES density. If the silanes are concentrated at one point on the surface, this part likely faces upwards, illustrated in Figure 45a. The microscope slide is hydrophilic and will thus prefer interaction with the non-functionalized hydrophilic part of the particle surface. A possible way to verify this proposed explanation is by examining the influence of multiple layers of coating. If there is indeed a preferable orientation of the particles on the substrate, a second layer of coating should give a different, more hydrophilic contact angle. The oil droplet will then be predominantly exposed to the non-functionalized silica surface, see Figure 45b. When the DTES density increases, the silane molecules might be forced to distribute more evenly over the particle surface. A more homogenous coating allows for more hydrophilic silica surface to be exposed to the oil droplet, see Figure 45c. Hence, the oil droplet is less likely to spread on the surface. As depicted in Figure 45d an increase in DTES coverage now leads to a more hydrophobic coating. This could explain the drop in contact angle going from 20% DTES coverage to 40% DTES coverage, and the increase in θ going from 40% to 60% DTES coverage.

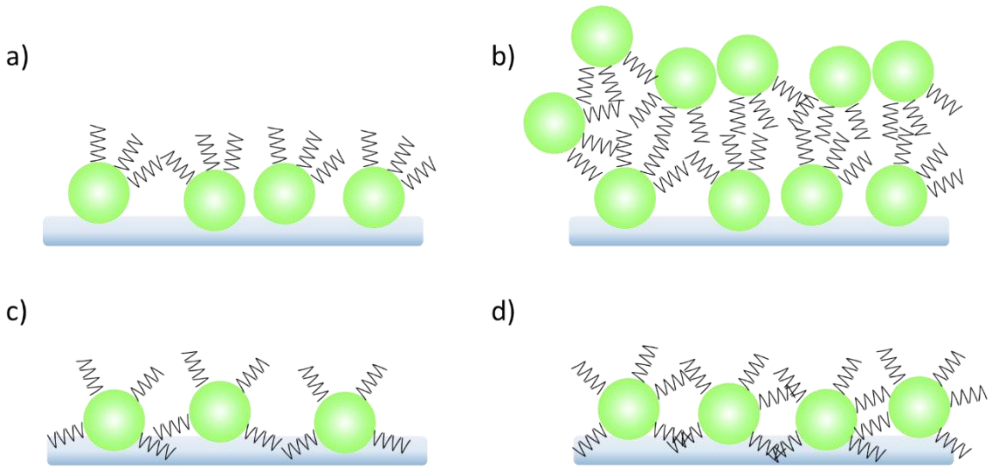

Figure 45 Possible orientations of functionalized particles coated on a hydrophilic microscope slide. a) Inhomogeneous coverage can result in a preferred orientation where the hydrophobic silanes are facing upwards. b) When there are two layers of inhomogenously covered particles coated on the slide, the hydrophobicity is inverted. c) and d) More homogenously covered particles allow for more hydrophilic silica surface to be exposed. However, the more silanes are attached to the surface the less accessible the silica surface.

The increase in θ is steepest when going from 60% DTES coverage to 100% DTES coverage. Intuitively, this would indicate that the more functionalized the particles are, the more hydrophobic the surface becomes. However, the TGA results show that the 60% and 100% DTES functionalized particles have the same amount of DTES molecules attached to their surface. As mentioned in Section 2.4.4 the favorable grafting mode of trifunctional silanes depends on the silane concentration. At high silane concentrations the ladder-like grafting mode is the most likely grafting mode (35). This mode results in less silanol groups and is thus more hydrophobic than the mono-grafting mode that is preferred at low concentrations. Presumably, the grafting mode changes from mono grafting at 60% DTES coverage to more and more ladder-like grafting when going towards the 100% DTES coverage. This explanation is in accordance with the FTIR peak Si-OH/Si-O-Si ratios. Here, the peak ratios continue to decrease from 60% DTES coverage to 100% DTES coverage.

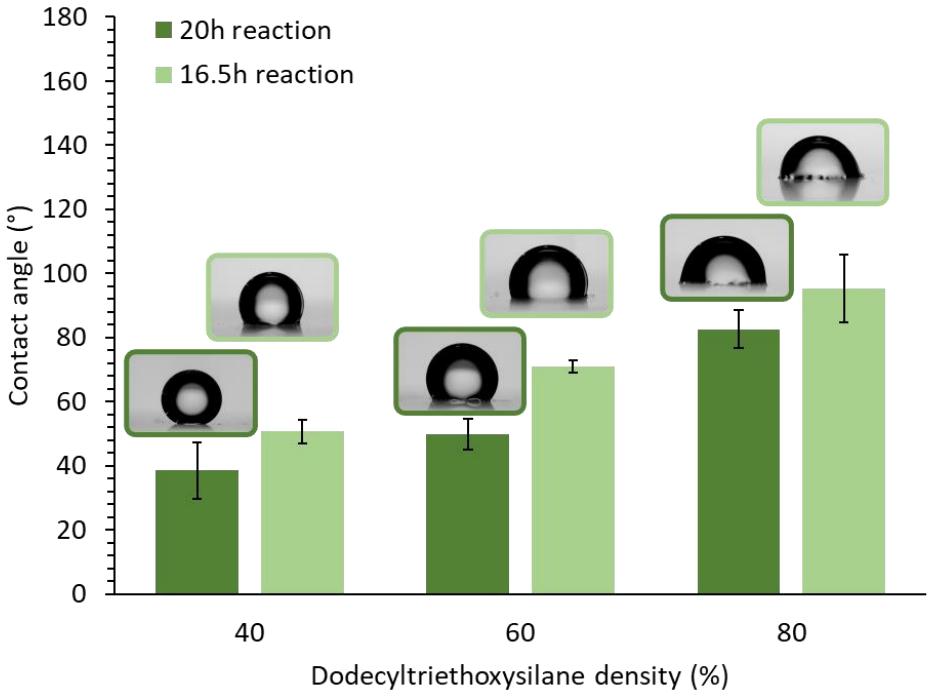

Figure 46 Contact angles for the DTES functionalized particles using a slightly different reaction time.

To demonstrate the reproducibility of the functionalization method the procedure was repeated for the 40%, 60% and 80% DTES density, only with a slightly shorter reaction time of 16.5 hours. The three-phase contact angles measured for these particles are given in Figure 46 together with the contact angles of the particles functionalized using 20 hours of reaction time. Both reaction times resulted in an increase in the contact angle with increasing amount of added DTES, showing that the previous results could be reproduced. It appears that the shorter reaction time yields slightly more hydrophobic particles. However, there is still a theoretical DTES density of 80% required to obtain particles with a contact angle close to the neutral wetting angle of 90°.

The contact angles measured directly after the functionalization prove that DTES can modify the surface of the silica particles such that the surface changes from hydrophilic to hydrophobic. A theoretical DTES density close to 80% should tailor the contact angle to be close to 90°. To gain insight in the stability of the particle dispersion in water the contact angle of the particles with 20 hours reaction time was monitored over time, see Figure 47. Measuring the contact angle one week after the functionalization revealed a decrease in contact angle for all degrees of functionalization. For 40% and 60% DTES coverage the contact angle was brought back to the value measured for non-functionalized Ludox TM-50 particles. For the other degrees of functionalization the contact angles were in the hydrophilic regime but not yet brought back to non-functionalized Ludox TM-50 contact angle value. The DEP droplets formed on top of the coated slides with water as ambient phase are illustrated in Figure 47.

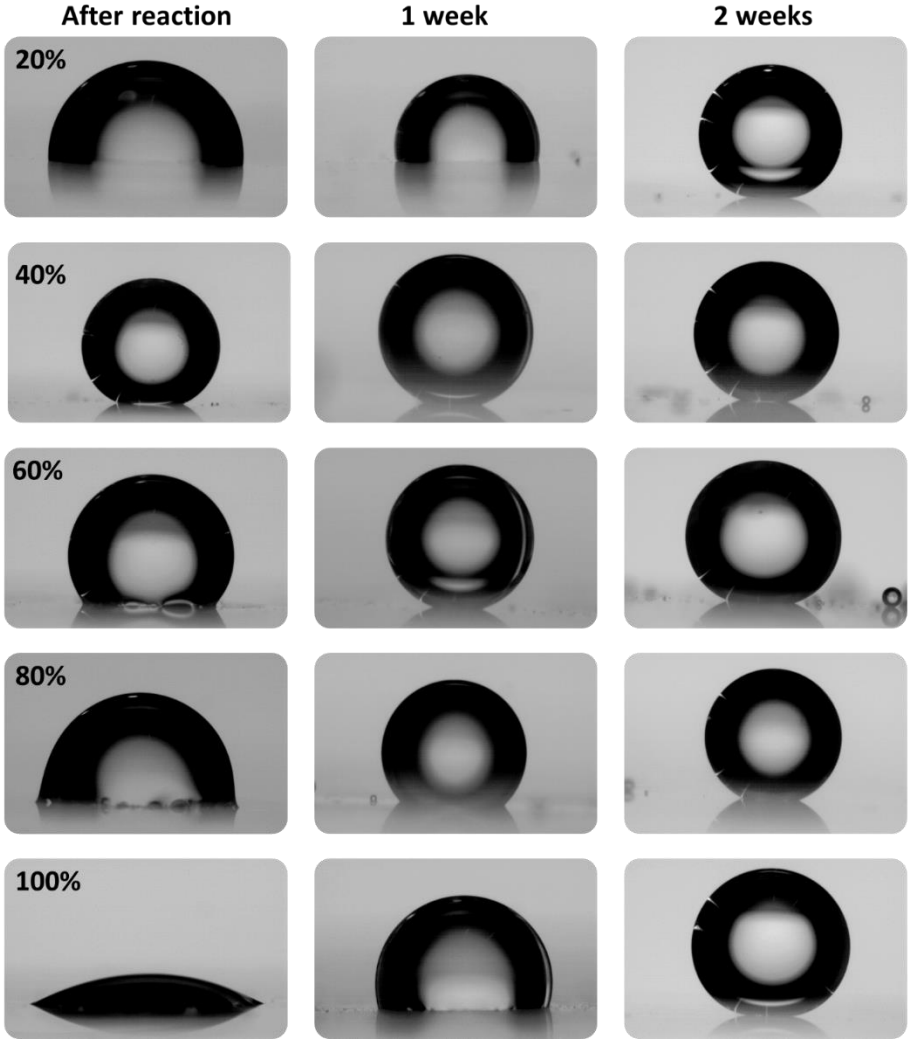

Figure 47 DEP droplets formed during the contact angle measurements. Over time the droplet becomes more and more spherical, illustrating the unfavorable interaction between the drop phase and the coating.

The measurements done two weeks after the functionalization show that within two weeks the contact angle values are returned to the initial value of the non-functionalized particles. Figure 48 depicts the contact angle valued measured via the water phase for the different functionalizations. Here, the decrease in contact angle is clearly observable. This decrease can be well understood. The functionalized particles are stored in water, the principal component in the functionalization. As discussed in Section 2.4 the presence of water is required for hydrolyzation. Upon storing the particles in water, water is accessible at every point in time. The condensed DTES molecules can thus readily "post-hydrolyze", hydrolyze after the functionalization. In the post-hydrolyzation the bond formed between the surface silanol and DTES molecule is hydrolyzed, resulting in the recovery of the hydrophilic surface silanol group. After two weeks likely all the DTES molecules bound to the surface were post-hydrolyzed, returning all the silanol groups that were substituted in the functionalization and thereby the initial hydrophilicity. This led to the conclusion that functionalized particles cannot be stored in water. Possibly, this can also explain the small differences in contact angel observed for slightly different reaction times in Figure 46. The reaction mixture contains water. The longer the reaction time, the longer the functionalized particles are exposed to water. This might already allow for some post-hydrolyzation.

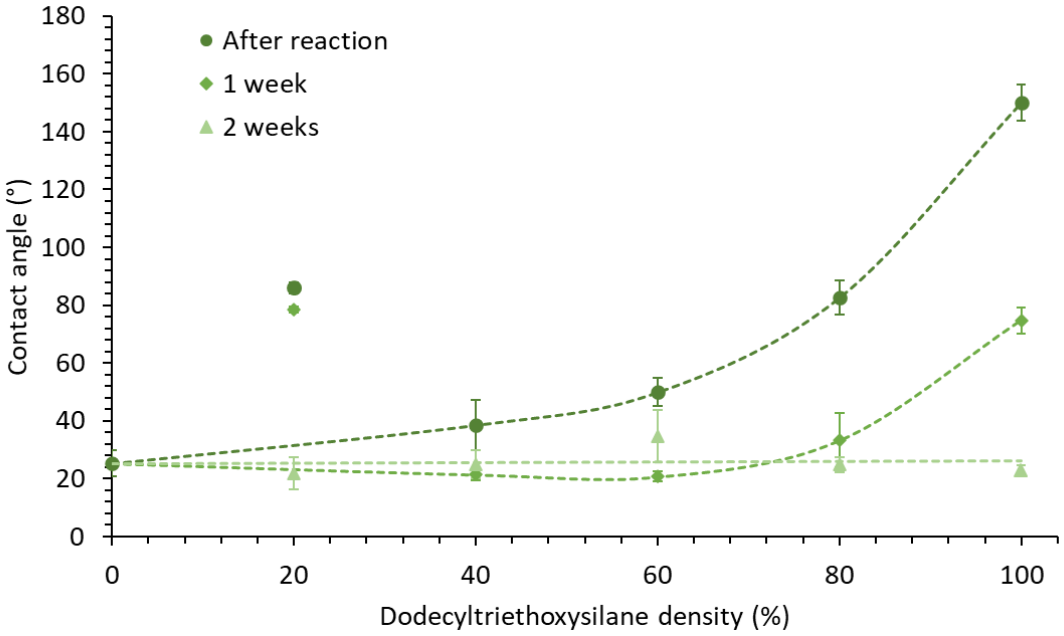

Figure 48 Contact angle versus DTES density for different moments in time. Clearly, the contact angles decrease with time.

The high pH of 11.1 could have enhanced the post-hydrolyzation. Both the hydrolysis and condensation rate are pH-dependent, see Figure 49. At neutral pH the hydrolysis rate is relatively slow. Both at low and high pH the hydrolysis rate is significantly higher. Hence, the high condition pH of the DTES functionalized particles could have intensified the post-hydrolyzation. Conditioning at more neutral pH could slightly increase the stability of the functionalized particles in water.

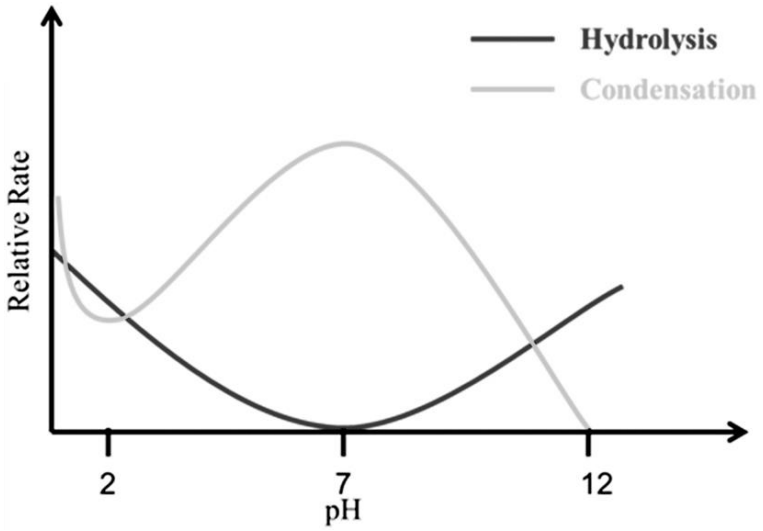

Figure 49 The pH effect on both the hydrolysis and condensation rate. Reprinted from Li et al. (56).

4.3 Functionalization of SiO_2 nanoparticles with DTES – dispersion in 1-propanol

The above discussed three-phase contact angle measurements clearly show that by keeping the particles in water the functionalization is reversed. Hence, the shelf life of the functionalized particle dispersions is short. To preserve the functionalization it might help to change the dispersion medium. Despite the fact that dispersibility in water is desired to enhance the precursor mixture stability, it is first and foremost of importance to retain the functionalization. In order to achieve this the functionalization is repeated but now 1-propanol is used as dispersion medium.

4.3.1 Experimental method functionalization

The experimental method used to obtain DTES-functionalized particles in 1-propanol is similar to the method described in Section 4.1.2. The previous results gave an indication for the DTES density range that results in contact angles close to 90°. Hence, we choose DTES densities of 60%, 75% and 90%. The corresponding added amounts of DTES were 0.744 mL, 0.930 mL and 1.116 mL, respectively. Prior to the third washing step the pH was brought up to 11.6 with NaOH. To remove the residual water the sediment was washed with 1-propanol before dispersing the particles in 1-propanol using vortex mixing (Scientific Industries Vortex-Genie 2) and ultrasonication (Branson 1800).

4.3.2 Three-phase contact angle for functionalized particles stored in 1-propanol

Figure 50 gives the three-phase contact angles measured for the 60%, 75% and 90% DTES surface coverage dispersed in 1-propanol directly after the reaction and after 7 weeks. Strikingly, there is no clear difference observable between the three different degrees of functionalization while the largest difference in contact angles for the particles dispersed in water could be observed between 60% DTES and 100% DTES density. All three types of particles give a three-phase contact angle close to 50°. This value is larger than the 25° for the unfunctionalized Ludox TM-50, indicating that there is DTES attached to the particles. Additionally, this value of approximately 50° is similar to the value found for the 60% DTES covered particles in water. The TGA results revealed that the number of bound silanes is comparable for both 60% DTES and 100% DTES density. Hence, it might actually be reasonably expected that the 60%, 75%, and 90% DTES densities give rise to same extent of hydrophobicity. However, when dispersed in water a decrease in contact angle was seen between 60% and 100% DTES density which was ascribed to a decrease in silanol groups due to the ladder-like grafting mode. When dispersed in 1-propanol it appears like the change in silane grafting mode with increasing silane concentration does not influence the contact angle as there is no increase in contact angle observable. Why this is the case remains unclear, but is does show that the dispersion

medium can influence the obtained hydrophobicity. Based on these results the maximum contact angle that could be achieved using DTES as silane is 50°. Consequently, DTES is, just like TMSPM, not hydrophobic enough to realize neutral wetting behavior of the Ludox TM-50 particles in the water/DEP system.

The stability of the DTES functionalization was assessed by measuring the contact angles a second time after 7 weeks. Now the particles are stored in 1-propanol, water should be less accessible and thus it is expected that there is no or less post-hydrolyzation. The measured contact angle values indeed show that there is no significant change in the hydrophobicity over time. Thus, it can be concluded that by dispersing the particles in 1-propanol the functionalization is preserved.

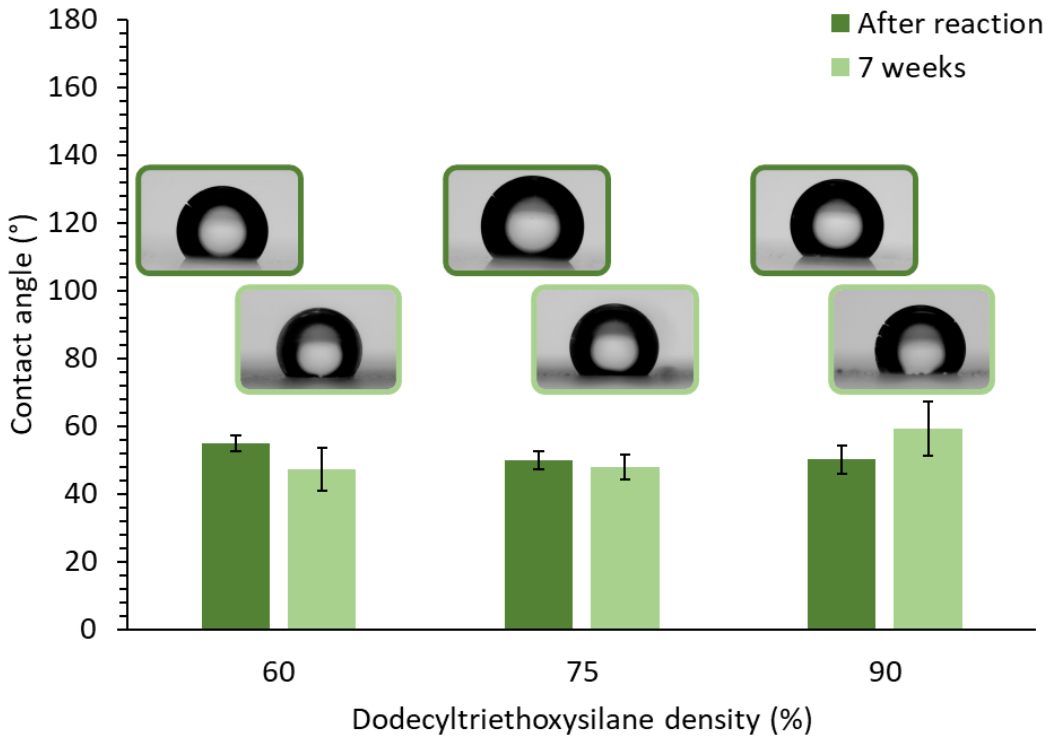

Figure 50 Three-phase contact angles of the DTES functionalized particles dispersed in 1-propanol measured directly after the functionalization reaction and after 7 weeks. The insets show the DEP droplet formed on top of the particle coating during the contact angle measurements.

Chapter 5

Hexamethyldisilazane

TMSPM and DTES are both trifunctional silanes. Their ability to bind to the silica surface in multiple ways makes it more difficult to interpret the data obtained for these silanes. Moreover, if only one bond is formed between the trifunctional silane and the silica surface, this leaves two silanol groups unreacted. Silanol groups are hydrophilic and thus by using trifunctional silanes hydrophilicity can be introduced simultaneously to introducing hydrophobicity via the hydrophobic organic group R'. To circumvent the possibility of introducing hydrophilicity while aiming for solely introducing hydrophobicity monofunctional silanes can be used. Hexamethyldisilizane (HMDS), see Figure 51, is such a monofunctional silane. Cai and Clegg (57) have already used HMDS to alter the silica surface chemistry, making them suitable for bijel formation. Besides the advantage of the monofunctional reaction with the surface, HMDS also allows for more gentle reaction conditions (31). When using HMDS as silylation agent there is only one possible way of binding. The trimethylsilyl group either binds to the silica surface, forming one Si-O-Si bond, or not. Upon binding there are only hydrophobic methyl groups introduced. This possibly allows for adding more hydrophobicity compared to the silanol-introducing trifunctional silanes. Additionally, it might be easier to interpret the data obtained on HMDS-functionalized particles as the type of binding does not have to be considered. In this chapter we explore the ability of HMDS to render the Ludox TM-50 silica particle partly hydrophobic. First, the functionalization protocol will be discussed. Subsequently, the functionalization will be assessed by FTIR, zeta potential and contact angle measurements.

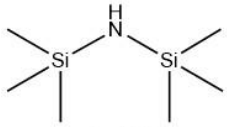

Hexamethyldisilazane

Figure 51 Chemical structure of hexamethyldisilazane.

5.1 Functionalization of SiO_2 nanoparticles with hexamethyldisilazane

The method used for the functionalization with hexamethyldisilizane (HMDS) is based on the method reported by Cai and Clegg (57). A schematical overview of the experimental method is depicted in Figure 52. The reaction mixture consists of 11 w% ammonia solution, 85 w% ethanol, 3 w% silica particles (HDK H30 fumed silica) and 1 w% HMDS. After mixing the different components the mixture is placed on a vortex mixer for 10 seconds. Subsequently, the mixture is subjected to ultrasonication for 30 minutes. The mixture was left 20 hours at room temperature before washing the functionalized particles with ethanol. The particles were dried for 24 hours at 50°C prior to redispersing them in the desired solvent using tip sonication (57,58). This base-catalyzed procedure requires a large excess of silane. Using the calculation described in Section 2.4.4 the above described method uses a silane coverage of 600%. This is significantly higher than the silane coverages needed in the acid-catalyzed procedure used for the TMSPM and DTES functionalization, making the base-catalyzed reaction less controllable.

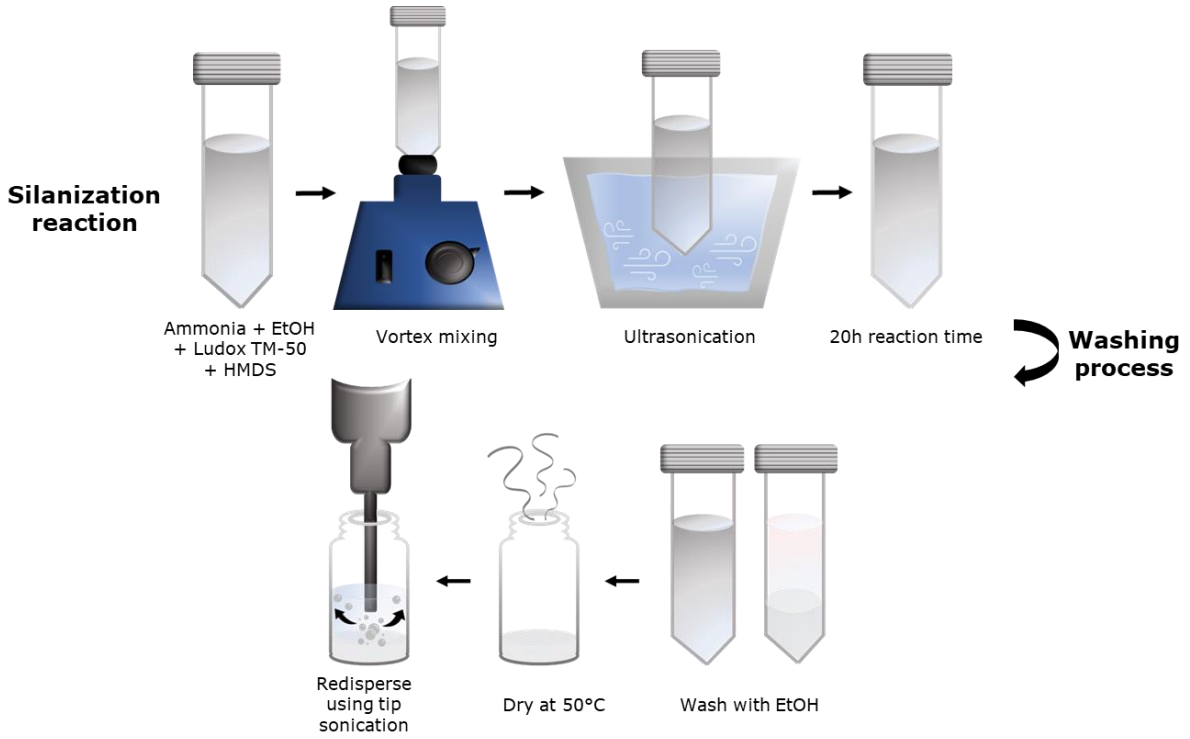

Figure 52 Schematical overview of the experimental method described by Cai and Clegg (57) *to functionalize silica nanoparticles with HMDS. After the silylation reaction the particles are washed with ethanol and subsequently dried. The particles are then dispersed in 1-propanol using tip sonication.*

The drying step was implemented to allow the particles to be dispersed in a binary mixture of ethylene carbonate and *p*-xylene (57). Although not specifically mentioned in the procedure by Cai and Clegg (57,58) the reaction mixture was stirred during the 20 hours of reaction time. In the first attempt drying step was included. However, redispersing the dried particle in 1-propanol showed to be difficult, even if tip sonication was used. Hence, the experimental method was adjusted by leaving out the drying step and adding a washing step with 1-propanol, see Figure 53.

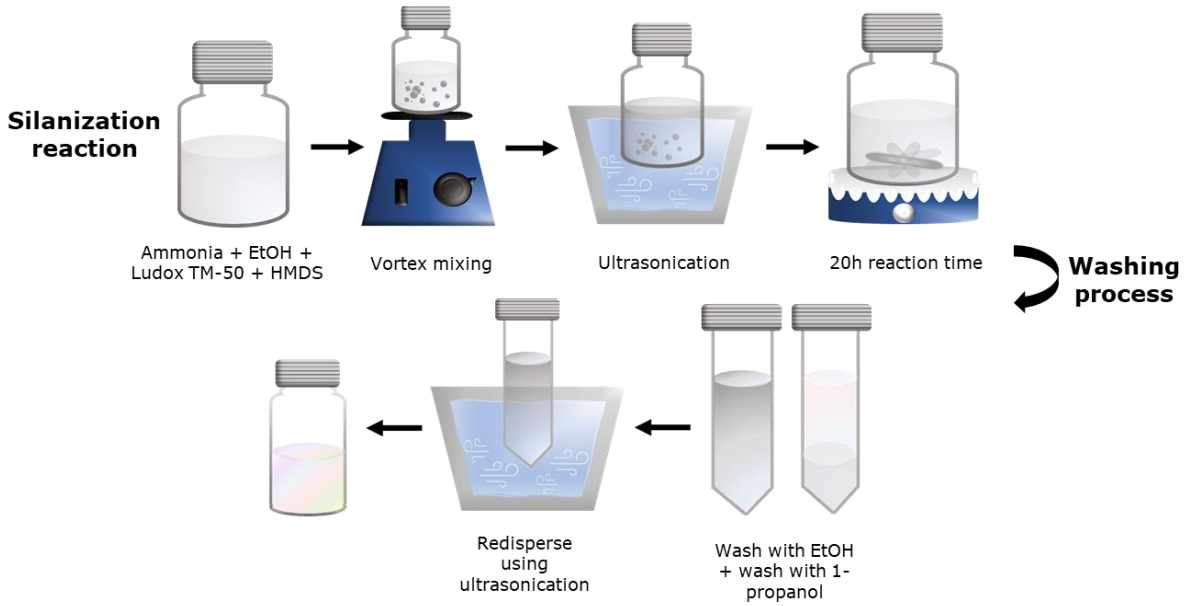

Figure 53 The adjusted experimental method for the HMDS-functionalization. After the silane reaction the particles are washed with ethanol and 1-propanol. Subsequently, the particles are redispersed in 1-propanol using ultrasonication.

5.1.1 Chemicals

The hexamethyldisilizane used in the HMDS-functionalization is purchased from Sigma Aldrich and has a purity of 99%. The ammonia solution, 30 w% solution of NH_3 in water, is purchased from Acros Organics.

5.1.2 Experimental method functionalization

The reaction was carried out in a 100 mL bottle. To the bottle 7 mL ammonia, 53 mL ethanol, 2 mL Ludox TM-50 and the calculated amount of HMDS were added. Table 9 gives the amounts added for 600%, 900%, 1100% and 1200% HMDS surface coverage. The mixture was vigorously mixed using the Scientific Industries Vortex-Genie 2 vortex mixer for 15 seconds. Subsequently, the mixture was placed in the ultrasonic bath (Branson 1800) for 30 minutes. The mixture was placed on a stirring plate for 20 hours. After 20 hours of reaction time the functionalized particles were washed with ethanol thrice. Each washing step consisted of redispersing the particles using vortex mixing and collecting the particles via centrifugation using the Beckman Coulter Allegra® X-12R centrifuge for 20 minutes at 3750 rpm. In the first washing step 30 mL ethanol was added. In both the second and third step 20 mL ethanol was added. For 1200% HMDS density the particles were dried at 50°C for 24 hours. Once completely dry, 1-propanol was added and the dispersion was subjected to tip sonication (amplitude of 35%). The pulse option was used to reduce heating of the sample. For the 900%, 1100%, and 1200% HMDS the particles were washed once with 10-20 mL of 1-propanol after the washing with ethanol. Subsequently, 5-8 mL of 1-propanol was added. Vortex mixing and ultrasonication was applied to redisperse the particles.

For the weight fraction determination the mass of 100 µL dispersion and the mass of the particles present in 100 µL of dispersion were weighted.

Table 9 Added amounts of HMDS for different surface coverages together with the particle weight fraction of the dispersions.

Degree of functionalization (%)	Amount of added HMDS (mL)	Particle weight fraction (w%)
600	0.819	14
900	1.229	18
1100	1.502	18
1200	1.640	5

5.1.3 Sample preparation for DLS, zeta potential, FTIR, TGA, and contact angle measurements

The sample preparations were performed as described in Section 4.1.3. For the zeta potential and DLS samples the pH had drifted to pH values below 10. Hence, 0.1M NaOH was used to bring the pH up to 10 again.

5.2 Results and discussion

The calculated weight fractions are given in Table 9. Similar to the TMSPM and DTES functionalization the HMDS functionalized particles are subjected to FTIR, zeta potential and three-phase contact angle measurements to examine the functionalization.

5.2.1 Determining the presence of HMDS functional groups using FTIR

Similar to DTES, HMDS only introduces hydrocarbon functional groups. It is thus to be expected that the FTIR spectra of the HMDS functionalized particles resemble that of the DTES functionalized particles. On first sight, see Figure 54, the average spectra of the HMDS functionalized particles appear to resemble the Ludox TM-50 spectra rather than the DTES functionalized particles.

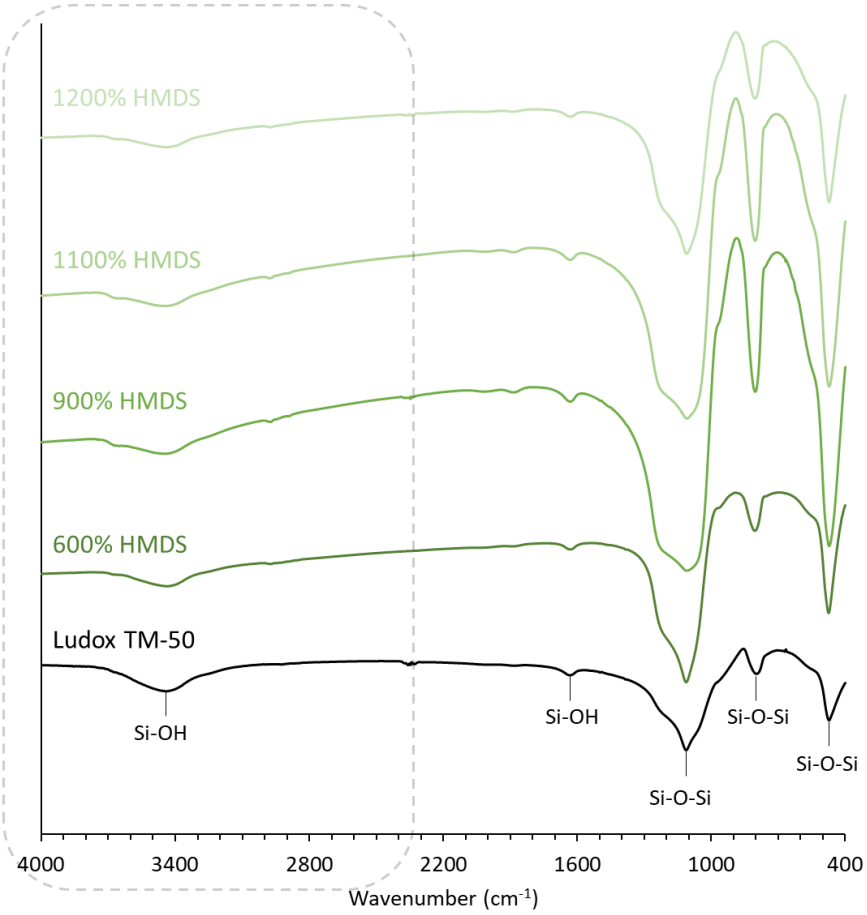

Figure 54 The average FTIR spectra of the HMDS-functionalized particles. The spectra are plotted with an offset.

However, zooming in on the wavenumber range 4000-2400 cm^{-1}, see Figure 55, revealed that the HMDS functionalized particles do give rise to the expected CH_3 stretch at 2970 cm^{-1} (46). An overview of the peaks present in the FTIR spectra of the HMDS functionalized particles is given in Table 10. Additionally, a very weak peak can be observed at 2890-2880 cm^{-1} which can be ascribed to the CH_2 group (46). Although weak in intensity, the presence of the peak around 2970 cm^{-1} does indicate that there is HMDS attached to the silica surface. The lower intensity compared to the DTES functionalized particles can readily be understood because the number of hydrocarbons is less in HMDS than in DTES. HMDS only introduces one methyl group whereas DTES introduces an alkyl chain of 12 carbon atoms. The HMDS functionalized particles were dispersed in 1-propanol. Hence, the presence of the CH_2 stretch could be explained by substitution of part of the methyl groups by propyl groups. However, based solely on the very weak peaks in the FTIR spectra this cannot be concluded.

Table 10 Overview of the peaks observable in the FTIR spectra of the HMDS functionalized particles.

Wavenumber (cm^{-1})	**Species**	**Appearance**
3437	Si-OH	Broad
2970	CH_3	Weak
2890-2880	CH_2	Very weak
1632	Si-OH	Weak
1113	Si-O-Si	Strong
797	Si-O-Si	Medium
473	Si-O-Si	Strong

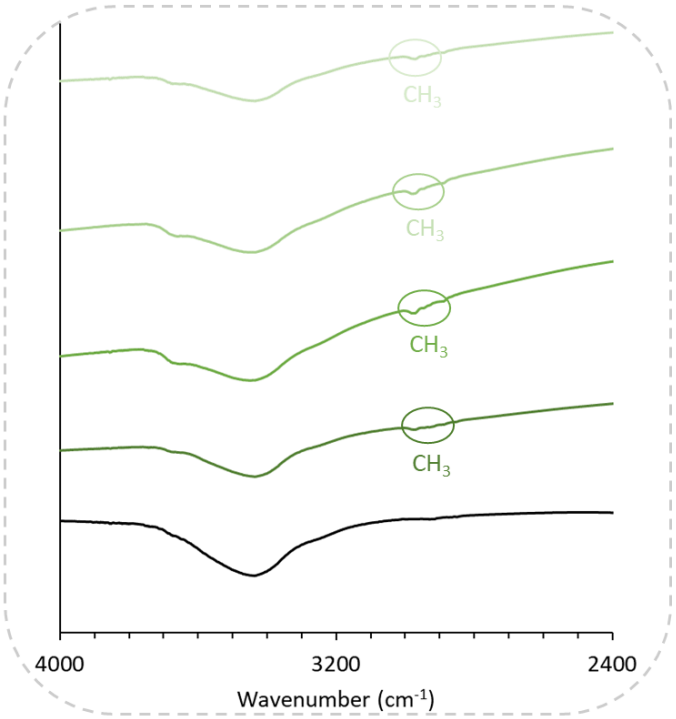

Figure 55 Zoom in on the spectral region 4000 cm^{-1}-2400 cm^{-1}. Upon zooming in the FTIR spectra of the HMDS functionalized particles show peaks around 2900 cm^{-1}.

The Si-OH to Si-O-Si ratio in Figure 56 confirms that the HMDS molecules reacted with the silica surface. Upon reaction surface silanol groups are substituted by the HMDS molecule which results in a decrease in Si-OH/Si-O-Si ratio. This decrease is clearly observable in Figure 56. The peak ratios for the 900%, 1100% and 1200% HMDS density are comparable. Therefore, it is likely that the maximum coverage of 40% is achieved by adding an excess of HMDS molecules corresponding to a coverage of 900%.

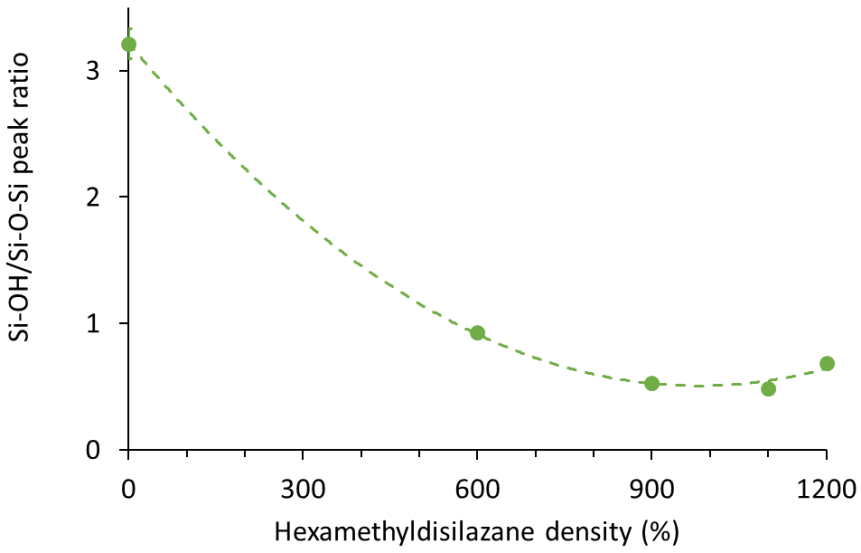

Figure 56 The average Si-OH/Si-O-Si peak ratios of the HMDS functionalized particles. The error bars indicate the standard deviation in the data. The standard deviation of the HMDS functionalized particles is too small to be observable in the graph. A second order polynomial trendline was added which has a R^2 value of 0.9988.

5.2.2 Change in surface charge examined by zeta potential measurements

The average zeta potential distribution is given in Figure 57a. Except for the 1200% HMDS functionalized particles, the distributions are broad and contain multiple peaks. For the 600%, 900%, and 1100% HMDS density the samples thus contained particles with different surface charges. The distributions corresponding to 900% and 1100% HMDS density show significant overlap, and therefore likely have comparable surface charges. Figure 57b shows the average zeta potential for the different HMDS densities. Here, it can be observed that both the 900% and 100% HMDS density give rise to a zeta potential of -62 mV. Remarkably, the absolute value of the zeta potential increases with increasing HMDS densities. HMDS is a monofunctional silane and therefore is not able to introduce additional silanol groups. To explain this increase in absolute zeta potential it is necessary to look into the DLS results.

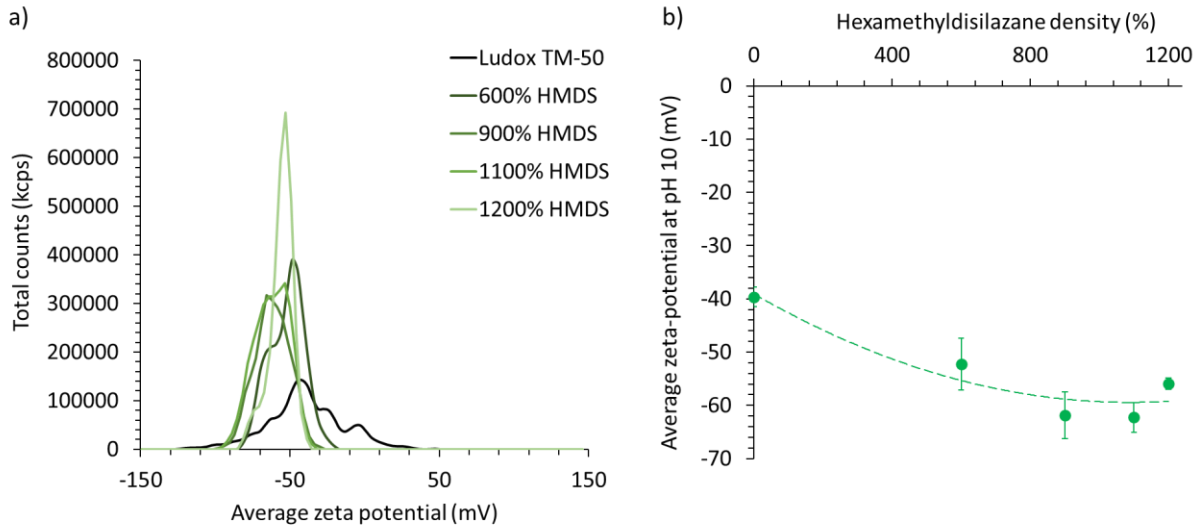

Figure 57 Zeta potential results. a) Average zeta potential distribution. b) Average zeta potential for the different degrees of functionalization. The error bars represent the standard deviation in the data. To the average zeta potential a second order polynomial was fitted. The R^2 is 0.8898.

The DLS results in Figure 58 show that the particles more than doubled in size compared to the unfunctionalized Ludox TM-50 particles. In Figure 58a a shift in the average size distribution can be observed towards larger sizes for all the degrees of functionalization. The size distributions are relatively broad, suggesting that the particles exhibit a significant polydispersity. The average sizes for the different used HMDS densities are depicted in Figure 58b. The increase in size is most pronounced for the particles functionalized using 600% HMDS density. There is no clear trend observable in the average size. The increase in size indicates that the particles have aggregated, making the zeta potential result unreliable. Based on these zeta potentials it is thus difficult to gain information on the extent of the functionalization as the particle size has changed significantly.

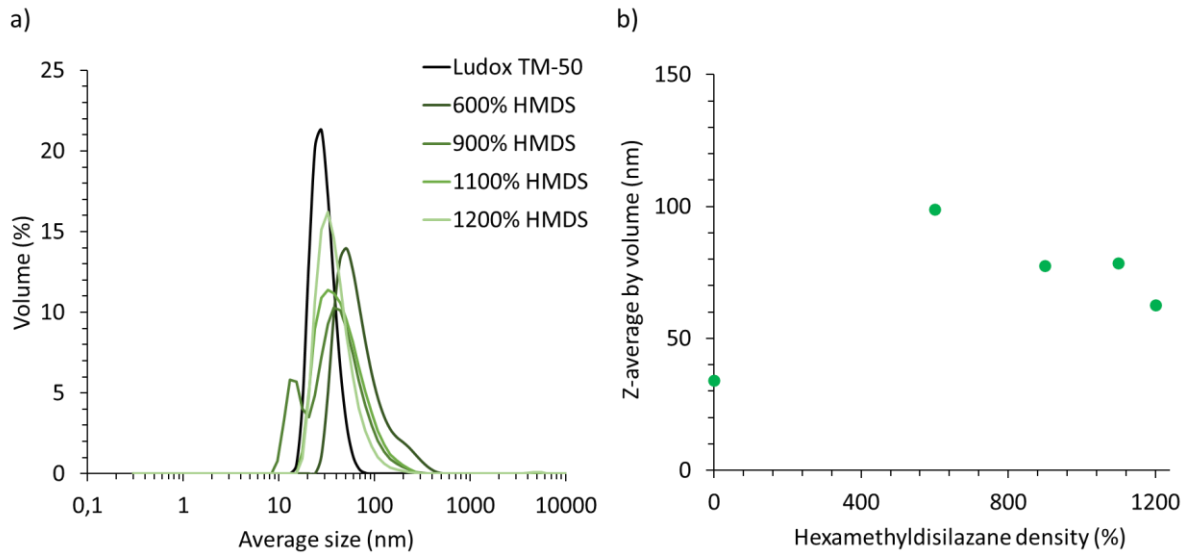

Figure 58 Results of the DLS measurement. a) Average size distribution by volume. b) Average volume-weighted size for the different DTES densities. The standard deviation in the average size is too small to be visible in the graph.

5.2.3 Three-phase contact angles for functionalized particles stored in 1-propanol – a time dependent study

The contact angles formed by the HMDS functionalized particles were monitored over time, as depicted in Figure 59. The particles are dispersed in 1-propanol, and thus it is not expected that the HMDS molecules detach due to post-hydrolyzation.

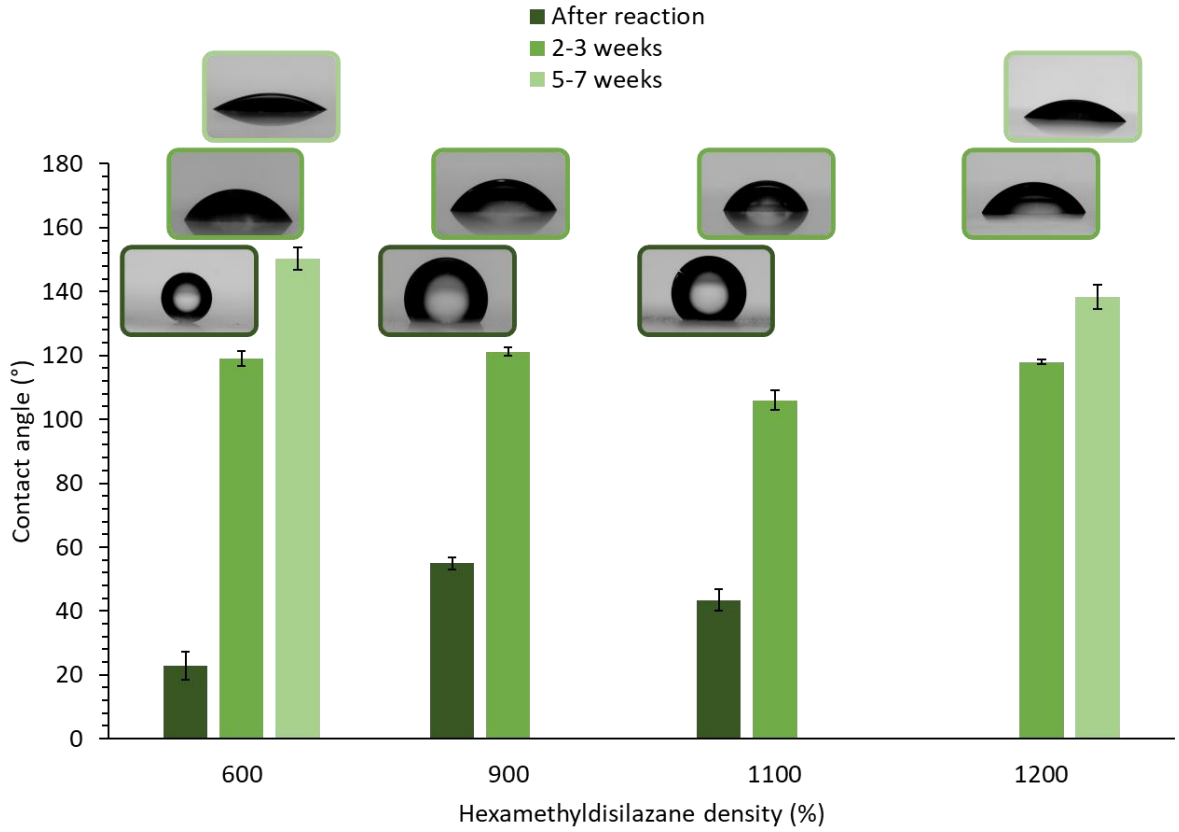

Figure 59 Time-dependent three-phase contact angles measured for the HMDS functionalized particles. Over time the contact angle increases significantly.

The contact angles measured directly after the functionalization reaction show that the particles remained hydrophilic using 600%, 900% and 1100% HMDS density. For the 600% the contact angle was similar to that of nonfunctionalized Ludox TM-50. For 900% and 1100% the contact angle was increased to 55° and 43°, respectively. When measured after 2 to 3 weeks a steep increase in contact angle can be observed. All the different degrees of functionalization researched here have a contact angle between 106° and 121° after 2 to 3 weeks. In this time span the minimal contact angle increase was 63°. After 5 to 7 weeks the particles appear to become even more hydrophobic with contact angles of 140° to 150°. Contrary to the DTES functionalized particles in water where the contact angle decreased over time, the contact angle of the HMDS functionalized particles in 1-propanol increases over time. A possible explanation for this could be that the -Si(CH_3)$_3$ groups introduced by the HMDS are substituted by -O-(CH_2)$_2$$CH_3$ groups originating from the solvent, 1-propanol. The FTIR spectra already showed a CH_2 signal which is in accordance with the proposed idea. The propyl group consists of a longer alkyl chain and is therefore more hydrophobic than the methyl groups of the HMDS functional group. Besides using silanes as silylation agents, they are also applied as alcohol protection groups in the organic chemistry. Often this alcohol protection is achieved by the formation of a trialkylsilyl ether via the reaction of an alcohol with a chlorotrialkylsilane. In this S_N2 reaction an oxygen-silicon bond is formed between the alcohol and the silane and the bond and the silicon-chloride bond is broken, see Figure 60a (59). Perhaps a similar reaction can take place between 1-propanol and the surface silicon that was involved in the functionalization reaction, see Figure 60b. This is a hypothetical reaction. Whether this is indeed the reaction that took place and caused the increase in hydrophobicity is difficult to determine. For the TMSPM and DTES functionalized particles in 1-propanol there was no increase in contact angle observed. The functional groups of these silanes are large compared to the methyl group of HMDS. Probably, these groups are poor leaving groups, and are therefore not substituted by propyl groups.

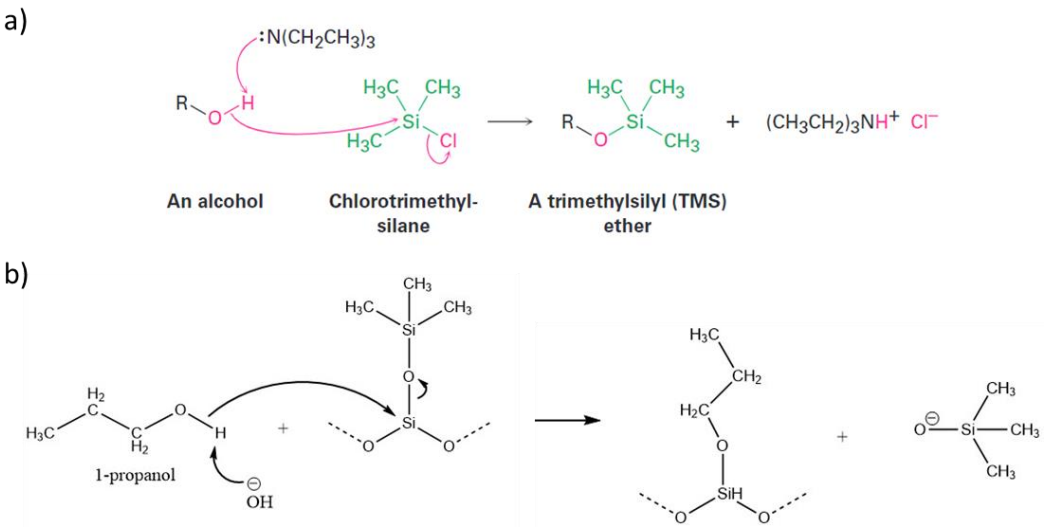

Figure 60 Alcohol protection reaction with chlorotrimethylsilane. Reprinted from McMurry (59). *b) Hypothetical reaction between 1-propanol and the surface silicon.*

Chapter 6

Silane comparison

Thus far, the focus has mainly been on characterizing the functionalization. However, it is also of interest to compare the three different silanes researched in this work. Is it preferable to work with monofunctional silanes if it is desired to make the silica surface more hydrophobic? Or do trifunctional silanes work better? What is the effect of the organic substituent on the achievable hydrophobicity? To address these questions the Si-OH to Si-O-Si peak ratio deduced from the FTIR spectra and the three-phase contact angles measured for dispersions in 1-propanol are compared. In addition, the stability of the particles in 1-propanol is compared.

6.1 Si-OH to Si-O-Si peak ratio

The Si-OH/Si-O-Si peak ratio gives information on the relative amount of residual silanol groups. The TGA results on the DTES functionalized particles showed that the 60% DTES and 100% DTES covered particles have a comparable silane content. Both have an actual silane density close to 40%. This led to the conclusion that for the Ludox TM-50 particles it is likely that there is a maximum coverage of 40%. Assuming that the maximum coverage is invariant with different silanes, the 60%, 80% and 100% covered particles should have the same silane coverage for both TMSPM and DTES. The peak ratios in Figure 61 for TMSPM and DTES at these theoretical densities, however, show to be different. For the TMSPM functionalized particles the peak ratio indeed appears to plateau, especially for 80% and 100%. The peak ratios corresponding to DTES, on the other hand, show a significant decrease. This decrease can only be due to a different binding mode of the DTES molecules as there is no increase in silane content. DTES thus changes the way it binds to the silica surface, and thereby decreases the number of hydrophilic silanol groups, whereas TMSPM does not change the binding mode. Presumably, TMSPM binds via the ladder-like mode even at lower silane concentrations. DTES likely first binds via the mono- and di- grafting mode until a threshold silane concentration is reached. Once this threshold concentration is reached, the DTES molecules also bind via the ladder-like grafting mode. The influence of the additional hydrophilic silanol groups appears to be more pronounced for DTES than for TMSPM. At a density of 100% both TMSPM and DTES give rise to a peak ratio of approximately 1, indicating that both silanes can attach to the silica surface in a comparable manner if the silane concentration is high enough.

The HMDS peak ratios are significantly lower than the ones corresponding to TMSPM and DTES. This confirms the idea that when using HMDS as the silylation agent there is no hydrophilicity introduced by additional silanol groups. Based on the peak ratios, it could be concluded that the monofunctional HMDS introduces the least hydrophilicity, and thereby may achieve the most hydrophobic silica surface. When aiming for a hydrophobic surface, it is thus best to utilize monofunctional silanes. Yet, the hydrophobicity of the silane surface does not only have to be dictated by the number of silanol groups present at the surface. The organic groups R’ can also contribute to the surface hydrophobicity. This contribution can be assessed by the three-phase contact angle.

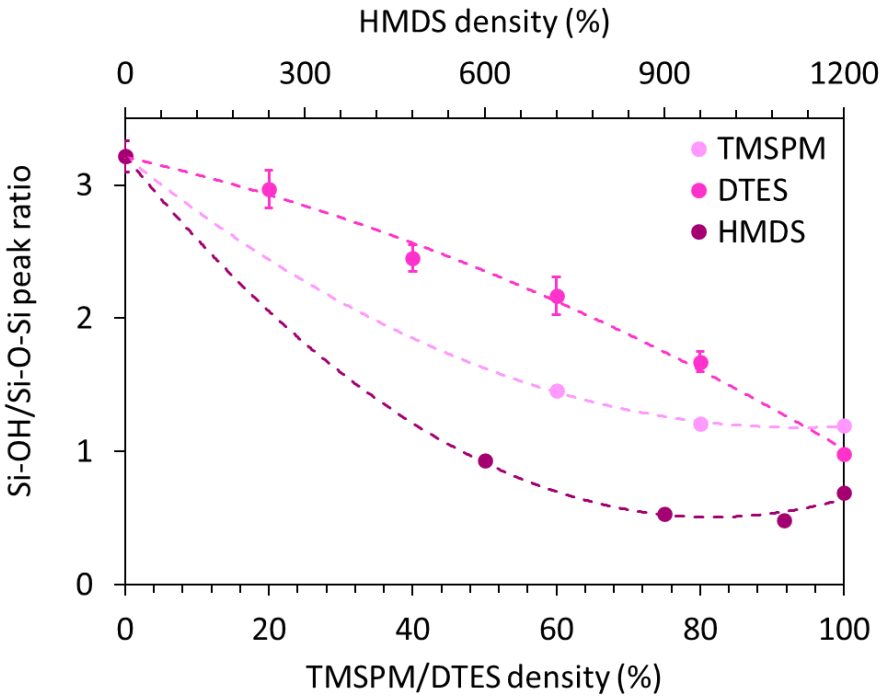

Figure 61 The FTIR Si-OH to Si-O-Si peak ratios for the three different researched silanes.

6.2 Three-phase contact angle & particle stability

To compare the hydrophobicity of the silane functionalized particles the three-phase contact angles are plotted together in Figure 62 for the dispersions in 1-propanol. Here, it can be observed that there is not much difference between the two trifunctional silanes, TMSPM and DTES. Both gave rise to contact angles of 50° to 60°. These contact angles remained relatively stable over time in 1-propanol. For TMSPM a slight decrease in θ could be observed. This might be due to the presence of a small amount of water in the 1-propanol that allows for post-hydrolyzation. Previous results showed that the influence of the hydrophilic silanol groups is larger for DTES compared to TMSPM. Yet, the contact angles are similar. This indicates that the organic group has a significant influence on the surface hydrophobicity, and can compensate for the introduced hydrophilicity. The initial contact angles measured for the HMDS functionalized particles are unexpectedly small. With a monofunctional silane there is no additional hydrophilicity introduced and thus it is to be expected that this functionalization yields large contact angles. However, the organic groups are relatively small, and thereby may introduce limited hydrophobicity. Over time the HMDS covered particles exhibit a significant increase in three-phase contact angle. This increase was ascribed to substitution of the HMDS methyl groups by the 1-propanol propyl groups. A monofunctional silane with larger hydrophobic groups can thus hydrophobize the Ludox TM-50 silica to such extent that contact angles of 150° can be achieved. This shows the potential of monofunctional silanes as silylation agent for generating neutral wetting behavior of Ludox TM-50 particles with respect to water and DEP. Utilizing larger organic groups presumably also allow the functionalization to be stable in 1-propanol as substitution would be less favorable if the leaving group is significantly large. Generating sufficiently hydrophobic Ludox TM-50 nanoparticles that are stable over time should therefore be achievable using monosilanes with organic groups of 3 or more carbon atoms.

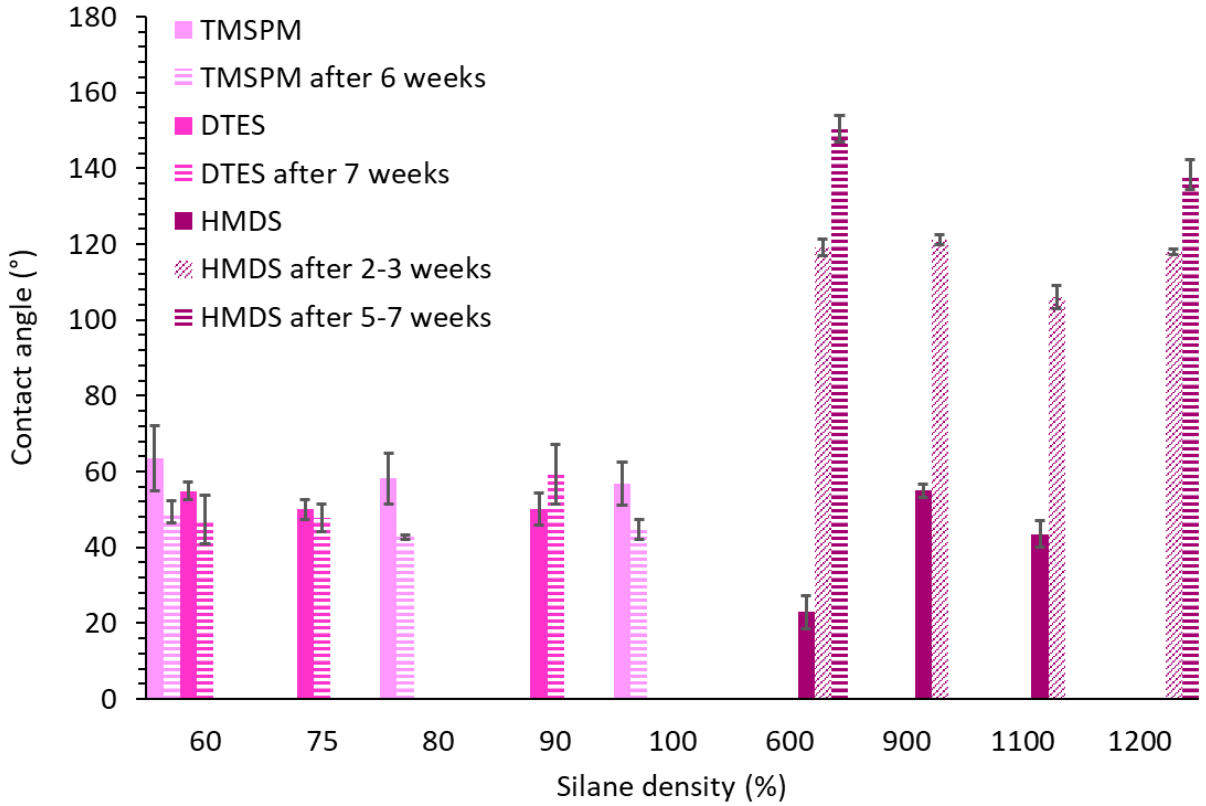

Figure 62 The three-phase contact angles of the silane functionalized particles dispersed in 1-propanol.

Chapter 7

Conclusions & outlook

To conclude this master thesis the main findings are summarized. Additionally, follow-up research ideas are proposed.

7.1 Conclusions

To address whether covalent modification of Ludox TM-50 nanoparticles can be used to generate neutrally wetting nanoparticles for the stabilization of bijels formed with the water/DEP/1-propanol system, we have researched three different silanes TMSPM, DTES, and HMDS in this work. Besides researching their ability to hydrophobize Ludox TM-50 silica nanoparticles, we have also looked at the stability of the functionalization, and at the dispersibility of the functionalized particles in the water/DEP/1-propanol bijel precursor mixture.

Using the method described by Boakye-Ansah et al. (9) Ludox TM-50 silica nanoparticles were successfully functionalized with the trifunctional silanes TMSPM and DTES. The introduction of the corresponding functional groups was confirmed by FTIR. The difference in the Si-OH/Si-O-Si peak ratio between the different degrees of functionalization was small for TMSPM, suggesting that the TMSPM coverage is similar for theoretical TMSPM densities of 60%, 80% and 100%. The TMSPM functionalized particles dispersed in 1-propanol gave rise to a water/particle/DEP three-phase contact angle close to 50° for 60%, 80% and 100% TMSPM coverage, indicating that TMSPM is not sufficiently hydrophobic to generate neutrally wetting silica nanoparticles for bijels formed using the water/DEP/1-propanol system. Even though the particles are still classified as hydrophilic, the TMSPM functionalized particles dispersed in 1-propanol were not stable in the precursor mixture consisting mainly of water and 1-propanol. Therefore, it was concluded that the hydrophobicity required for neutrally wetting differs significantly from the hydrophobicity that allows the particles to be dispersed in the precursor mixture.

To create a more hydrophobic silica surface DTES was applied as silylation agent, using 20%, 40%, 60%, 80% and 100% DTES densities. When the DTES functionalized particles are dispersed in water, the contact angle increased significantly from 50° to 150° going from 60% DTES coverage to 100% DTES coverage. The Si-OH/Si-O-Si peak ratios showed a decrease in the number of silanol group for increasing DTES densities, indicating that the higher the DTES density the more surface silanol groups are replaced by DTES molecules. Based on the TGA results the actual silane coverage was calculated to be 17.5% for the 20% DTES density and 42.6% and 39.8% for 60% and 100% DTES density, respectively. This showed that the maximum silane coverage that can be achieved on Ludox TM-50 particles is likely close to 40%, and that this maximum coverage is reached for silane densities of 60% and higher. Knowing that the maximum coverage is reached for 60% DTES density and higher, the decrease in silanol groups for DTES densities larger than 60% indicates that the grafting mode of DTES changes when the DTES density is increased above 60%. Monitoring the contact angle over time revealed that in the presence of water the silanes post-hydrolyze. Hence, the functionalized particles cannot be stored in water. Consequently, the particles must be dispersed in 1-propanol. For 60%, 75% and 90% DTES covered particles in 1-propanol the contact angle showed to be constant at 50°, suggesting that there is no change in grafting mode if the particles are dispersed in 1-propanol, and that the functionalization is relatively stable in 1-propanol. However, similar to TMSPM, DTES does not introduce enough hydrophobicity to allow for neutral wetting behavior of the Ludox TM0-50 silica nanoparticles in the water/DEP system.

The introduction of additional hydrophilicity by hydrolyzed silane alkoxy groups was eliminated by using the monofunctional HMDS. Applying the method reported by Cai and Clegg (57), HMDS was successfully attached to the Ludox TM-50 surface according to FTIR. The maximum coverage

appeared to be reached when 900% HMDS density was used, and gave rise to a contact angle of 55°. Contrary to the DTES functionalized particles, the time dependent study of the contact angle showed that for HMDS functionalized particles dispersed in 1-propanol the contact angle increased significantly over time to vales up to 150°. For small functional groups the silane functionalization is not stable in 1-propanol as the functional groups are presumably substituted by propyl groups.

Comparison of the Si-OH/Si-O-Si peak ratio revealed that DTES introduces the most hydrophilic silanol groups and HMDS, as expected, the least. The contact angles of the TMSPM and DTES functionalized particles in 1-propanol were similar, suggesting that the hydrophobicity of the organic group can compensate for the hydrophilicity introduced by the additional silanol groups. The large contact angles obtained by the substitution of the methyl groups by propyl groups reveals the potential of using monofunctional silanes with longer alkyl chains as silylation agent. Stable, neutrally wetting particles should be achievable using these type of silanes. Dispersing the functionalized particles in the water/DEP/1-propanol bijel precursor mixture, on the other hand, will remain very challenging. The hydrophobicity of the particles, the stability of the functionalization, and the dispersibility of the particles in the precursor mixture are key aspects for covalent modification to be successful in generating bijels. The results obtained in this work suggest that the requirements for the hydrophobicity, stability and dispersibility cannot be met simultaneously for the water/DEP/1-propanol system using covalent modification, and thereby suggest that in-situ modification might be the only route to "small domain" bijels using the water/DEP/1-propanol system.

7.2 Outlook

Although this work revealed interesting aspects of the silane functionalization of Ludox TM-50 silica nanoparticles, neutral wetting with respect to DEP and water could not be achieved with the researched silanes. To enhance the hydrophobicity, it would be interesting to look at monofunctional silanes with a longer alkyl chain. By increasing the alkyl chain the functionalized particles presumably also exhibit stability in 1-propanol. Additionally, relatively low silane density would be required to reach neutral wetting behavior. If more hydrophobic particles could be achieved using such a monofunctional silane these could be applied in a more hydrophobic bijel precursor mixture.

The base-catalyzed procedure used for the HMDS functionalization required a large excess of HMDS. The acid-catalyzed procedure used for the TMSPM and DTES functionalization, on the other hand, could be well controlled by the amount of silane that was added to the reaction mixture. It would be interesting to perform the HMDS functionalization with the acid-catalyzed experimental method. Perhaps this allows the reaction to be more controlled, eliminating the need for a large excess of silane.

Aside from precisely pinpointing the required silane density for a three-phase contact angle of 90°, hydrophilic and hydrophobic particles can also be mixed to stabilize bijels. Previous research has shown that bijels with μm domain size could be obtained using a mix of hydrophilic and hydrophobic silica particles by both temperature quenching (57) and STrIPS (60). Perhaps, this approach can also be implemented in the water/DEP/1-propanol bijel system. The additional benefit to this approach is that the individual particle fraction of both the hydrophilic and hydrophobic particles is significantly less than the particle weight fraction required for creating bijels with only one type of particle. Possibly, this improves the dispersibility of the particles in the precursor mixture.

Acknowledgements

To start, I would like to thank Alessio for his daily supervision, his relaxed attitude that compensated for my own stressful state of being, and his interesting research ideas. You taught me to do "sanity checks", simple experiments to test a characterization method, which certainly will help me in future research projects. During the first half of my project Katherine also supervised me, showing me around and teaching me the silane functionalization method, which I am very grateful for. I would like to thank Martin for the insightful discussions, his help with the functionalization method, and his involvement as project supervisor. Also, thanks to Joren for babysitting me when Alessio was absent.

In general, I would like to thank FCC for the enjoyable learning environment. Special thanks to Alex, Dominque and Bonny for running the lab, and always being available for questions. Besides the technical support I would like to thank Dominique for her help with the SEM and, most of all, for the supporting, interesting and inspiring conversations we have had about research, academia and industry. Azeem and Neshat for taking the time to give me helpful feedback on my poster about this project. Aside from FCC, I would like to thank Dennie Wezendonk from MCC for performing the TGA measurements and his help with the results.

Last but not least, a major "thank you" to my fellow master students (especially Bo, I know I distracted you way too often with my research struggles but I really appreciate our conversations about science and life, and your encouraging "Je bent gewoon goed bezig Tessa") who were always willing to think along, listen, and created a great and pleasant environment, also during the more stressful times of research.

References

1. Sholl DS, Lively RP. Seven chemical separations to change the world. Nature. 2016;532(7600):435–7.

2. di Vitantonio G, Wang T, Stebe KJ, Lee D. Fabrication and application of bicontinuous interfacially jammed emulsions gels. Vol. 8, Applied Physics Reviews. American Institute of Physics Inc.; 2021.

3. Cha S, Lim HG, Haase MF, Stebe KJ, Jung GY, Lee D. Bicontinuous Interfacially Jammed Emulsion Gels (bijels) as Media for Enabling Enzymatic Reactive Separation of a Highly Water Insoluble Substrate. Sci Rep. 2019 Dec 1;9(1).

4. Herzig EM, White KA, Schofield AB, Poon WCK, Clegg PS. Bicontinuous emulsions stabilized solely by colloidal particles. Vol. 6, Nature Materials. Nature Publishing Group; 2007. p. 966–71.

5. Haase MF, Stebe KJ, Lee D. Continuous Fabrication of Hierarchical and Asymmetric Bijel Microparticles, Fibers, and Membranes by Solvent Transfer-Induced Phase Separation (STRIPS). Advanced Materials. 2015 Nov 25;27(44):7065–71.

6. Khan MA, Sprockel AJ, Macmillan KA, Alting MT, Kharal SP, Boakye-Ansah S, et al. Nanostructured, Fluid-Bicontinuous Gels for Continuous-Flow Liquid–Liquid Extraction. Advanced Materials. 2022 May 1;34(18).

7. Haase MF, Boakye-Ansah S, di Vitantonio G, Stebe KJ, Lee D. CHAPTER 6 Bijels Formed by Solvent Transfer-induced Phase Separation. In: Bijels: Bicontinuous Particle-stabilized Emulsions . RSC publishing; 2020. p. 137–66.

8. Rubingh DN. The influence of surfactants on enzyme activity. Curr Opin Colloid Interface Sci. 1996 Oct;1(5):598–603.

9. Boakye-Ansah S, Schwenger MS, Haase MF. Designing bijels formed by solvent transfer induced phase separation with functional nanoparticles. Soft Matter. 2019;15(16):3379–88.

10. Butt HJ, Graf K, Kappl M. Physics and Chemistry of Interfaces. Weinheim: WILEY-VCH GmbH & Co. KGaA; 2003.

11. Pickering SU. CXCVI.-Emulsions. J Chem Soc. 1907;91:2001–21.

12. Ramsden W. Separation of Solids in the Surface-layers of Solutions and "Suspensions" (Observations on Surface-membranes, Bubbles, Emulsions, and Mechanical Coagulation). - Preliminary Account. Proceedings of the Royal . 1903;72:156–64.

13. Tran L, Haase MF. Templating Interfacial Nanoparticle Assemblies via in Situ Techniques. Langmuir. 2019 Jul 2;35(26):8584–602.

14. Chevalier Y, Bolzinger MA. Emulsions stabilized with solid nanoparticles: Pickering emulsions. Colloids Surf A Physicochem Eng Asp. 2013 Dec 20;439:23–34.

15. Cates ME, Clegg PS. Bijels: a new class of soft materials. Soft Matter. 2008;4(11):2132–8.

16. Stratford K, Adhikari R, Pagonabarraga I, Desplat JC, Cates ME. Colloidal Jamming at Interfaces: A Route to Fluid-Bicontinuous Gels. Science (1979). 2005 Sep 30;309(5744):2198–201.

17. Binks BP, Horozov TS. Colloidal particles at liquid interfaces. Cambridge Univ. Press; 2006.

18. Björkegren S, Nordstierna L, Törncrona A, Palmqvist A. Hydrophilic and hydrophobic modifications of colloidal silica particles for Pickering emulsions. J Colloid Interface Sci. 2017 Feb 1;487:250–7.

19. Gupta S, Saxena A. Negative Gaussian curvature distribution in physical and biophysical systems-Curved nanocarbons and ion-channel membrane proteins. J Appl Phys. 2012 Dec 1;112(11).

20. McDevitt KM, Thorson TJ, Botvinick EL, Mumm DR, Mohraz A. Microstructural characteristics of bijel-templated porous materials. Materialia (Oxf) [Internet]. 2019 Sep;7:100393. Available from: https://linkinghub.elsevier.com/retrieve/pii/S2589152919301899

21. Orts-Gil G, Natte K, Drescher D, Bresch H, Mantion A, Kneipp J, et al. Characterisation of silica nanoparticles prior to in vitro studies: From primary particles to agglomerates. Journal of Nanoparticle Research. 2011 Apr;13(4):1593–604.

22. Wang T, di Vitantonio G, Stebe KJ, Lee D. Scalable Manufacturing of Hierarchical Biphasic Bicontinuous Structures via Vaporization-Induced Phase Separation (VIPS). ACS Mater Lett. 2020 May 4;2(5):524–30.

23. Cai D, Clegg PS, Li T, Rumble KA, Tavacoli JW. Bijels formed by direct mixing. Soft Matter. 2017;13(28):4824–9.

24. Clegg PS, Thijssen JHJ. CHAPTER 1: Introduction to Bijels. RSC Soft Matter. 2020;2020-January(10):1–33.

25. Khan MA, Sprockel AJ, Macmillan KA, Alting MT, Kharal SP, Boakye-Ansah S, et al. Supporting Information Nanostructured, Fluid-Bicontinuous Gels for Continuous-Flow Liquid–Liquid Extraction. Advanced Materials. 2022 May 1;34(18).

26. Wang Y, Zhang L, Hu Y, Li C. In situ Surface Functionalization of Hydrophilic Silica Nanoparticles via Flame Spray Process. J Mater Sci Technol. 2015 Sep 1;31(9):901–6.

27. Arkles B. Tailoring surfaces with silanes. Chemtech. 1977;7(12).

28. Arkles B. Hydrophobicity, Hydrophilicity and Silane Surface Modification. Gelest, Inc. 2011;547–1015(215).

29. Hertl W, Hair ML. Reaction of Hexamethyldisilazane with Silica. J Phys Chem [Internet]. 1974;75(14):2181–5. Available from: https://pubs.acs.org/sharingguidelines

30. Gun'Ko VM, Vedamuthu MS, Henderson GL, Blitz JP. Mechanism and kinetics of hexamethyldisilazane reaction with a fumed silica surface. J Colloid Interface Sci. 2000 Aug 1;228(1):157–70.

31. Park JW, Park YJ, Jun CH. Post-grafting of silica surfaces with pre-functionalized organosilanes: New synthetic equivalents of conventional trialkoxysilanes. Chemical Communications. 2011 May 7;47(17):4860–71.

32. Jones FR. Optimization of the Reaction of Hexamethyldisilazane on a Fumed Silica Surface [Internet] [Masters]. [Charleston]: Eastern Illinois University; 1999. Available from: https://thekeep.eiu.edu/theses/1669

33. Boakye-Ansah S, Schwenger M, Haase MF, University R, Rowan HM. Supporting Information Designing Bijels formed by Solvent Transfer Induced Phase Separation with Functional Nanoparticles. 2019.

34. LUDOX TM-50 colloidal silica Aldrich CAS No.7631-86-9 (principal component) [Internet]. [cited 2022 Dec 19]. Available from: https://www.sigmaaldrich.com/NL/en/product/aldrich/420778

35. Wu J, Ling L, Xie J, Ma G, Wang B. Surface modification of nanosilica with 3-mercaptopropyl trimethoxysilane: Experimental and theoretical study on the surface interaction. Chem Phys Lett. 2014 Jan 20;591:227–32.

36. Erné B. Colloidal Analysis Techniques. Utrecht; 2022 Jan.

37. Lowe BM, Skylaris CK, Green NG. Acid-base dissociation mechanisms and energetics at the silica-water interface: An activationless process. J Colloid Interface Sci. 2015 Aug 1;451:231–44.

38. Duval Y, Mielczarski JA, Pokrovsky OS, Mielczarski E, Ehrhardt JJ. Evidence of the existence of three types of species at the quartz-aqueous solution interface at pH 0-10: XPS surface group quantification and surface complexation modeling. Journal of Physical Chemistry B. 2002 Mar 21;106(11):2937–45.

39. Spin Coater Chucks | Compatible with the Ossila Spin Coater | Ossila [Internet]. [cited 2022 Nov 28]. Available from: https://www.ossila.com/en-eu/products/spin-coater-chucks

40. Spin Coating: Complete Guide to Theory and Techniques | Ossila [Internet]. [cited 2022 Nov 28]. Available from: https://www.ossila.com/en-eu/pages/spin-coating

41. Zhou G, He J. Antireflective coatings on fresnel lenses by spin-coating of solid silica nanoparticles. J Nanosci Nanotechnol. 2013 Aug;13(8):5534–41.

42. Brassard JD, Sarkar DK, Perron J. Fluorine based superhydrophobic coatings. Applied Sciences (Switzerland). 2012 Jun 1;2(2):453–64.

43. Lopes IMF, Abersfelder K, Oliveira PW, Mousavi SH, Junqueira RMR. Flower-like silicon dioxide/polymer composite particles synthesized by dispersion polymerization route. J Mater Sci. 2018 Aug 1;53(16):11367–77.

44. Launer PJ, Arkles B. INFRARED ANALYSIS OF ORGANOSILICON COMPOUNDS: SPECTRA-STRUCTURE CORRELATIONS [Internet]. Morrisville; 2013. Available from: www.gelest.com

45. Wagh PB, Kumar R, Patel RP, Singh IK, Ingale S v., Gupta SC, et al. Hydrophobicity Measurement Studies of Silica Aerogels using FTIR Spectroscopy, Weight Difference Method, Contact Angle Method and K-F Titration Method [Internet]. Article in Journal of Chemical, Biological and Physical Sciences. 2015. Available from: https://www.researchgate.net/publication/277608386

46. Kulkarni SA, Ogale SB, Vijayamohanan KP. Tuning the hydrophobic properties of silica particles by surface silanization using mixed self-assembled monolayers. J Colloid Interface Sci. 2008 Feb 15;318(2):372–9.

47. Castaneda-Gill J. Zetasizer pro and zetasizer ultra. Malvern Panalytical.

48. Karmakar S. 5 Particle Size Distribution and Zeta Potential Based on Dynamic Light Scattering: Techniques to Characterize Stability and Surface Charge Distribution of Charged Colloids.

49. Winkler PM, McGraw RL, Bauer PS, Rentenberger C, Wagner PE. Direct determination of three-phase contact line properties on nearly molecular scale. Sci Rep. 2016 May 17;6.

50. Teo W, Caprariello A v, Morgan ML, Luchicchi A, Schenk GJ, Joseph JT, et al. Nile Red fluorescence spectroscopy reports early physicochemical changes in myelin with high sensitivity. Available from: https://www.pnas.org

51. Roe B, Kotek R, Zhang X. Durable hydrophobic cotton surfaces prepared using silica nanoparticles and multifunctional silanes. Journal of the Textile Institute. 2012 Apr;103(4):385–93.

52. Pyo CE, Chang JH. Hydrophobic Mesoporous Silica Particles Modified with Nonfluorinated Alkyl Silanes. ACS Omega. 2021 Jun 22;6(24):16100–9.

53. PerkinElmer. A beginner's guide to Thermogravimetric Analysis (TGA). Waltham;

54. Sehlleier YH, Abdali A, Schnurre SM, Wiggers H, Schulz C. Surface functionalization of microwave plasma-synthesized silica nanoparticles for enhancing the stability of dispersions. Journal of Nanoparticle Research. 2014;16(8).

55. Roboz J. A History of Ion Current Detectors for Mass Spectrometry. In: Gross ML, Caprioli RM, editors. The Encyclopedia of Mass Spectrometry. Elsevier Science; 2016. p. 183–8.

56. Li H, Chen X, Shen D, Wu F, Pleixats R, Pan J. Functionalized silica nanoparticles: Classification, synthetic approaches and recent advances in adsorption applications. Vol. 13, Nanoscale. Royal Society of Chemistry; 2021. p. 15998–6016.

57. Cai D, Clegg PS. Stabilizing bijels using a mixture of fumed silica nanoparticles. Chemical Communications. 2015 Oct 8;51(95):16984–7.

58. Cai D, Clegg PS. Supplementary Information (SI) Stabilizing bijels using a mixture of fumed silica nanoparticles. 2015.

59. McMurry JE. Organic Chemistry. Cengage Learning; 2011. 648–650 p.

60. di Vitantonio G, Lee D, Stebe KJ. Fabrication of solvent transfer-induced phase separation bijels with mixtures of hydrophilic and hydrophobic nanoparticles. Soft Matter. 2020 Jul 7;16(25):5848–53.